
**INSTITUTO SUPERIOR DE ENGENHARIA DE LISBOA**

**Área Departamental de Engenharia de Electrónica e Telecomunicações e de Computadores**


# Robust cardiopulmonary antenna design for any body mass index


**João Filipe Ferreira da Silva Tenente Cardoso**

Licenciado


Dissertação para obtenção do Grau de Mestre
em Engenharia Eletrónica e Telecomunicações


Orientadores : Prof. Doutor Pedro Pinho
Prof. Doutor Daniel Albuquerque


Júri:

Presidente: [Grau e Nome do presidente do juri]

Vogais: [Grau e Nome do primeiro vogal]
[Grau e Nome do segundo vogal]

**September, 2022**

# Acknowledgements

Firstly i would like to thank my family, for all the sacrifices, for helping me during all these years, providing conditions for my studies, and throughout all my life. To my girlfriend for her motivation and strength, fundamental in not getting discouraged and losing focus during the work.

I would like to thank my supervisor Dr. Pedro Pinho and co-advisor Dr. Daniel Albuquerque for the sharing of knowledge and for all the help and availability provided throughout this year. I would also like to thank Carolina Gouveia for all the help provided, it was fundamental to this work.

I thank Instituto Superior de Engenharia de Lisboa for the teachings that were important for the development of this work. Thanks to the Instituto de Telecomunicações - Aveiro for the manufacture of the antenna and providing the required materials and equipments to support the measurements.

Lastly, a big thanks to my friends, for the great memories and support during all these years. A special thanks to Tiago who has been with me throughout my academic journey.

To all, a heartfelt thank you!

# Abstract

With the advancement of wireless diagnostic and treatment technologies, antennas implanted inside and outside the human body are now widely used. The use of antennas on the body, along with other technologies, presents itself as an innovative method for detecting and monitoring vital signs. These antennas can be placed in direct contact with the human body or on clothing making vital signs monitoring with these methods more comfortable and less invasive when compared to traditional methods, allowing home monitoring of elderly patients or high risk workers such as police, firefighters and military personnel. A gap was found in the literature regarding the development of a standard antenna model that can be used by anyone, regardless of their physiognomy.

In this dissertation, a robust high bandwidth antenna was developed to operate in the ISM frequency band, namely at 2.45 GHz, capable of monitoring vital signs in any subject. In order to increase its bandwidth, parasitic patches placed on top of the radiating element were used to obtain resonances adjacent to the center frequency, thus increasing the bandwidth of the antenna. After the antenna design, the antenna was simulated, built, and the vital signs monitoring of 5 subjects with different body physiognomies was performed. The effectiveness of the chosen design was proven, being able to monitor the respiratory signal in all test subjects.

**Keywords:** On-Body antenna, Patch antenna, high bandwidth, vital signs

# Resumo

Com o avanço das tecnologias de diagnóstico e tratamento sem fios, as antenas implantadas no interior e no exterior do corpo humano são agora amplamente utilizadas. A utilização de antenas no corpo, juntamente com outras tecnologias, apresenta-se como um método inovador para a deteção e monitorização de sinais vitais. Estas antenas podem ser colocadas em contacto direto com o corpo humano ou em roupas tornando a monitorização dos sinais vitais com estes métodos mais confortável e menos invasiva quando comparado com os métodos tradicionais, permitindo a monitorização em casa de pacientes idosos ou trabalhadores de alto risco, tais como polícia, bombeiros e militares. Foi encontrada uma lacuna na bibliografia relativamente ao desenvolvimento de um modelo de antena padrão que possa ser utilizado por qualquer pessoa, independentemente da sua fisionomia.

Nesta dissertação, foi desenvolvida uma antena robusta de elevada largura de banda para operar na banda de frequência ISM, nomeadamente a 2.45 GHz, capaz de monitorizar sinais vitais em qualquer sujeito. Com o propósito de aumentar a sua largura de banda, recorreu-se à utilização de patchs parasitas colocadas por cima do elemento radiante, obtendo-se assim ressonâncias adjacentes à frequência central, aumentando-se assim a largura de banda da antena. Após o design da antena, esta foi simulada, construída e realizada a monitorização dos sinais vitais de 5 sujeitos com fisionomias corporais diferentes. Comprovou-se a eficácia do design escolhido, conseguindo-se realizar a monitorização do sinal respiratório em todos os sujeitos teste.

**Palavras-chave:** On-body, Antena patch robusta, sinais vitais

# Contents

# List of Figures

# List of Tables

# 1

# Introduction

Cardiovascular diseases are responsible for 17,1 million deaths annually according to the World Health Organization [1]. That number tends to increase as population aging increases as well as the problems related with overweight. Respiratory diseases have as well a major effect on society as over 3 million deaths are associated with chronic respiratory diseases [2]. There is a need for monitoring non-critical patients at their homes rather than the hospitals. That way, by creating a reliable home healthcare device it is possible to reduce hospitalizations. Vital signs (breathing rate (BR) and heart rate (HR)) monitoring is one of the key features for these devices. The most traditional methods for heart rate monitoring include electrocardiography and plethysmography as shown in Figure 1.1. The use of methods that require the patient to wear biomedical devices, such as a capnometer or a pulse oximeter are valid options as well but are still inconvenient and uncomfortable to use.

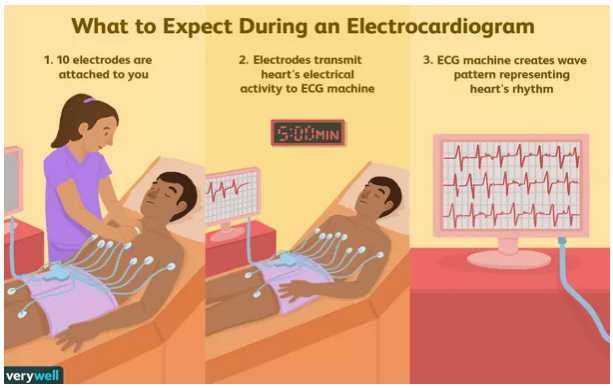


Figure 1.1: Example of an Electrocardiography [3].

The techniques for breathing rate monitoring include capnography and spirometry which involve breathing into tubes, as shown in Figure 1.2. All these methods are uncomfortable, require constant contact (inhibiting movement) and are expensive. Alternative devices should be non-invasive, more comfortable, cost effective, portable, reliable, and accurate. Noninvasiveness is especially important in case of infants, burnt victims, etc.

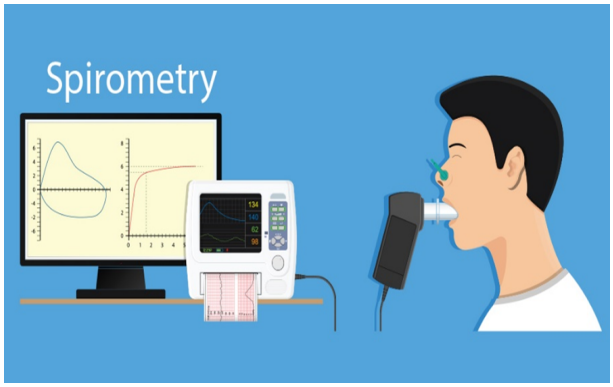


Figure 1.2: Example of a Spirometry [4].

Non-contact and noninvasive detection of vital signs such as heartbeat and breathing rates is recently becoming the object of various research. Moreover, the recent advances in integrated electronics and wireless technology, together with the reduced hardware costs, make off-the-shelf devices available directly for the not-specialized final user. Thus, home systems are becoming popular for monitoring known syndromes where intrusive and uncomfortable traditionally prescribed chest-strap monitors could be replaced by contactless monitoring instruments [5], [6], [7]. Further applications include sports training, police, firemen and military etc. Making it that uncomfortable strap belts and electrodes could be replaced by a single compact device. Although these antennas are simpler and more comfortable to use, as shown in Figure 1.3, it is difficult to adapt the antenna for all patients. Human's body electromagnetic characteristics will be different according with the person using the antenna because all humans body are different, regarding the composition of the different layers, such as fat tissue, bone, and muscle.


Figure 1.3: Example of an On-Body antenna [8].

## 1.1 Motivation

From the first medical equipment developed in the mid-19th century to the present day enormous progress has been made [9]. In recent years, devices that can be used for constant health care by a non specialized user at home or devices that can be used in a controlled environment by medical professionals are a growing area of research [5]. In particular, antennas for on-body communications and vital signs monitoring have been the subject of a large number of studies due to their different possible uses, as shown in the Figure 1.4.

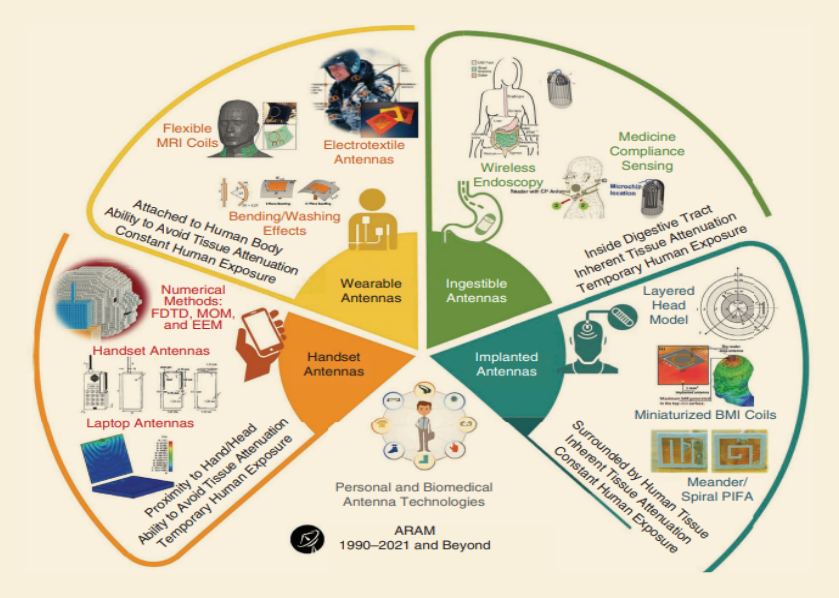


Figure 1.4: Personal and biomedical antenna technologies [10].

In recent years, advances have been made in the use of this type of antennas to monitor the vital signs of patients in a non-intrusive, highlighting the study carried out in [5]

and [11]. The use of a single antenna to monitor vital signs has important advantages when compared to other methods, since it is possible to integrate these antennas into garments and be able to monitor both vital signs simultaneously, achieving a constant and comfortable monitoring during the subject's daily life. Nonetheless in order to guarantee the effectiveness of the methods, these antennas need to be designed considering the human body, regardless of its constitution, which is one of the main objectives of this dissertation. In this aspect, there is a gap in the state of the art regarding the adaptation of this type of antenna to any human body.

## 1.2 Dissertation goals

The main objective of this dissertation will be the design and development of an antenna for the On-Body detection of vital signs, namely heart and respiratory. The antenna must be robust in order to be used by any individual, regardless of their physical constitution, the different layers of the human body and their different thicknesses will influence the behavior of the antenna. The robustness of the antenna will be achieved by increasing its bandwidth through different designs, including clipping the radiating element and using parasitic patches. After the development of the antenna, its ability to monitor vital signs was tested on 5 subjects, all of them with different physiognomies.

## 1.3 Document organization

This document will be divided into 5 chapters. In the first chapter an introduction will be given to the conventional methods of vital sign detection as well as the more recently developed alternative methods. The state of the art of this dissertation is presented in chapter 2. This chapter is dedicated to the presentation of the different types of antennas for on-body vital sign monitoring, as well as the impact of the human body on the antenna's performance and how to keep the antenna's matching close to the body. In chapter 3 the patch antenna to monitor vital signs is designed. First is designed a patch antenna to operate in free space and matched to the human body. In order to counteract the influence of the human body, different methods to increase the antenna bandwidth were studied and two specific methods were implemented. In chapter 4 the designed antenna is built and tested for its operation in contact with the human body as well as its ability to monitor vital signs. Finally, in chapter 5 the conclusions are presented as well as the possibility for future improvements.

## 1.4 Original contribution

Published papers:

**J. Cardoso, P. Pinho, C. Gouveia, D. Albuquerque,** "Design of a Cardiopulmonary Antenna for Vital Signs Monitoring Robust to Different Subjects", EuCAP 2023, from 26 - 31 March at Florence, Italy.

# 2

# State of the art

Over the years there has been an increase in interest and consequent development of the technology necessary for the use of On-Body antennas. The architecture typically used in the antennas designed need to be adapted to work close to the human body. It will also be necessary to not harm patients as these antennas will work almost attached to the patient's body. This chapter will be divided into two sections,the traditional and alternative methods to monitor vital signs, with the focus on the use of on-body antennas, in this second part will be presented the type of antennas that can be used for the detection of vital signs and their characteristics (architecture, resonant frequency, etc.) and where it be discussed the impact of the human body on the antennas matching as well as solutions to overcame these impacts.

## 2.1 Vital sign detection - Classic methods

Vital signs are physiological measurements recorded to assess the basic body functions. In most cases vital signs include the following four measurements [12]:

- Heart Rate (HR)
- Breathing Rate (BR)
- Blood pressure
- Body temperature

Vital signs are generally recorded in clinical and emergency situations to determine what illnesses a person may have. The onset of certain physiological conditions can be determined by changes in vital signs.

### 2.1.1 Cardiac rhythm monitoring techniques

Pulse rate is representative of the heart rate and rhythm. The heart rate in adults is normally between 50 and 90 beats per minutes [12]. Some people have heart rates slightly outside of this range, but a heart rate that is radically outside this range is an indicator of cardiac anomalies [12]. The most common method for monitoring heart rhythm is the electrocardiogram (ECG), one of the most widely performed tests worldwide. This method consists of using 10 electrodes placed on the patient chest, as shown in Figure 2.1, to detect the heart's electrical signals, in other words, the timing and strength of electrical impulses in the heart. Each contraction of the heart muscle or heart valves emits an electrical impulse comparable to a standard that is considered normal. The ECG can be performed either at rest, while the patient is lying on the couch, or during exertion, while the patient walks on a treadmill or rides on an exercise bike.

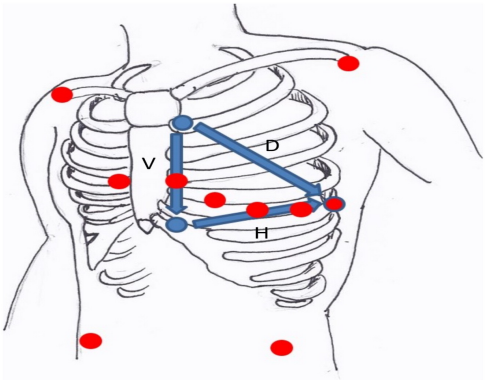


Figure 2.1: Location of electrodes in an ECG [13].

Although it is a reliable way of monitoring, there are some disadvantages in doing it. Electrodes need to be attached to the person's skin via cables. These cables restrict movement and the electrodes themselves can cause irritation to the skin of certain patients. Loose electrode connections can also bring about unwanted motion artefacts on the ECG signals. Moreover, since the voltage detected by the ECG is under 12 mV if the skin of the patient is unclean or has a lot of hair the results obtained can be incorrect [12]. Pulse oximeters which are attached to finger tips can also be used to measure pulse rates, can be another way to monitor the cardiac rhythm. Pulse oximeter monitors the oxygen saturation of the patient's blood. Polar straps (electric chest straps) are

also used to monitor heart rate during exercises [14]. They produce a pulse when an R-wave is encountered and using the timings of the generated pulses, the pulse rate is calculated. In this way they measure a bipolar electrocardiogram. It does not provide a true electro cardiogram and is inaccurate if skin under the strap is not moistened properly.

### 2.1.2 Respiratory rhythm monitoring techniques

The normal respiration rate in adults is 16 to 24 breaths per minute [12]. It can go down to 8 breaths per minute for very healthy people, but a respiratory rate out of this range is usually an indicator of respiratory system problems. Breathing rate, pattern, effort, and volume of respiration together can provide a clear picture of respiratory physiology. Respiration can be measured by:

- Measurement of air-flow;
- Measurement of chest movement or effort due to respiration;
- Oxygen Saturation Measurement.

The most commonly performed test in respiratory monitoring is spirometry. It is a simple test used to help diagnose and monitor certain lung conditions by measuring how much air you can breathe out in one forced breath. It is carried out using a device called a spirometer, which is a small machine attached by a cable to a mouthpiece, as shown in Figure 2.2. Spirometry is helpful in assessing breathing patterns that identify conditions such as asthma, pulmonary fibrosis, cystic fibrosis, and COPD (Chronic obstructive pulmonary disease). It is also helpful as part of a system of health surveillance, in which breathing patterns are measured over time [15].

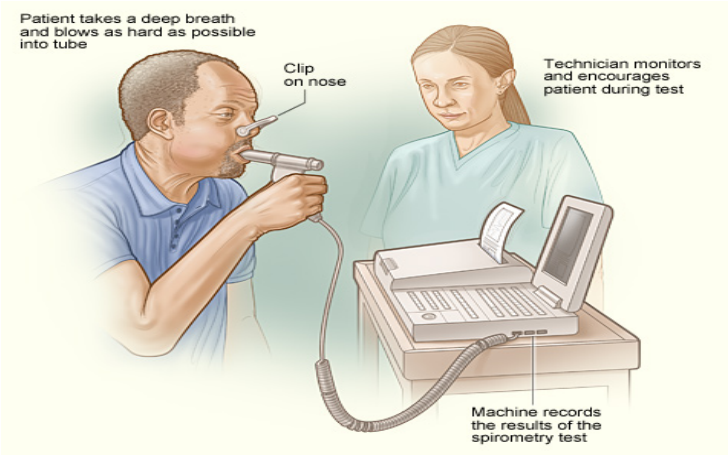


Figure 2.2: Example of a spirometry exam [15].

Pulse oximetry and Plethysmography are other possibilities to monitor the respiratory health. Pulse oximetry devices measure the oxygen saturation of blood. They are incapable of measuring respiration rate or flow but can measure respiratory disturbances [16]. Plethysmography involves the measurement of change in volume of various organs or parts of the body. These measurements give rise to respiration waveforms from which the rate can be calculated although they cannot measure exact respiratory volume. It is also possible to measure the respiratory rhythm by detecting temperature changes. Thermocouples measure the respiration rate by detecting the temperature in front of the mouth or nose [17]. Inhaled air is cool while exhaled air is warm. The difference between the two with time gives an indication of respiration rate.

## 2.2 Vital signs detection using different technologies

As previously mentioned, cardiopulmonary diseases affect a large part of the world's population. Traditional methods of detecting this type of problem, namely electrocardiograms and spirometrys, are exams that require a trip to the hospital, are invasive, being therefore ineffective in terms of time spent. Alternative methods, such as the use of a Doppler radar or an On-Body antenna, are solutions that allow for greater patient comfort as well as remote monitoring [5].

### 2.2.1 Contactless methods

As the name suggests, contactless methods are technologies that do not require a direct contact with the patient, making them non-invasive, allowing remote monitoring. Doppler radar is one of those technologies, which can be used to monitor vital signs in a completely non-invasive way, like is shown in Figure 2.3, improving the quality of care and mobility for the users. Its benefits and functioning for the detection of vital signs are adressed in [18] , [19].

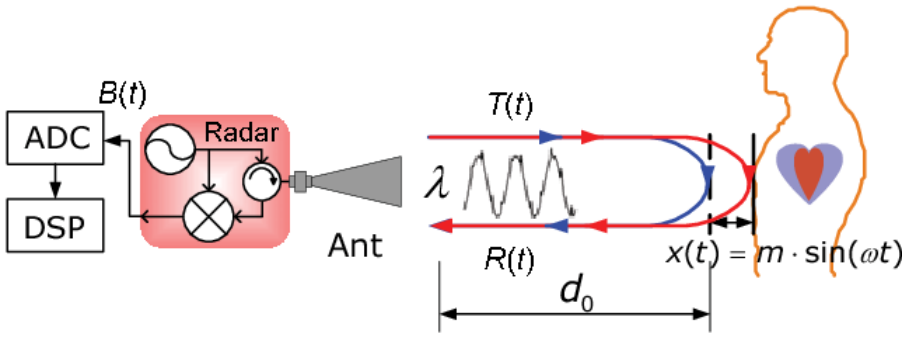


Figure 2.3: Doppler radar for heart rate monitoring [20].

Other technologies are also used in this area, namely in [21] with the use of a reclining chair with two accelerometers placed in order to detect the patient's vital signs in a non-invasive way. Another example is presented in [22], using video surveillance and photoplethysmography techniques, which made it possible to extract the patient's heart rhythm.

### 2.2.2 On-Body antennas

On-Body antennas can be used to monitor the heart rate (HR) and respiratory rate (RR). These types of antennas can be attached directly to the skin or embedded in clothes, making its usage more comfortable and less invasive in comparison with the most traditional methods. This approach is much more accurate and requires significantly less power than the Doppler radars [5]. For instance, the antenna can be embedded in the clothes worn by elderly people who need a continued care at home, allowing their caregiver to better monitor the patient's health. In [23] it is presented a review of wearable and body mounted antennas designed and developed for various applications, at different frequency bands, which were made in the last decade. The authors in [11] and in [5] came to the conclusion that it is possible to obtain the HR and RR when the antenna is placed in contact with the patient's skin. This is possible using the phase analysis of $S_{11}$ parameter (reflection coefficient). The main obstacle of using these antennas is the impact produced by the human body on the antenna matching. As we all know no one is equal to anyone else, so each person will have a different physical stature. For example, a man's chest has a thicker muscle mass than a woman's [24]. These conditions will change the behavior and matching of the antenna (this topic will be discussed in more detail later in the document). There is a lack of information on this topic, making it difficult to standardize this type of antennas, which are the focus of this dissertation.

#### 2.2.2.1 Type of On-Body antennas for vital sign monitoring

Considering the different antennas types available, it is necessary to check which is the most suitable for monitoring vital signs working in contact with the patient's body. The main parameters that must be considered during the design of an antenna is the bandwidth, the return losses, gain, impedance, directivity, polarization, and efficiency [25]. These parameters will have to be adapted according to the target application. Based on the study done in [5], eight different types of antennas were tested regarding its usage as a vital sign detector, of which, seven are narrowband and one broadband (Figure 2.4a. High bandwidth can be a factor to help maintain the matching on On-Body antenna. As addressed in [26], when placed close to the body, narrowband antennas, suffer a large deviation in the resonance frequency. Although the same happen to wideband antenna, they remain between reasonable matching levels. The antennas used in [5] are presented below and shown in Figures 2.4a to 2.4h:

- CPW planar monopole (CPWM) (Figure 2.4a);
- Coplanar waveguide 3d monopole antenna (CPW3dM) (Figure 2.4b);
- Dipole antenna (Figure 2.4c);
- Loop antenna 1 (loop1) (Figure 2.4d);
- Patch Antenna (Figure 2.4e);
- Loop Antenna 2 (loop2) (Figure 2.4f);
- 3d Monopole Antenna (3dM) (Figure 2.4g);
- Inverted F antenna (IFA) (Figure 2.4h).

To perform this test, all antennas were placed on subjects, and vital signs were measured using a VNA (Vector Network Analyzer). The subjects were also hooked up to an ECG and a respiratory monitoring belt, in order to obtain heart rate and reference respiratory movements. Narrowband antennas operated in the 2.45 GHz ISM band, with the UWB antenna operating in the 3.1 - 10.6 GHz frequency range. The obtained results are shown in Table 2.1. By analyzing, it is possible to verify that the antennas that had a better performance regarding precision and Signal to Noise Ratio (SNR) were the IFA, Loop1, CPWM loop antenna 2 and patch antenna radiating to chest.

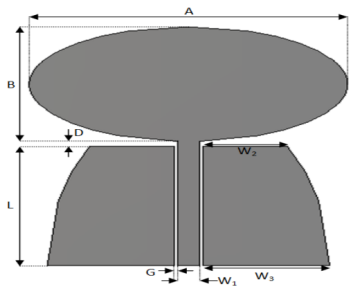


(a) Wideband antenna monopole [5];

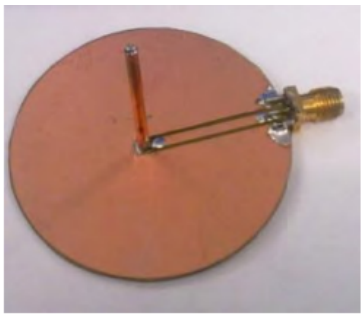

(b) CPW3dM [5];

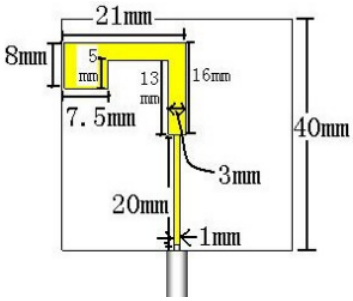


(c) Dipole antenna [5];

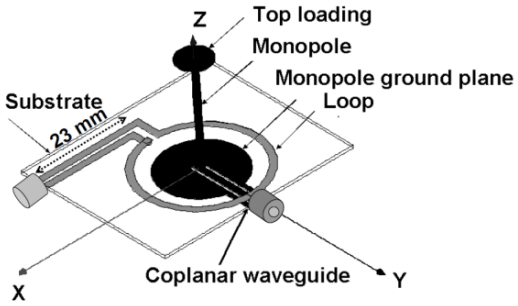


(d) Loop antenna [5];

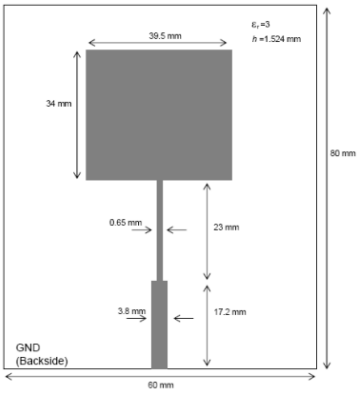


(e) Patch antenna [5];

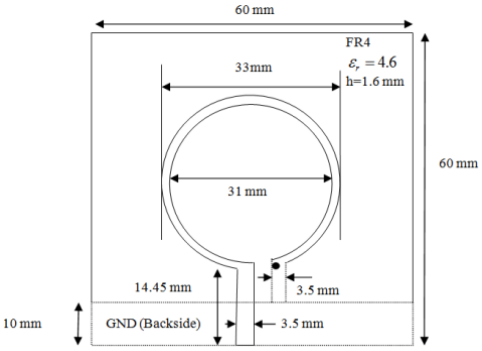


(f) Loop antenna 2 [5];

(g) 3d Monopole Antenna [5];

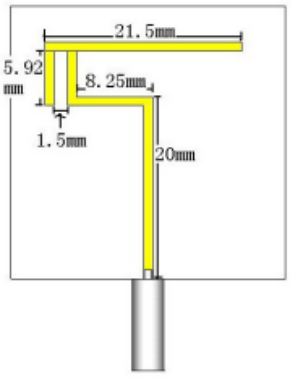


(h) Inverted f antenna [5];

Table 2.1: Statistical analysis of heart rate from ECG and On-Body Monitor for tested antennas [5].

| Antenna Type | IFA | CPW3dM | Dipole | Loop1 | PatchR | PatchG | Loop2 | 3dM | CPWM |
|---|---|---|---|---|---|---|---|---|---|
| SNR (dB) | 1.113 | 0.8188 | 0.6174 | 1.3735 | 1.2937 | 0.6266 | 1.06 | 0.6879 | 1.3223 |
| Accuracy (%) (within 1BPM) | 98 | 72.11 | 34.5 | 98.6 | 96.4 | 24.1 | 92.9 | 57.7 | 95.9 |
| Accuracy (%) (within 2BPM) | 100 | 75.1 | 44.9 | 100 | 99.66 | 33 | 96.94 | 70.58 | 99.8 |
| Accuracy (%) (within 3BPM) | 100 | 75.1 | 48.8 | 100 | 100 | 39.3 | 98.3 | 74 | 100 |
| Accuracy (%) (within 4BPM) | 100 | 79.3 | 51.2 | 100 | 100 | 43.7 | 98.5 | 75.7 | 100 |
| Accuracy (%) (within 5BPM) | 100 | 82.1 | 56 | 100 | 100 | 49.1 | 98.6 | 76.4 | 100 |
| ECG Heart Rate (BPM) | 70.52 | 77.9 | 75.92 | 75.23 | 76.37 | 79.4 | 88.12 | 80.18 | 87.38 |
| On-Body Heart Rate (BPM) (BA) | 70.37 | 75.84 | 76.7 | 75.1 | 76.21 | 73.34 | 87.64 | 76.32 | 87.16 |
| Mean Diff (BA) | 0.145 | 2.0641 | -0.7804 | 0.1372 | 0.1554 | 6.0548 | 0.617 | 3.8607 | 0.2166 |
| Standard Deviation (BA) | 0.4347 | 4.3185 | 9.0052 | 0.3862 | 0.4701 | 8.0829 | 3.8279 | 6.9860 | 0.4301 |
| d+1.96 Sd (BA) | 0.99 | 10.53 | 16.87 | 0.89 | 1.08 | 21.9 | 8.12 | 17.55 | 1.06 |
| d-1.96 Sd (BA) | -0.71 | -6.4 | -18.43 | -0.62 | -0.77 | -9.79 | -6.88 | -9.89 | -0.63 |

This results shows that antennas with larger ground plane have a better performance. The reason for that better performance is that the antenna electric fields are concentrated in between the radiating element and the ground plane. If the ground plane is not present, these fields easily couple with the chest and the antenna's reflection coefficient becomes more sensitive to chest movements [5]. For instance, for the Patch Antenna and the Loop Antenna cases, it is possible to observe that, despite the Loop Antenna have better results, the ground plane of the Patch Antenna adds additional protection regarding the detection of unwanted movements that may influence the reflection coefficient [5]. It is then possible to conclude that a ground plane that covers the entire antenna presents itself as a fundamental characteristic in antennas for vital signs monitoring.

In [7] is address the use of monopoles and patch antennas for measuring vital signs in contact with the human body. Three antennas were used: one monopole working at 370 MHz and two patch antennas working at 900 MHz and 1.5 GHz, respectively. A VNA was used to measure the vital signs, like is shown in Figure 2.5. The 3 antennas were placed parallel to the chest in order to monitor vital signs, the monitoring was achieved through the analysis of the reflection coefficient phase. The author concluded that, with well-adapted antennas, it is possible to detect heart and respiratory rate.

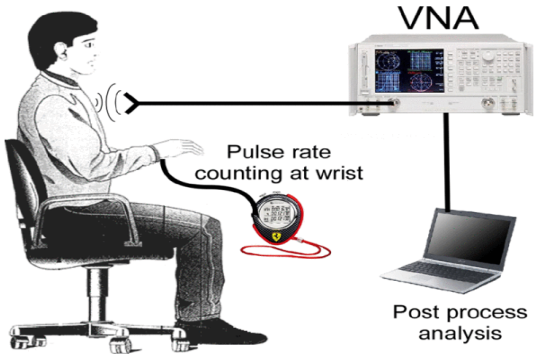


Figure 2.5: Experimental setup for the cardiopulmonary measurements.[7].

### 2.2.3 On-body patch antenna

With the need to keep the antenna matching in contact with the body, it is then necessary to choose the ideal antenna type for this purpose. The antenna must not only work in contact with the body, but also be able to detect the person's vital signs. As discussed in the section 2.2.2.1 there are several types of antennas that meet these requirements. It should be noted that some characteristics have proven to be fundamental to the proper functioning of the antenna, namely the ground plane. Therefore, considering the performance, reasonable size, planar nature and better isolation from unwanted movements, microstrip patch antenna with radiating element towards the skin was chosen to be the selected approach to monitor vital signs. An example of a patch antenna is shown in Figure 2.6.

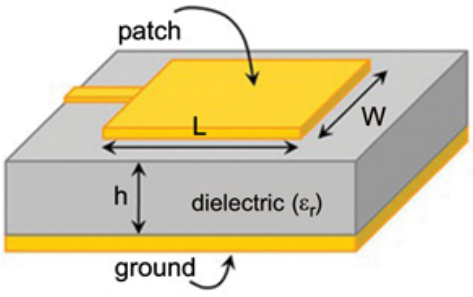


Figure 2.6: Example of a patch antenna [27].

### 2.2.4 Working frequency selection

As mentioned in [5] it is possible to use several antennas regarding the detection of vital signs when the antenna is placed on the human body. The authors have concluded that the patch antenna produced the better overall results, being the most viable to use.

It is then necessary to ensure that the antenna operates in an appropriate frequency band, since the frequency is relevant in the detection of vital signs. This is what will vary the reflection coefficient more or less sensitively, depending on the movement caused by breathing and the heartbeat [5]. Although with increasing frequency the penetration of electromagnetic waves is greater, the noise at high frequencies is also greater, and is an obstacle in the capture of vital signs [5]. To choose the working frequency of the antenna, it is necessary to take into account which frequencies can be used, that is, whether or not they belong to the ISM band (Industrial, Scientific and Medical Applications). According with ANACOM, there are a few frequency bands already tested that can be used to ISM applications in Portugal [28]. In [5] were tested the 2.4-2.5 GHz and 5.725-5.925 GHz bands, where the author concluded that the 2.45 GHz resonance frequency it is the proper one to use regarding the detection of vital signs using an antenna in contact with the human body. From the same author of [5], in [29] the use of antennas normally used for on body wireless body area networks such as dipole, monopole, loop and patch, etc. were tested to monitor vital signs, with the help of a VNA. The author carried out measurements for different frequencies, verifying which one has the highest accuracy. As shown in Table 2.2, the studied antennas behave better at 2.45 GHz, with the author mentioning that this is due to harmonic and intermodulation interference between the breathing and heart beating frequencies is higher at higher frequencies.

Table 2.2: Frequency vs. Accuracy when detecting vital signs [29].

| Frequency (GHz) | 2.45 | 3.5 | 5.8 | 7.5 | 9 |
|---|---|---|---|---|---|
| Accuracy | 100% | 95.7% | 76.1% | 74.8% | 53.4% |

### 2.2.5 Influence and challenges imposed by the human body

As mentioned in the subsection 2.2.2, the presence of the human body will cause the antenna to mismatch, making it impossible to use normal antennas for On-Body applications. This mismatching can be verified through the variation of the resonant frequency of the antenna. To counteract the mismatching suffered it will need to make some adjustments to the antenna architecture. Propagation on the human body creates a new challenge for the antenna design, because the human body is a very complex environment (lossy, dispersive, and inhomogeneous). Under these circumstances, anticipating and understanding the antenna behavior becomes difficult. To understand how a signal can propagate in different layers of tissues such as skin, fat tissue, muscle and so on. Each of these different layers have different dielectric properties, which can

vary with the frequency, temperature, and humidity [24]. The dielectric parameters of the human tissues change with the frequency, as can be seen in Table 2.3. As shown in Table 2.3, relative permeability ($\epsilon_r$) and conductivity ($\sigma$) are inversely proportional with increasing frequency. These properties also change according with the patient. The results of age's influence can be found in [24].

Table 2.3: Dielectric proprieties for different parts of the human body [24].

| Frequency (MHz) | Dielectric Prop. | Skin | Fat Tissue | Brest Tissue | Muscle | Bone | Nerves | Cerebrospinal fluid | Heart |
|---|---|---|---|---|---|---|---|---|---|
| 236 | $\epsilon_r$ | 53.0 | 11.9 | 5.57 | 59.3 | 13.7 | 38.5 | 74.9 | 72.6 |
| | $\sigma$ | 0.61 | 0.07 | 0.03 | 0.75 | 0.08 | 0.4 | 2.2 | 0.86 |
| 350 | $\epsilon_r$ | 45.8 | 11.6 | 5.5 | 56.8 | 13.0 | 34.9 | 70.5 | 65.0 |
| | $\sigma$ | 0.71 | 0.08 | 0.04 | 0.81 | 0.1 | 0.46 | 2.26 | 0.99 |
| 900 | $\epsilon_r$ | 41.4 | 11.3 | 5.42 | 55.0 | 12.5 | 32.5 | 68.6 | 59.9 |
| | $\sigma$ | 0.87 | 0.11 | 0.05 | 0.94 | 0.14 | 0.57 | 2.41 | 1.23 |
| 1500 | $\epsilon_r$ | 39.4 | 11.1 | 0.05 | 0.94 | 0.13 | 0.57 | 2.41 | 1.23 |
| | $\sigma$ | 1.07 | 0.16 | 0.08 | 1.19 | 0.23 | 0.74 | 2.72 | 1.57 |
| 1800 | $\epsilon_r$ | 38.9 | 11.0 | 5.27 | 53.6 | 11.8 | 30.9 | 67.2 | 56.3 |
| | $\sigma$ | 1.18 | 0.19 | 0.09 | 1.34 | 0.28 | 0.84 | 2.92 | 1.77 |
| 2450 | $\epsilon_r$ | 38.0 | 10.8 | 5.15 | 52.7 | 11.4 | 30.2 | 66.2 | 54.8 |
| | $\sigma$ | 1.46 | 0.27 | 0.14 | 1.74 | 0.39 | 1.09 | 3.46 | 2.26 |
| 5800 | $\epsilon_r$ | 35.1 | 9.86 | 4.5 | 38.5 | 9.67 | 27.2 | 60.5 | 49.0 |
| | $\sigma$ | 3.72 | 0.83 | 0.42 | 4.5 | 1.15 | 2.94 | 7.84 | 5.86 |

#### 2.2.5.1 Human Body Models

One of the main challenges that this method can face is the fact that no human body is equal, so an antenna working for one person may not work if it was used on another person. Thus, creating a generic on-body antenna is a difficult challenge. Depending on the intended location of the antenna, different models for the human body should be taken into account, as the different layers will have different thicknesses and electrical properties [30]. For simulation purposes an On-Body system for vital signs monitoring can be simplified by the model shown in Figure 2.7a. This simple model can be used for simulations when placing the antenna on the patient's chest or back and consists of 4 layers, skin, adipose tissue, muscle and bone. A representative circular model of the human body can also be used, represented in the Figure 2.7b, although for this project this model will not be considered, as it is not suitable for the human chest. The thickness of the models is shown in table 2.4.

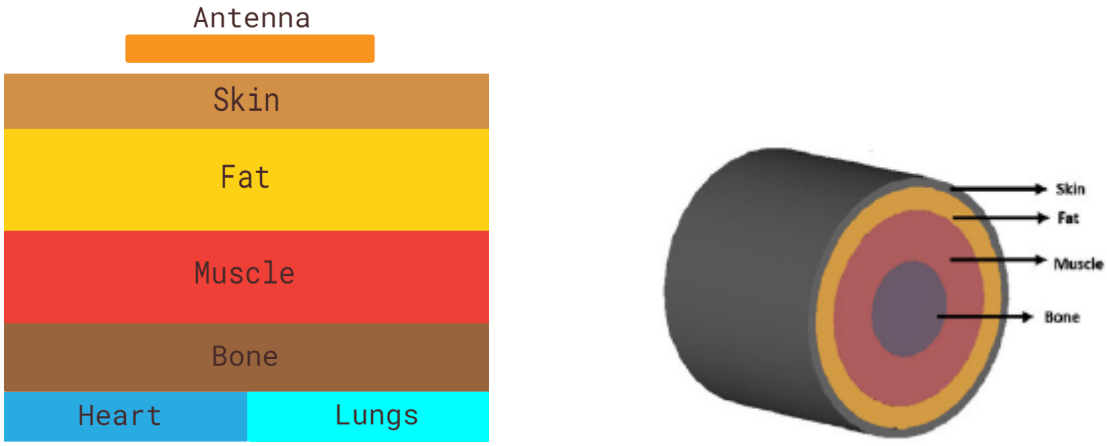


(a) Layered chest model; (b) Circular model [31];

Figure 2.7: Layered human body models.

Table 2.4: Thickness of the different tissues [30], [32], [33], [34], [35].

| Location | Tissue | Thickness (mm) | Total Thickness (mm) |
|---|---|---|---|
| Chest | Skin | 3.60 | 79 - 99 |
| | Fat | 7 - 27 | |
| | Muscle (front) | 15 - 35 | |
| | Muscle (back) | 8 - 28 | |
| | Bone | 25.40 | |
| Arm | Skin | 1.11 - 2.90 | 73.41 - 94.3 |
| | Fat | 0.4 - 33.50 | |
| | Muscle | 32 - 46 | |
| | Bone | 25.9 | |
| Thigh | Skin | 0.60 - 3.30 | 70.15 - 75.87 |
| | Fat | 3.65 - 9.87 | |
| | Muscle | 35.7 - 38.7 | |
| | Bone | 27.2 | |
| Abdomen | Skin | 1.30 - 3.30 | 78.95 - 100.11 |
| | Subcutaneous Fat | 19 - 41 | |
| | Visceral Fat | 36 - 58 | |
| | Muscle | 2.31 - 5.15 | |
| | Small Intestine | 2.2 - 4 | |
| | Visceral Fat 2 | 5.3 - 6 | |

As shown in Table 2.4, it is not possible to consider a fixed thickness for the models of the human body, as each person will have their own physical characteristics, and it is necessary, among other things, to adapt the resonance frequency of the antenna. A study on the ideal frequencies to be used for the different models is addressed in [32], with several simulations being carried out for different thicknesses of the human chest model, reaching the conclusion that the use of a frequency between 0.5 and 0.9 GHz would achieve good results when propagating in the human body.

With the goal of this project focused on standardizing the antenna for any body type

and consequent detection of vital signs, it is necessary to ensure that the model used is as real as possible. Although the CST Suite Studio software has phantoms of the human body, the high computational capacity required makes its use an obstacle. It was possible to conclude that the use of simplified models, as presented in Figure 2.7, can be enough, as long as they are built in a way that replicates the human body as much as possible, namely its dielectric characteristics, different thicknesses and elements.

### 2.2.6 Antenna matching to the human body

To counteract the strong influence of the human body, it is necessary to ensure the proper functioning of the antenna in contact with it. In [36], the author designs and simulates a patch antenna based on LTCC (Low-Temperature Cofired Ceramic) substrate for medical use which is shown in Figure 2.8. As can be seen from the observation of Figure 2.8, it is a complex antenna. The use of several slots in the patch as well as the presence of a superstrate guarantee the matching of the antenna with the presence of the human body. The superstrate is a dielectric material, supported on the surface of the radiant element, which protect the antenna and cause changes in efficiency, gain and on the antenna impedance, helping its matching as well [37]. Their use is fundamental since superstrates allow for a much smoother transition of propagation medium, essential to combat the large dielectric differences between the antenna and the human body.

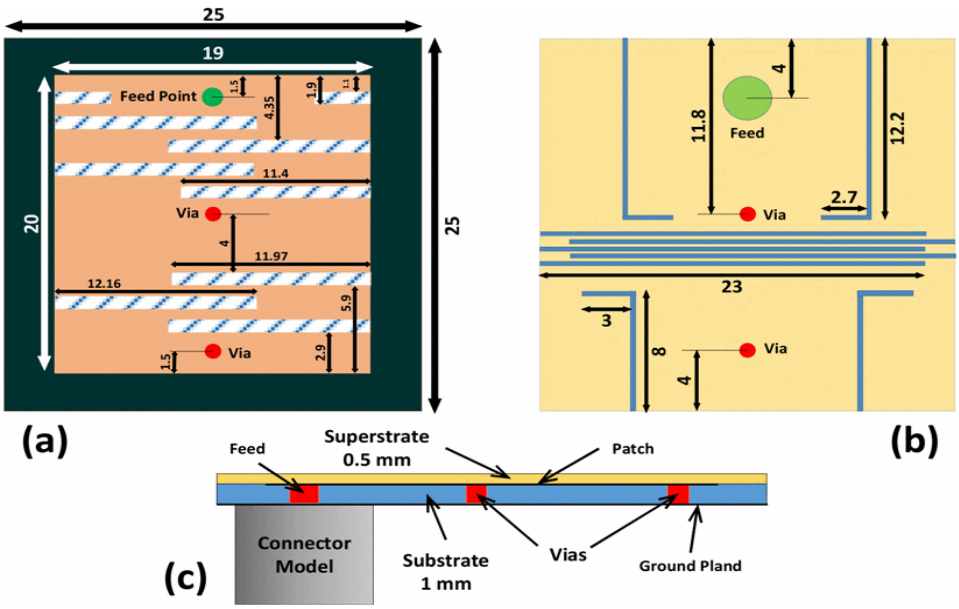


Figure 2.8: Proposed antenna geometry: (a) Top view of patch. (b) Bottom view shows slots on ground plane. (c) Side view shows feed location and vias.[36].

The high degree of complexity of the antenna shown in Figure 2.8 can be an obstacle to its replication and practical use. In [38] a simplification of the antenna previously presented is made and it is presented in Figure 2.9.

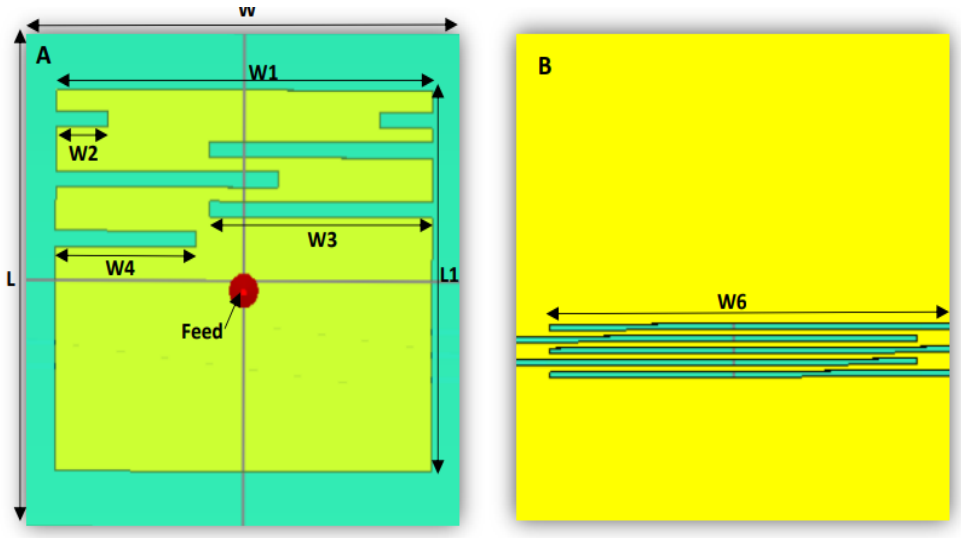


Figure 2.9: Patch and final ground plan design [38].

In the design of this antenna, a DuPont 951 LTCC substrate was initially used. Despite the increased use and advantages of LTCC technology, its rigorous manufacturing method causes problems in its use [39]. Considering this, the author used the Rogers RO4360G2 substrate. The differences between both substrates are shown in Table 2.5. For both studies, the same frequency band was used (ISM 915 MHz), they also used the same human body model during the antenna design, which is a multi-layer model (the possibility of using other models of the human body as well as their properties will be addressed later). From the work done by the authors of both works, it is possible to conclude that the use of superstrates proved to be a determining factor in maintaining antenna matching in the presence of the human body [36], [38].

Table 2.5: Antenna dimensions with Rogers RO4360G2 substrate and DuPont 951 LTCC substrate, in milimeters [38].

| Antenna | W | W1 | W2 | W3 | W4 | W6 | L | L1 | Feed | Superstrate Thickness |
|---|---|---|---|---|---|---|---|---|---|---|
| DuPont 951 LTCC | 25 | 21.5 | 3 | 12.7 | 8 | 23 | 25 | 19.2 | 9.1 | 1.5 |
| Rogers RO4360G2 | 25 | 21.8 | 3 | 13.8 | 7 | 23 | 25 | 22.6 | 14 | 1.62 |

These antennas will also have to have an additional protection in order to prevent to damage the user's skin. In [40] the authors created a patch antenna capable of operating in the vicinity of the human body. Its architecture allows its use on different parts

of the body thanks to its construction through multiple layers, ideal for use on more curvilinear body surfaces (per example, the women's chest) as shown in the Figure 2.10. The antenna shown in Figure 2.10 has a layer on the surface of the antenna that is in contact with the human body, increasing the antenna's energy efficiency. Although the initial use of this antenna is not for the detection of vital signs, its architecture as well as the lower layer that protects the human body are characteristics that can help when sizing and matching the antenna.

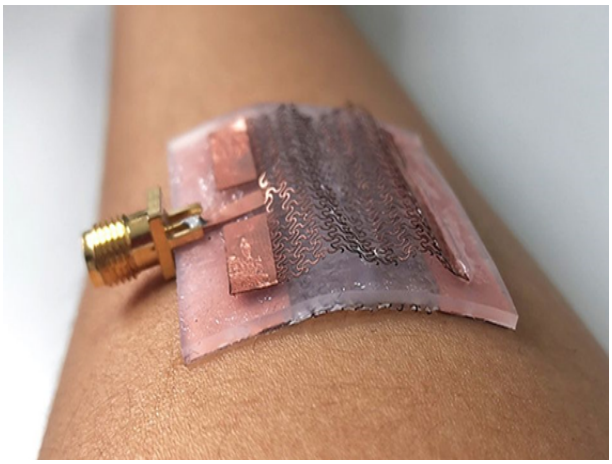

Figure 2.10: Wearable antenna built in layers [40].

### 2.2.7 Wideband patch antennas

There are numerous and well-known methods to increase the bandwidth of antennas, including increase of the substrate thickness [41], the use of a low dielectric substrate [41], the use of various impedance-matching and feeding techniques [42], the use of multiple resonators [43], and the use of slot antenna geometry [44]. However, the bandwidth and the size of an antenna are generally mutually conflicting properties, that is, improvement of one of the characteristics normally results in degradation of the other. A useful approach to design a microstrip antenna with both small patch size and high bandwidth was to fill in the volume between the patch and ground plane with magneto-dielectric material, whose permeability and permittivity are both larger than one [45, 46], as can be seen in Figure 2.11a. The basic principle of this approach is that the enhanced magnetic response of magneto-dielectric material lowers the quality factor of patch antenna while its refractive index lowers the resonant frequency as pure dielectric material does [46].

U-shaped patching is also a possible technique to increase bandwidth. In [47] a U-shaped patch antenna is developed, as shown in Figure 2.11b with the author achieving a 27.3% increase in antenna bandwidth at 5.5 GHz. In [48] an antenna with the U-shaped patch is also developed achieving an increase in bandwidth of approximately 20%. In [49] the author proposes an antenna model with a wider bandwidth while maintaining reasonable dimensions by clipping a small trapezoid, as shown in Figure 2.11c, thus creating a second resonance and increasing the bandwidth. In [50] the concept of parasitic patches is introduced as a way to increase bandwidth. The parasitic patches will overlap the main patch (radiating element), as shown in Figure 2.11d, creating a second.

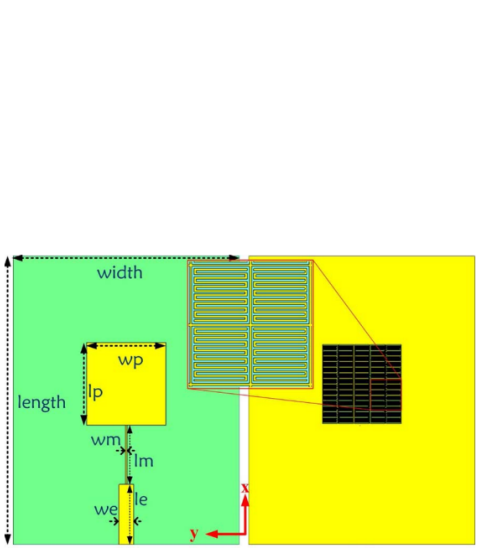


(a) Magnetic dielectrics [46];

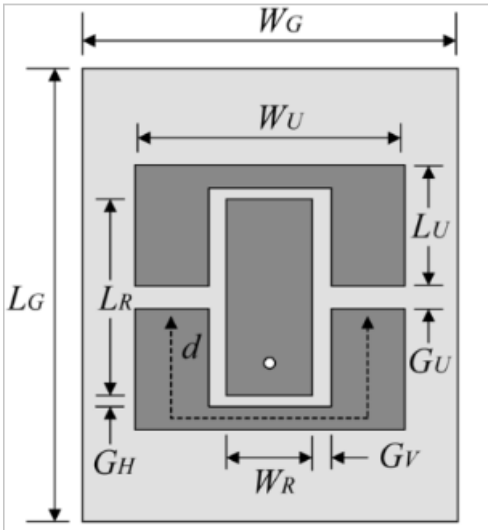


(b) U-Shape antenna [47];

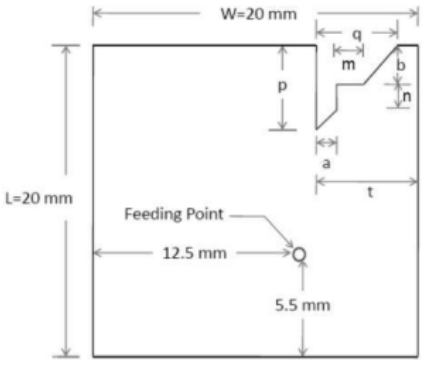


(c) Cropped patch antenna [49];

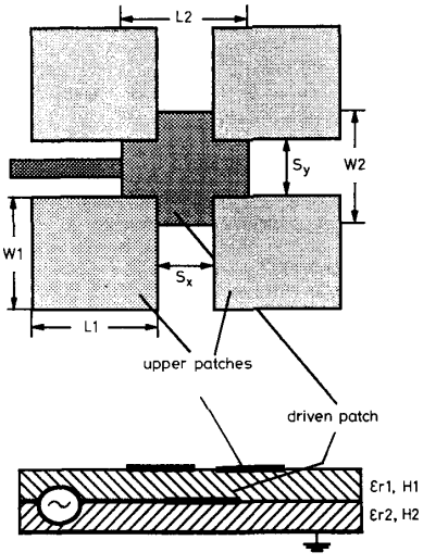


(d) Parasitc patch antenna [50];

Figure 2.11: Bandwidth increase techniques.

## 2.3 State of art conclusions

In this chapter it was intended to perform a literature review on the use of antennas for monitoring vital signs in contact with the human body. Initially a comparison was made between several types of antennas, taking into account their behavior with the human body. Next was addressed the biggest obstacle to the operation of on-body antennas, the human body, with the dielectric properties and characteristics of each layer presented. Finally were presented the characteristics that allow these antennas to work in contact with the human body. In an attempt to achieve a standard model, capable of withstanding the variations caused by different human bodies, bandwidth augmentation presented itself as an option, and its techniques were studied and presented. It was concluded that antennas with a larger ground plane (covering the entire antenna) perform much better compared to antennas with a smaller ground plane, thus becoming a key characteristic in the antenna. The human body presents itself as a factor that causes a great mismatching in the antenna, a mismatching that can be cancelled with the use of slots and/or superstrates. These last is fundamental for the antenna to operate in contact with the human body.

# 3

# On-body antenna design for vital signs monitoring

This chapter will introduce the antenna that will be used in this project as well as all the stages of its development to achieve the goal of detecting vital signs in contact with the body.

## 3.1 Considerations for the microstrip patch antenna design

When sizing an antenna, it is necessary to take into account several parameters so that the antenna is working for the desired frequency. The objective will be to obtain the best possible value (theoretically -$\infty$) for the reflection coefficient, in order to guarantee the antenna matching for a specific frequency. The patch width was calculated using equation (3.1) [51].

$$W = \frac{c}{2 \times f_r \times \sqrt{\frac{\epsilon_r + 1}{2}}} \tag{3.1}$$

Where:

$W$ = Patch width;

$c$ = Speed of light;

$f_r$ = Resonance frequency;

$\epsilon_r$ = Relative electrical permittivity of the patch substrate;

Ideally, in a microstrip antenna, the electric field lines between the patch and the ground plane run through the substrate. However, at the boundaries of the patch, due to its finite size, these electromagnetic waves simultaneously pass through the air and the substrate, creating the so-called fringe effect represented by Figure 3.1. With this it becomes necessary to treat these two media as one, homogenizing the permittivity of both layers, now given by the parameter $\epsilon_r$ expressed by equation (3.2), with the relation $\frac{W}{h} > 1$, since it is intended that radiation is more predominant than transmission.

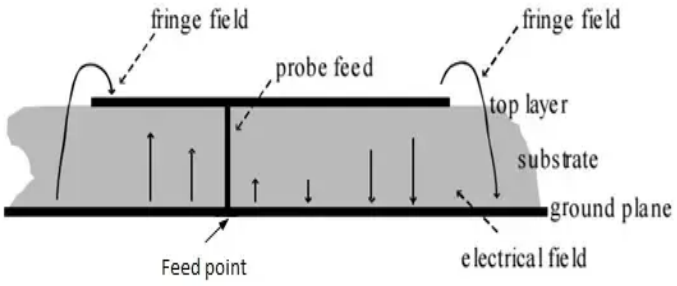


Figure 3.1: The fringe effect [51].

$$\epsilon_{ref} = \frac{\epsilon_r + 1}{2} + \frac{\epsilon_r - 1}{2} \times (1 + 12 \times \frac{h}{W})^{-\frac{1}{2}} \tag{3.2}$$

Where:

$h$ = substrate height;

After considering the air and the dielectric as one medium, it is possible to calculate the effective wavelength ($\lambda_{eff}$), given by the equation (3.3) [51].

$$\lambda_{eff} = \frac{c}{f_r \times \sqrt{\epsilon_{ref}}} \tag{3.3}$$

By standard, the effective patch length is half the effective wavelength ($L_{eff}$), as shown in the equation (3.4) [51].

$$L_{eff} = \frac{\lambda_{eff}}{2} \tag{3.4}$$

Due to the fringe effect, the electric field lines at the edges of the patch have a curved effect, which makes the dimensions of the patch appear larger than they actually are. It is therefore necessary to remove this contribution, thus obtaining the effective length. The fringe effect contribution is calculated using the equation 3.5 [51].

$$\Delta L = 0.412h \times \frac{(\lambda_{eff} + 0.3) \times (\frac{W}{h} + 0.264)}{(\lambda_{eff} - 0.258) \times (\frac{W}{h} - 0.8)} \tag{3.5}$$

Finally, the two contributions (since this effect occurs at both the upper and lower ends of the patch) of the fringe effect are then removed, thus obtaining, by the equation 3.6, the effective length of the patch [51].

$$L = L_{eff} - 2 \times \Delta L \tag{3.6}$$

### 3.1.1 Considerations on microstrip patch antenna feeding

The radiating element has different input impedance at different feed locations. Thus, the maximum impedance are at the extremes of the patch and the minimum at $\frac{\lambda}{4}$ of the end of the patch as shown in Figure 3.2, assuming $L \approx \frac{\lambda}{2}$, where $\lambda$ is the wavelength at the substrate. Thus, the approximate value of the input impedance ($Z_{in}$) can be calculated by equation (3.7) [51].

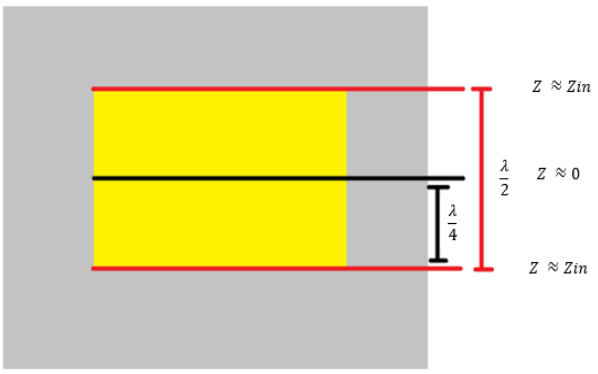


Figure 3.2: Patch impedance [51].

$$Z_{in} = \frac{60 \times \lambda_0}{W} \tag{3.7}$$

Where:

$\lambda_0$ = Wavelength in vacuum;

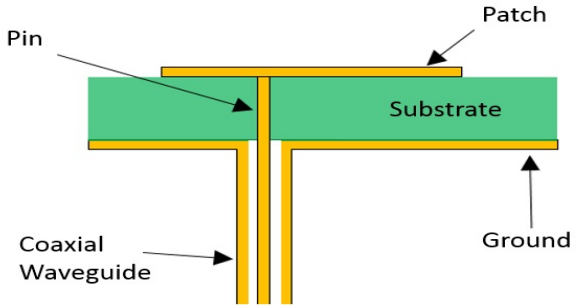


(a) Illustration of a patch antenna with coax feeding [53];

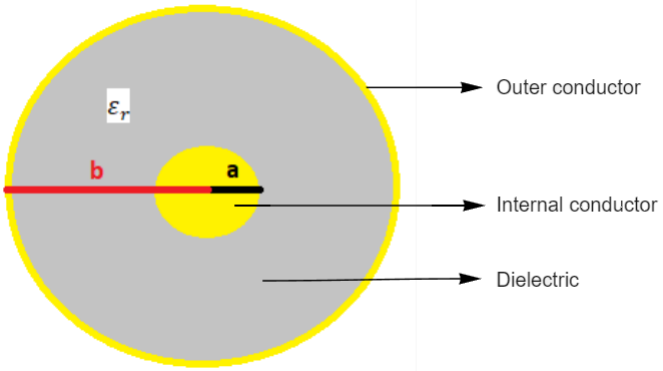


(b) Coaxial feeding schematic:

Figure 3.3: Coaxial cable description.

The antenna input impedance $Z_{in}$ must be made at the location where the input impedance of the patch equals the characteristic impedance $Z_0$ of the feed element. This value is normally 50 Ω, and this is the value used.

There are four types of the feeding techniques and they are coaxial probe, microstrip line, aperture coupled and proximity coupled [52]. For this project a coaxial feed was chosen, because in this type of feed it is easy to achieve very good approximations between the characteristic and input impedance. The coaxial cable consists of an inner conductor, a dielectric, and an outer conductor. The inner conductor is in direct contact with the patch, while the outer connector is in contact with the ground plane, as shown in the Figure 3.3a as well as its internal view in Figure 3.3b.

In order to match the feed impedance with the antenna input impedance, and thus obtain the best possible matching, it is necessary to dimension the diameters of the inner conductor and the dielectric, in this case Teflon with $\epsilon_r$ = 2.1, using the equation (3.8).

$$Z_0 = \frac{60}{\sqrt{\epsilon_r}} \times \ln(\frac{b}{a}) \tag{3.8}$$

Where:

$Z_0$ = Characteristic impedance of the coaxial cable;

$\epsilon_r$ = relative electrical permittivity of the coaxial dielectric;

$a$ = Radius of the coaxial outer conductor;

$b$ = Radius of the coaxial internal conductor;

Obtaining values of a = 0.635 mm and b = 2.12 mm.

### 3.1.2 Design of a patch antenna with CST

After choosing the patch antenna to be used as well as its operating frequency, 2.45 GHz, the CST Studio Suite simulation software was used to perform the simulations of the previously sized antenna. The antenna was first simulated to operate in free space. A ROGERS RO4360G2 substrate was used since it is the substrate with the highest electrical permittivity, thus providing an easier fit next to the body due to the high electrical permittivity of the skin. The substrate has a thickness of 0.81 mm (manufacturer's defined measurement), electrical permittivity $\epsilon_r = 6.15$ and loss tangent $\tan\delta = 0.0038$ at 10 GHz. The antenna matching started with the parameters obtained in the theoretical computations. Then, some adjustments were made to the dimensions of the patch and the feed point in order to have the best possible matching to the desired frequency. For the first antennas sized, namely for free space and simpler body models a discrete port was used for simplicity reasons, this type of feed simulates the behavior of a coaxial cable model. In final versions of the antenna a coaxial feed was introduced. The antenna obtained in simulation is shown in Figure 3.4. The parameter Fp indicates the feed position of the antenna relative to the bottom edge of the patch. In Table 3.1 the results obtained theoretically and by simulation for the antenna dimensions are presented.

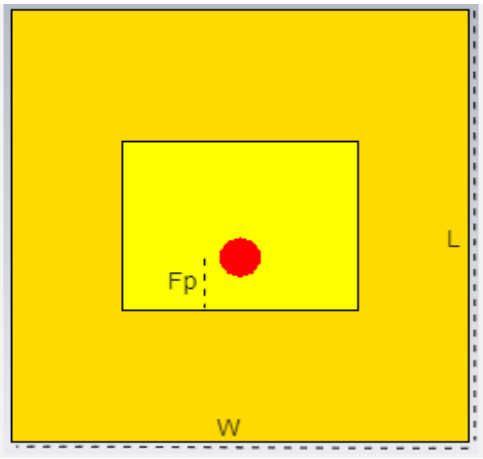


Figure 3.4: Single microstrip patch antenna to operate in free space.

Table 3.1: Patch dimensions

| | Theoretical (mm) | Simulated (mm) |
|---|---|---|
| W | 31.82 | 30.85 |
| L | 23.795 | 23.526 |
| FP | 6.2439 | 7.43 |

In order to achieve a matching antenna for the desired frequency, it was necessary to vary the patch dimensions. To do this it is necessary to understand the behavior of the antenna when its parameters are varied. In Figure 3.5a it is possible to verify that with the variation of the patch length occurs a displacement of the resonance frequency. The variation of the patch width, shown in Figure 3.5b, causes variations in the resonance frequency but much smaller than through the variation of the length, having its greatest influence on the value of the magnitude of the reflection coefficient. As discussed in section 3.1.1, it is necessary to match the impedance of the feed with that of the antenna (in this case 50 Ω). For that it is necessary do adjust the Fp to achieve the matching between both impedance. In Figure 3.5c is shown that a variations on the Fp causes the magnitude of the $S_{11}$ parameter to vary a lot, with its variations being a central point in the antenna matching.

As can be seen from Figure 3.6 the antenna presents an excellent matching at the frequency desired.

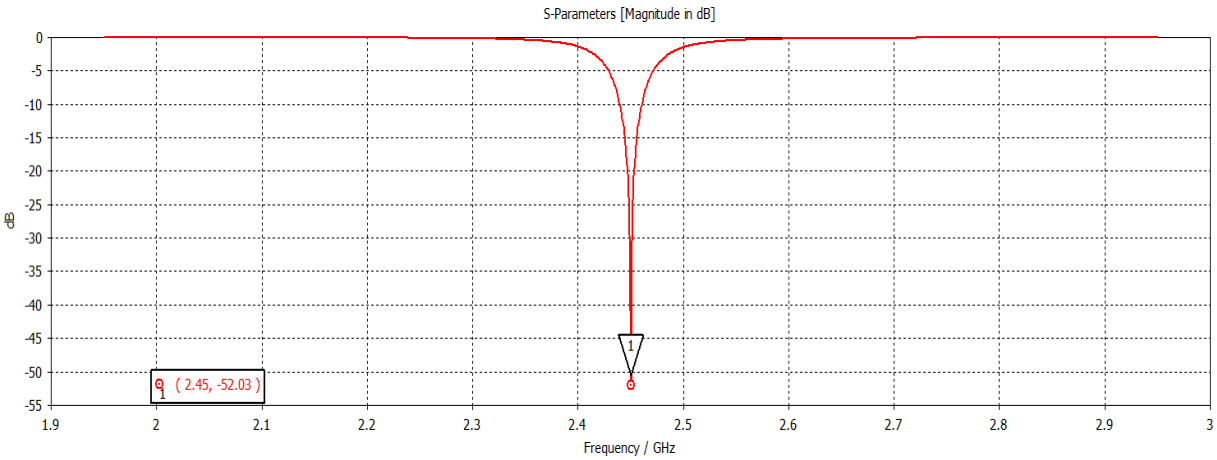


Figure 3.6: Reflection coefficient in free space.

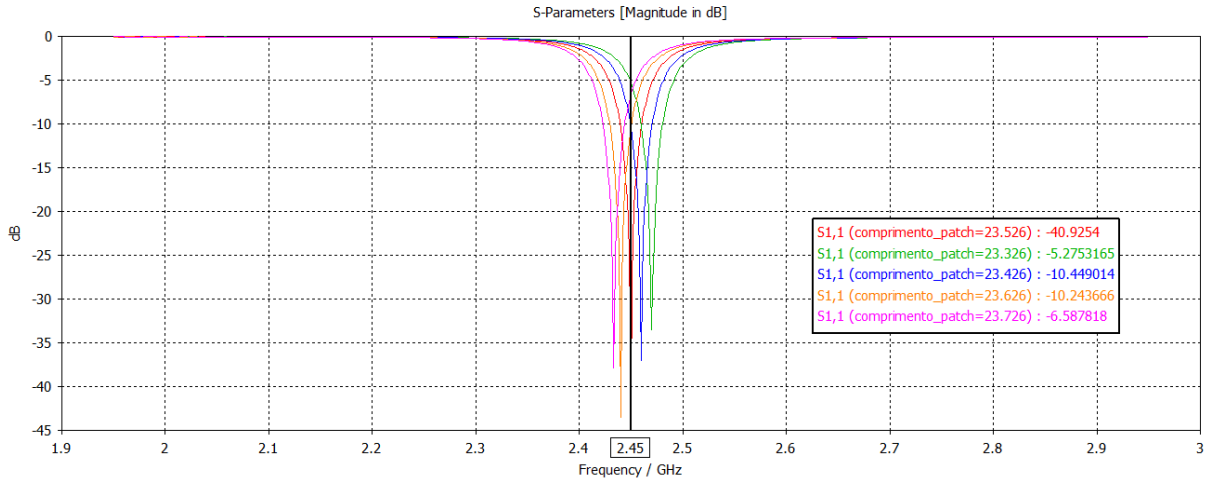


(a) in function of L;

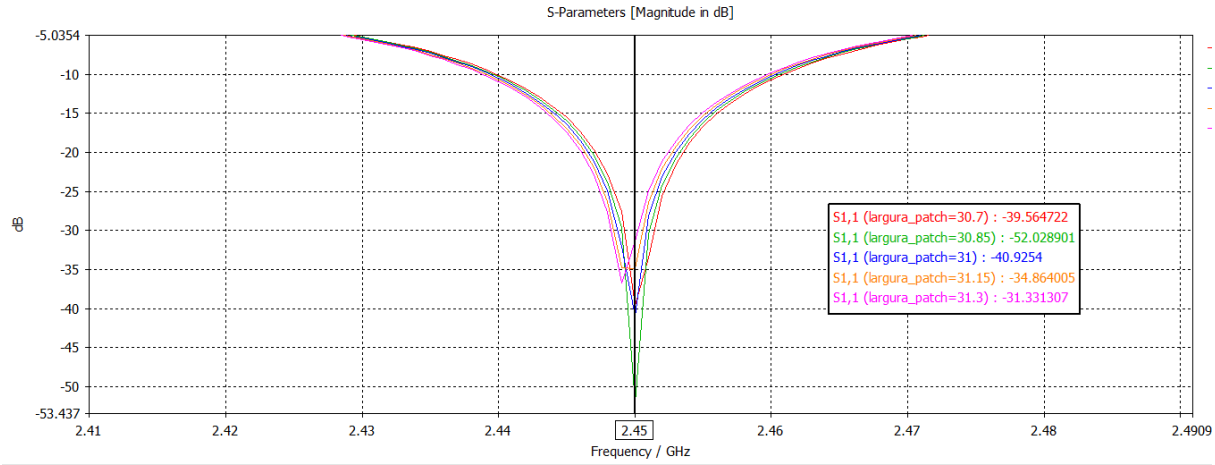


(b) in function of W;

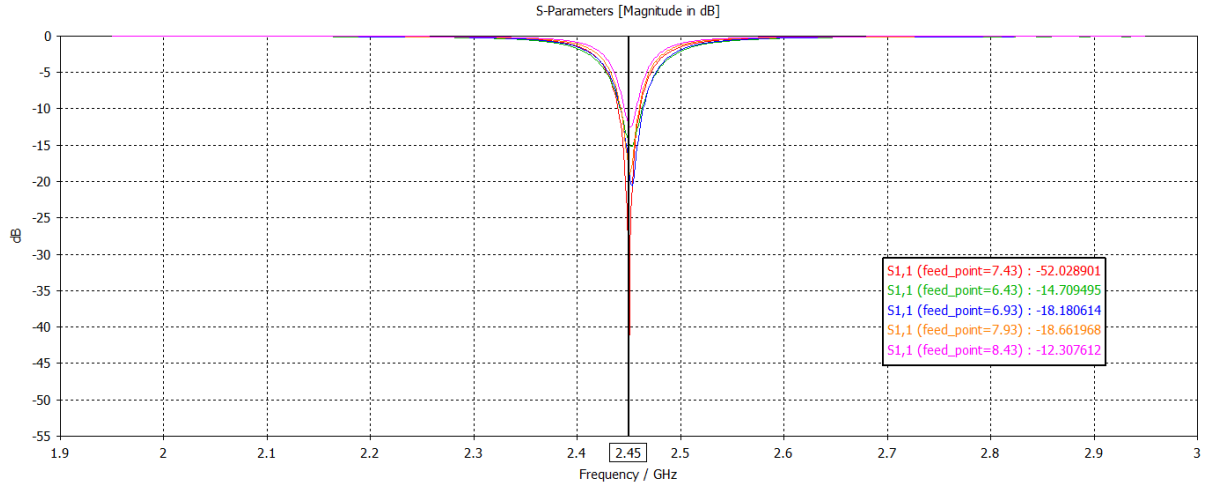


(c) in function of Fp;

Figure 3.5: S11 variation.

## 3.2 Human body as a propagation medium

Although the antenna has an excellent matching operating in free space, with the introduction of the body this will change dramatically. As presented in the section 2.2.5 each layer of the body will have its own dielectric properties, which will vary depending on the age and gender of the person [24]. That said, it is necessary to ensure that the antenna works considering these adversities. To ensure this, three models of the human chest were developed, where the level of complexity was gradually increased in order to make the antenna simulation as real as possible. In this section we will present the 2 models used and their characteristics, as well as the design changes that were made to the antenna in order to ensure that it works in the presence of the human body.

### 3.2.1 Human chest models

As mentioned, 2 different models of the human chest were used throughout this project. The first model was a simple 3-layer model that evolved into a cubic model of the human chest, where the rib cage, lungs and heart are introduced. This last model already allowed the simulation of cardiac and respiratory motion by varying the size and dielectric properties of the organs.

#### 3.2.1.1 Human chest models - 3 layer model

The first body model to be developed was a simple 3-layer model, similar to the one shown in Figure 2.7a, although it is simpler, consisting of a layer of skin, fat and muscle as shown in Figure 3.7.

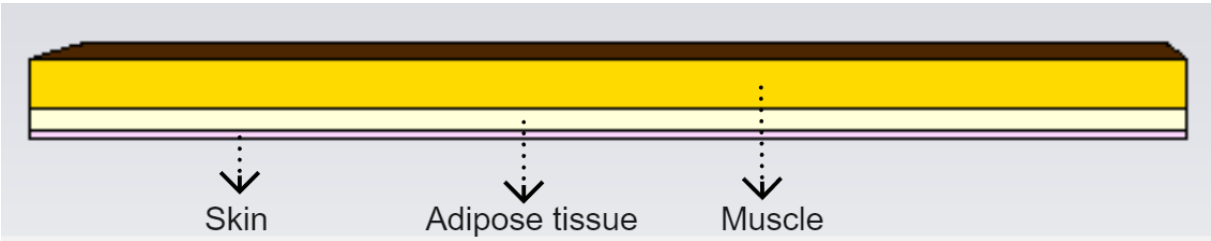


Figure 3.7: 3 Layer model.

To develop the model it was then necessary to complement the study done in the sections 2.2.5 and 2.2.5.1. It was then found that the most important properties are the electrical permittivity ($\epsilon_r$), relative permeability ($\mu_r$), density ($\rho$), electrical conductivity

($\sigma$) and thermal conductivity (k). In Table 3.2 the dimensions of the layers and in Table 3.3 the dielectric properties of the layers are shown for the frequency of 2.45 GHz.

Table 3.2: Layer dimensions - 3 layer model [24, 30, 32].

| | Length (mm) | Width (mm) | Thickness (mm) |
|---|---|---|---|
| Skin | 350 | 350 | 2.3 |
| Adipose Tissue | 350 | 350 | 7 |
| Muscle | 350 | 350 | 15 |

Table 3.3: dielectric properties of the human body layers[24, 54].

| | $\epsilon_r$ | $\mu$ | $\rho$ [kg/[$m^3$]] | $\sigma$ [$S/m$] | k [$W/Km$] |
|---|---|---|---|---|---|
| Skin | 38 | 1 | 1109 | 1.46 | 0.326 |
| Adipose Tissue | 5.28 | 1 | 911 | 0.105 | 0.205 |
| Muscle | 51.7 | 1 | 1090 | 1.74 | 0.385 |

After the model was defined, the antenna previously matched to operate in free space was tested in contact with the body, as shown in Figure 3.8. As can be seen from the Figure 3.9a, the antenna is completely mismatched. This is due to the large differences in dielectric properties between the antenna and the human body. Those abrupt changes in the propagation medium cause the antenna to completely mismatch. In order to better understand the impact of the body, the antenna was tested at different distances from the body with the results being shown in Figure 3.9b.

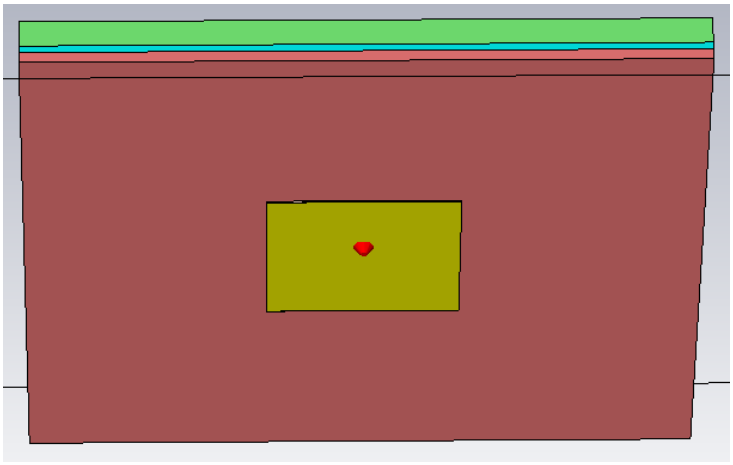

Figure 3.8: Simple microstrip patch antenna in contact with the human body.

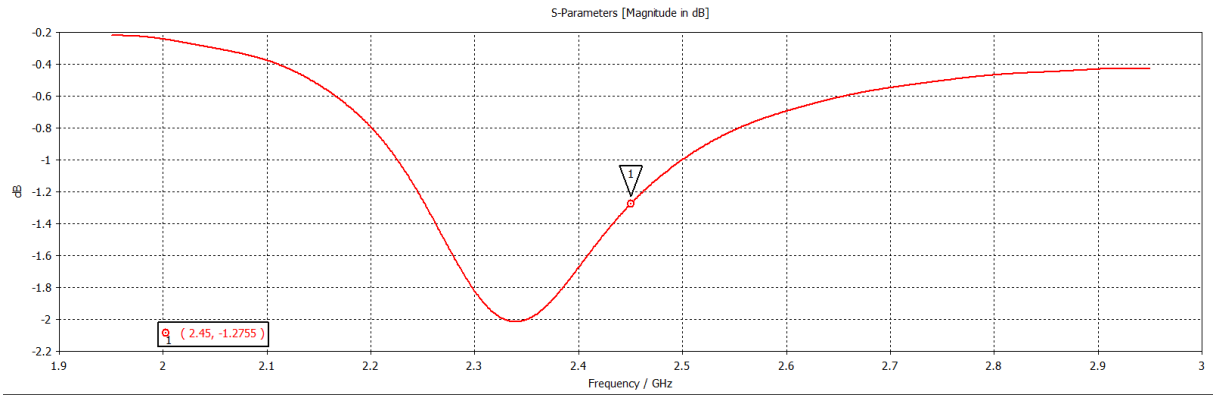


(a) in contact with the body;

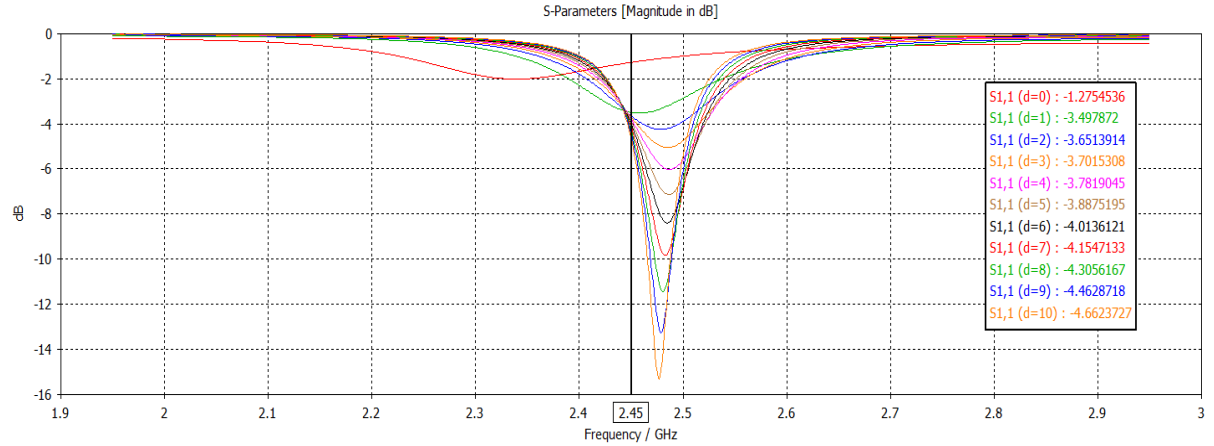


(b) 0 to 10 mm from the body;

Figure 3.9: $S_{11}$ of the on-body antenna located at different distances.

As can be seen from the Figure 3.9b with the distance of the antenna from the body its matching improves. These results are to be expected since the further away from the body the antenna is the more its behavior approaches the free space behavior.

The antenna was then matched to the distances closer to the body, namely 1, 2, 3 and 4 mm. It turned out that for distances less than 4 mm it is practically impossible to get a good fit for the antenna, since the feed point is very close to the patch boundary. Figure 3.10 shows the result of the antenna matching when operating at 4 mm from the human body.

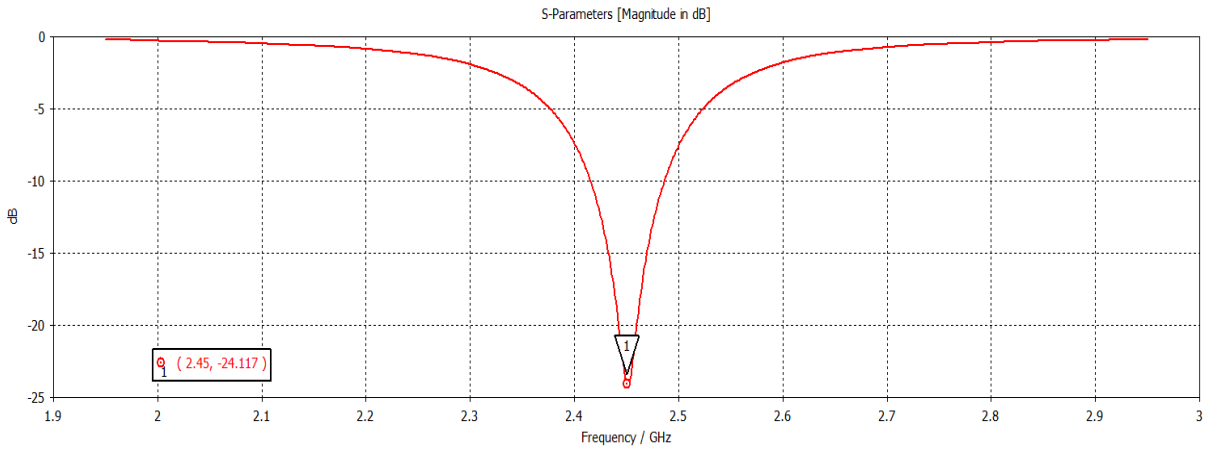


Figure 3.10: $S_{11}$ with the antenna 4 mm from the body.

As it was possible to verify from the results presented in this subsection, the presence of the body has a huge impact on the antenna matching, considering that the closer the antenna is to the body, the greater the difficulty in its matching. Therefore, it is necessary to resort to design changes to ensure its operation in contact with the body. In addition, the antenna will also have to withstand variations in the morphology of the human body, since each person has different dielectric and layer thickness characteristics.

#### 3.2.1.2 Human chest models - Cubic model

In order to be able to simulate cardiac and respiratory motion while ensuring a realistic approximation to a model of the real human body, the model presented in section 3.2.1.1 will have to be greatly improved. The remaining constituent layers of the human chest were added, namely the rib bones and their cartilages, as well as the heart, lungs and diaphragm. The property values, at 2.45 GHz, of the new layers added to the model are shown in Table 3.4 [55–57] . During breathing, the volume of the lungs will change, causing their properties to change as well. This change will cause variations in the phase of the reflection coefficient, thus allowing the antenna to detect the breathing rhythm [5].

Table 3.4: Human body dielectric properties [54].

| | $\epsilon_r$ | $\mu_r$ | $\rho$ [kg/[$m^3$]] | $\sigma$ [S/m] | k [W/k m] |
|---|---|---|---|---|---|
| Bone | 14.95 | 1 | 1543 | 0.5995 | 0.315 |
| Cartilage | 38.8 | 1 | 1100 | 1.76 | 0.49 |
| Full lungs | 20.5 | 1 | 394 | 0.84 | 0.39 |
| Intermediate lungs | 34.45 | 1 | 722 | 1.26 | 0.39 |
| Empty lungs | 48.4 | 1 | 1050 | 1.68 | 0.39 |
| Heart | 54.8 | 1 | 1081 | 2.26 | 0.56 |
| Diaphragm | 52.7 | 1 | 1090 | 1.74 | 0.49 |
| Visceral Fat | 5.46 | 1 | 900 | 0.05 | 0.21 |

The implementation of the remaining layers in the model was performed. The first thing to do is to add the rib cage. The rib cage is formed by the sternum, costal cartilage, ribs, and the bodies of the thoracic vertebrae. That surrounds the lungs and the heart, serving as an important mean of bony protection for these vital organs. The rib cage also assists in respiration, and provides support for the upper extremities. Although the human body is made of 24 ribs (grouped in 12 pairs), only the first 7 pairs are considered "real ribs" (Figure 3.11) with the cartilages connecting them to the sternum [58].

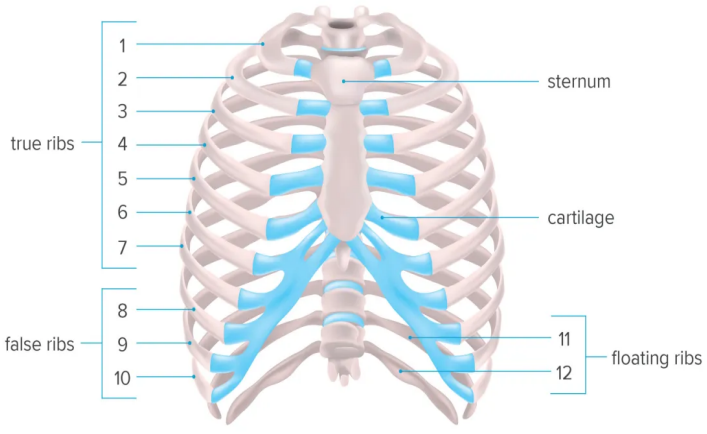


Figure 3.11: Rib cage structure [58].

The addition of the sternum, ribs and respective cartilages to the developed model is shown in Figure 3.12.

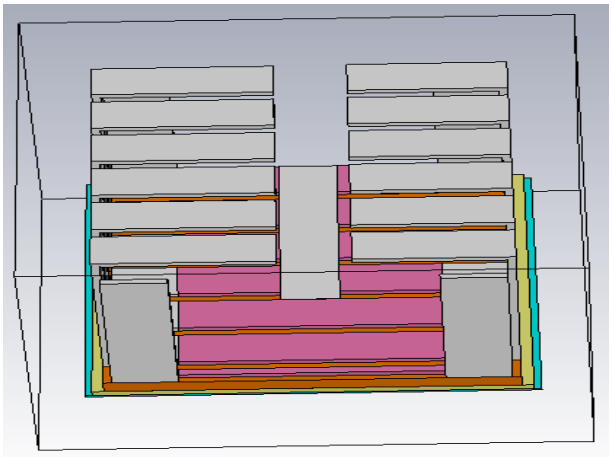

Figure 3.12: Sternum, ribs and cartilage on CST.

The thoracic cavity has the fundamental function of protecting the vital organs of the human being, namely the heart and the lungs. The variation of these allows the cardiac and respiratory movements, indispensable for human life and also for this project. The addition of these organs, along with the diaphragm, was the next step in the model building. In order to finish off the bone structure of the rib cage, the spinal column was also added.

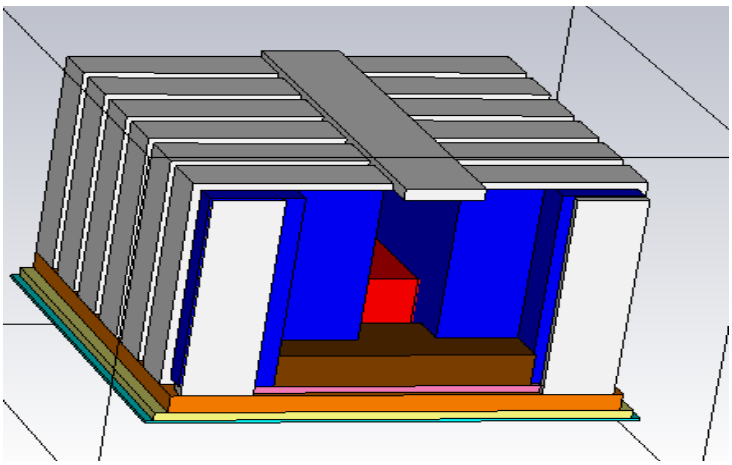

Figure 3.13: Bone structure and vital organs on CST.

Finally the layers of the back were added, namely layer of muscle, fat and skin, placed over the back of the ribs and spine. Side layers were also added to cover the entire model except the top and bottom edges, thus simulating the opening to the neck and abdominal region. The final step in the construction of this model was the introduction of the visceral fat layer. This is a type of fat present in the human body whose main function is to protect the organs of the human body. Although this type of fat is mostly

found in the abdominal region, its use is the best option for filling the model. The final model of the human chest is shown in the Figure 3.14.

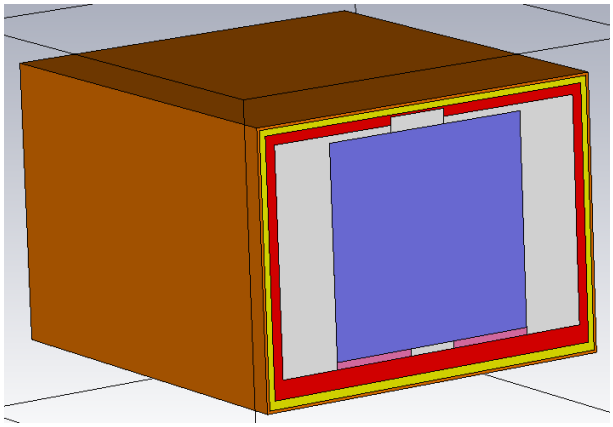

(a) Side view;

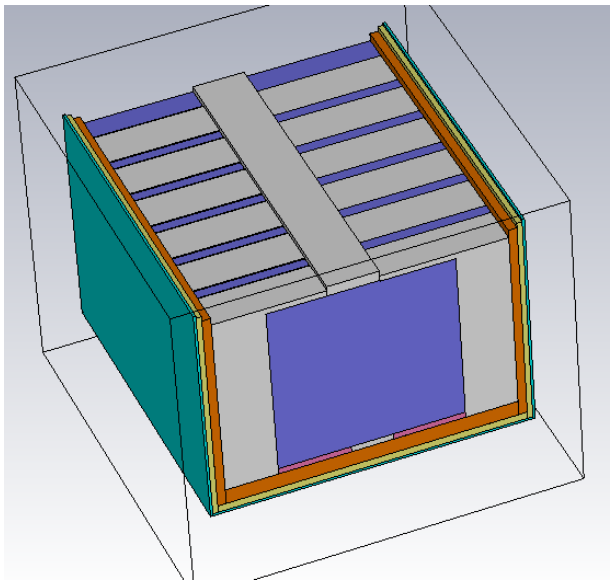

(b) Up view;

Figure 3.14: Human chest full model on CST.

The development of this model has tried to follow the actual dimensions of the human body as closely as possible. The dimensions considered for this model are shown in Table 3.5.

Table 3.5: Dimensions of the layers of the rib cage [56, 57].

| | Heart | Left Lung | Right Lung | Cartilage | Bone | Sternum |
|---|---|---|---|---|---|---|
| Thickness (mm) | 60 | 171 | 170 | 5.74 | 5.74 | 5.74 |
| Width (mm) | 85 | 100 | 114 | 87.5 - 178.19 | 87.5 | 39.17 |
| Length (mm) | 120 | 265 | 269 | 39.16 | 39.16 | 200 |

#### 3.2.1.3 Human body matching - Superstrates

According to what was studied in section 3.2.1.1 the morphology of the human body has a very large impact on the reflection coefficient of the antenna. It will improve or worsen depending on the distance from the antenna to the body. Taking into account the obtained results and the studies presented in section 2.2.6, the use of superstrates presents itself as a fundamental element in the matching of antennas in contact with the human body. The superstrate is a dielectric material supported on the surface of the radiating element, as shown in Figure 3.15, which protects the antenna from abrupt variations between propagation media, thus helping to maintain the matching of the antenna.

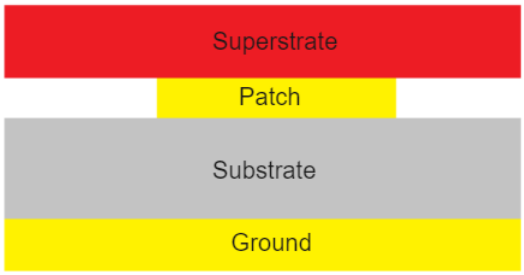


Figure 3.15: Structure of an antenna using superstrate.

To the antenna previously matched to operate within 4 mm of the human body, layers of substrate were added so that the distance between the antenna and the body is filled. Three different sets of substrates were used and later compared, shown in Table 3.6.

Table 3.6: Superstrates properties and dimensions for a 4 mm gap between the body and the antenna.

| Superstrate | Antenna 1: 3 x ROGERS RO4725JXR | Antenna 2: 5 x ROGERS RO4360G2 | Antenna 3: 2 x ROGERS4725JXR + 2 x ROGERS RO4360G2 |
|---|---|---|---|
| $\epsilon_r$ | 2.55 | 6.15 | 2.55+6.15 |
| Height (mm) | 3.86 | 4.05 | 3.94 |

For the Antenna 1, three layers a low permittivity superstrate were used. For the Antenna 2, 5 layers of the highest permittivity superstrate available (equal to the antenna substrate) were used, in order to reduce the impact of the propagation transition to the human body as much as possible. Finally, for the Antenna 3 a combination of the two dielectric materials presented above was used, where the lowest permittivity layer was in contact with the antenna and the highest permittivity layer in contact with the body.

For each antenna was then necessary to adjust there parameters. Those parameters are shown in Table 3.7.

Table 3.7: Antenna dimensons after superstrate optimization.

| | Antenna 1 | Antenna 2 | Antenna 3 |
|---|---|---|---|
| W (mm) | 21.7 | 17.1 | 23 |
| L (mm) | 23.73 | 22.532 | 23.67 |
| Fp (mm) | 2.5 | 1.9 | 2.1 |

Observing the values of the reflection coefficient obtained after the readjustment of the antennas, presented in Figure 3.16, it is verified that all antennas present very good matching levels (always lower than -45 dB). It was thus proven that the use of the superstrate allows the antenna to operate in direct contact with the human body while maintaining very good matching levels. Regarding the 3 antennas presented, it is necessary to analyze beyond the reflection coefficient, since it is very good for all three. In this context, should be noted that the Antenna 3 proved to be easier to match. Since the presence of two substrates with different properties makes the transition from propagation to the human body smoother compared to the other antennas tested. The use of two different superstrate adds robustness to the antenna.

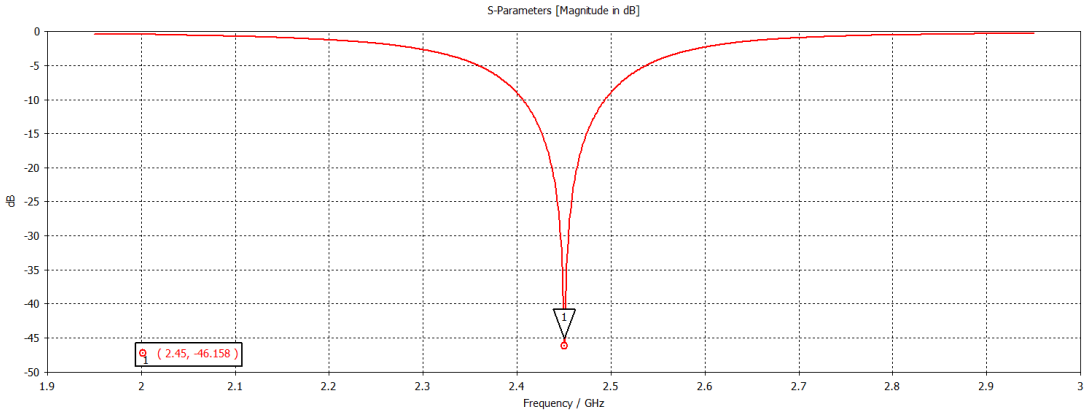


(a) Antenna 1;

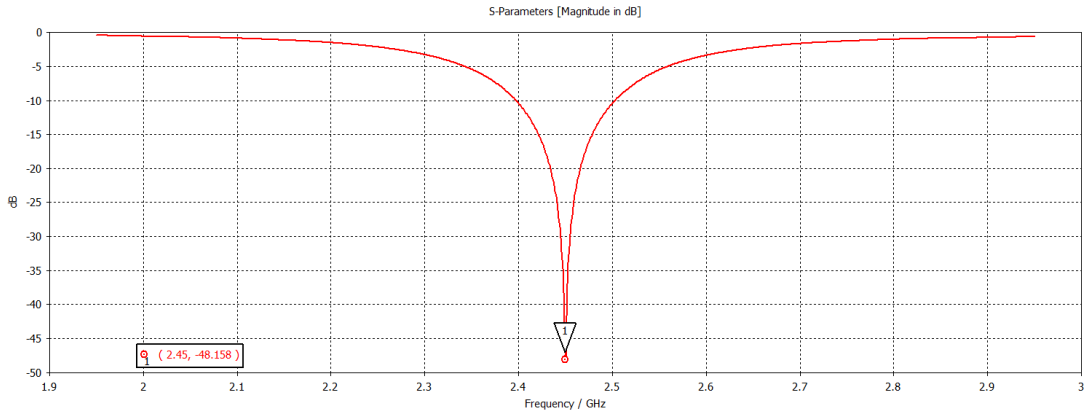


(b) Antenna 2;

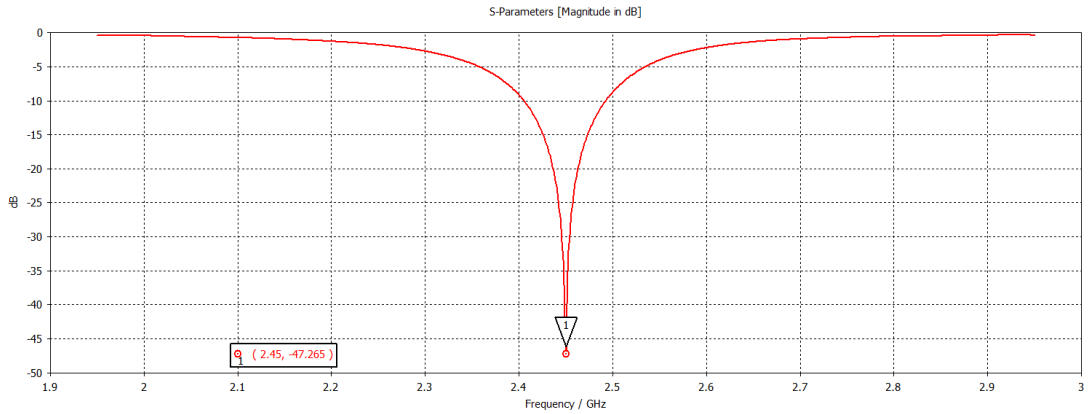


(c) Antenna 3;

Figure 3.16: $S_{11}$ for all superstrate antennas.

## 3.3 Bandwidth increase in patch antennas

Microstrip patch antenna has been widely used in mobile communications due to its simple structure and low cost. The major disadvantage of this antennas is its inherently narrow bandwidth of only a couple of percent. Intensive research has been done in

recent years to develop bandwidth increase techniques for patch antennas. This section will implement some of the methods, for increasing the bandwidth, presented in the section 2.2.7 and how this could be a solution to maintain antenna matching for any body type.

### 3.3.1 Parasitic patches method

The first method implemented was the use of parasitic patches used in [50] for bandwidth augmentation. Its implementation consists of using 4 parasitic patches placed on a substrate placed on top of the radiating patch. The substrate plates used have a relative permittivity ($\epsilon_r$) = 2.55 and height ($h$) = 1.58 mm. Following the design shown in Figure 3.17, the antenna parameters are shown in Table 3.8. Therefore, to understand how this method work, the first step was to study how a single parasite patch will affect the antenna, by verifying the influence of the variation of the parameters of the parasite.

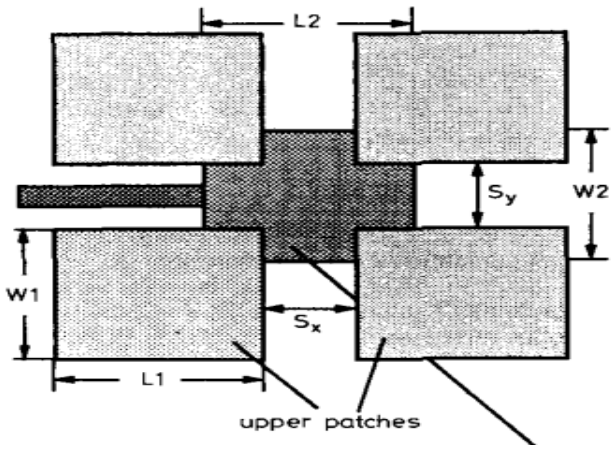


Figure 3.17: Parasite antenna design [50].

Table 3.8: Parameter value for the parasite antenna proposed in [50].

| Parameter | L1 | W1 | L2 | W2 | Sx | Sy |
|---|---|---|---|---|---|---|
| Values (mm) | 20 | 16 | 21.3 | 20 | 16 | 16 |

#### 3.3.1.1 Study of the influence of the parasitic patches

The initial implementation is shown in Figure 3.18 and its $S_{11}$ parameter in Figure 3.20. In this work stage, some changes were made regarding the substrate used: Rogers substrate was used due to its easy experimental implementation, since FR4 substrate

may present volatility in the experimental process. The substrate used was then Rogers RO4725JXR with $\epsilon_r$ = 2.64 and height (h) = 1.54 mm.

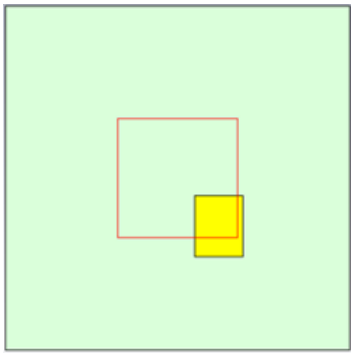

Figure 3.18: Parasite patch antenna with 1 parasite element.

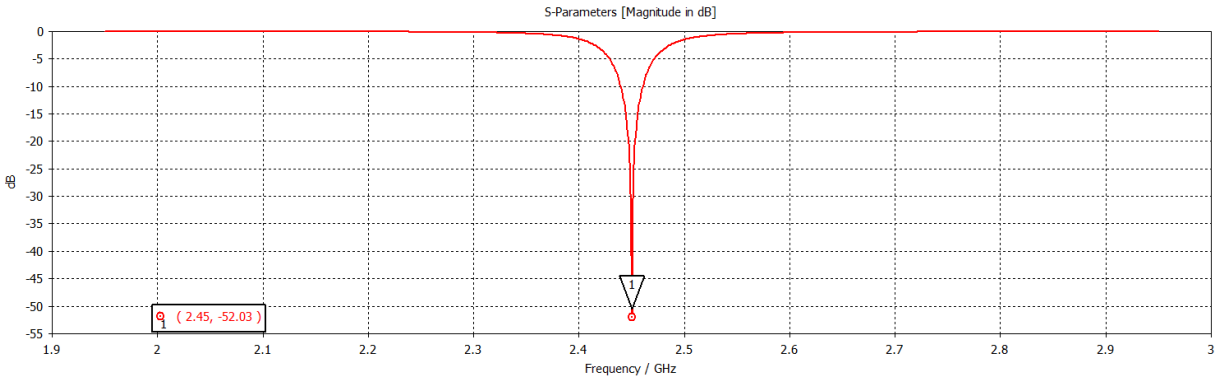


Figure 3.19: $S_{11}$ parameter before the parasitic patch addition.

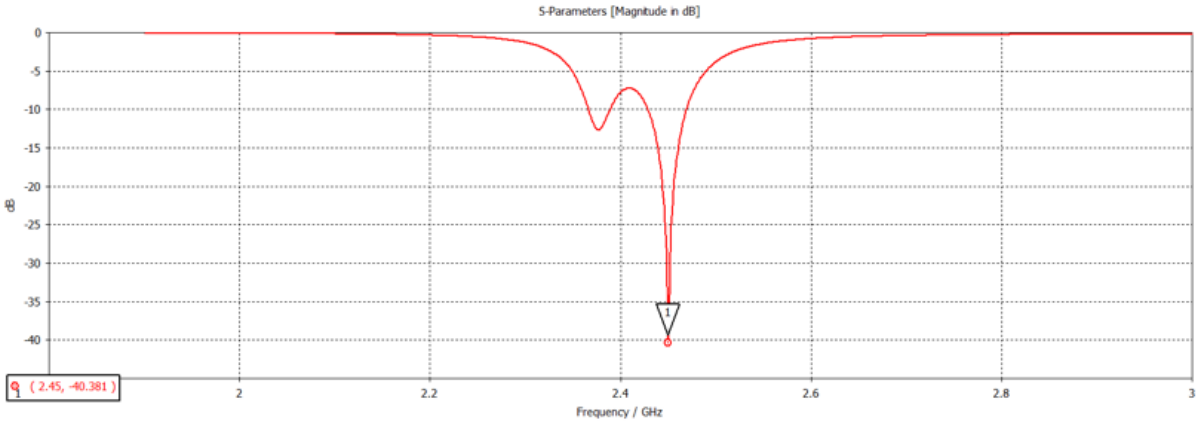


Figure 3.20: $S_{11}$ parameter of parasite patch antenna with 1 parasite element.

As can be seen by comparing Figure 3.19 and Figure 3.20 the introduction of one parasitic patch introduces a new resonant frequency, thus increasing the total bandwidth of

the antenna. Further matching was needed, with the new parameter values presented in Table 3.9. The behavior of the variation of patch parameters, namely the width ($W1$), length ($L1$) and distance between patch centers ($Sx$ and $Sy$), was also studied. The results of the variation of width and length are shown in Figure 3.21.

Table 3.9: Parameter value for the parasite antenna.

| Parameter | L1 | W1 | L2 | W2 | Sx | Sy |
|---|---|---|---|---|---|---|
| Values (mm) | 19 | 14 | 34.55 | 35 | 10 | 10 |

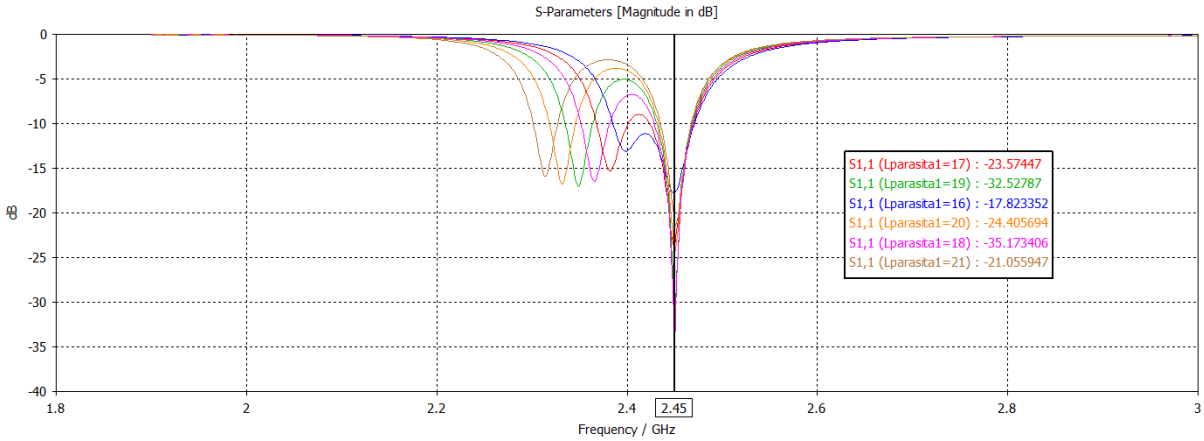


(a) Length variation;

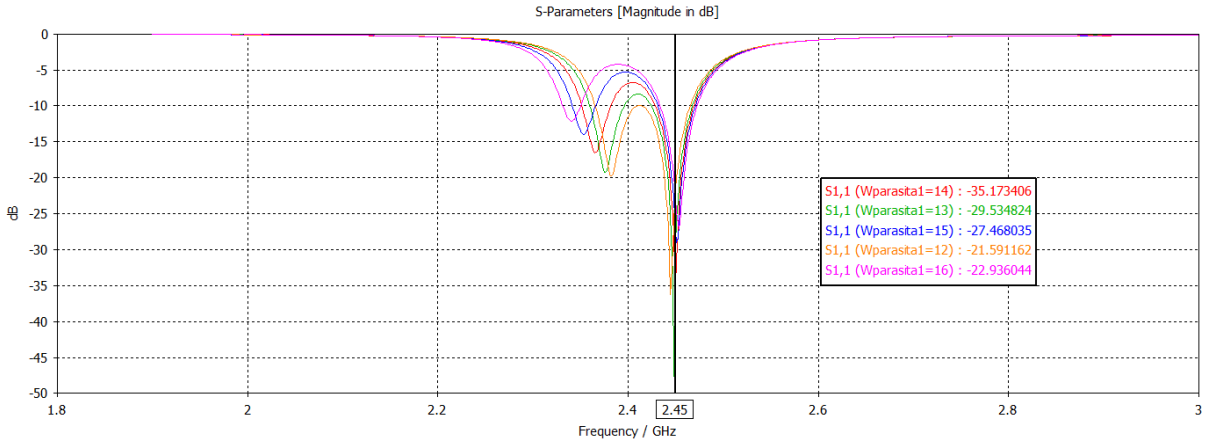


(b) Width variation;

Figure 3.21: Parameter variation of the parasite patch.

The behavior of the variation of the parasite dimensions show similar results as the variation of the main patch. The variation of the width will vary the magnitude of the reflection coefficient and causes small shifts to the second resonance. The variation of the patch length will cause a bigger shift to the resonance frequency obtained by

the parasitic patch. The distance from the parasitic patch to the main patch was also studied. This shows the distance between the center of the main patch and the center of the parasitic patch. The distance was decreased to 4 mm, with the $S_{11}$ shown in Figure 3.20. As can be seen, moving the center of the parasite closer to the center of the main patch will cause an increase in the magnitude of the $S_{11}$ parameter of the second resonance. As presented in Figure 3.23, moving the parasitic patch closer will cause the second resonance to be attenuated. Despite this attenuation, with increasing distance there was an increase in the bandwidth of the antenna, reaching values of approximately 130 MHz. It is then possible to conclude that by varying the parameters of the parasite together, it is possible to increase the bandwidth of the antenna while maintaining its matching to the desired frequency.

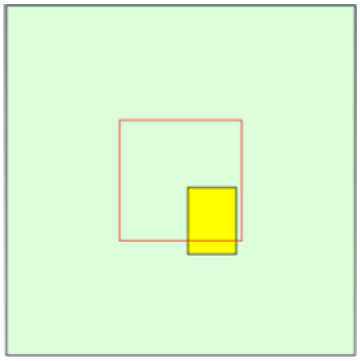

Figure 3.22: Parasite patch antenna with 1 parasite element, decreaed distance to the main patch.

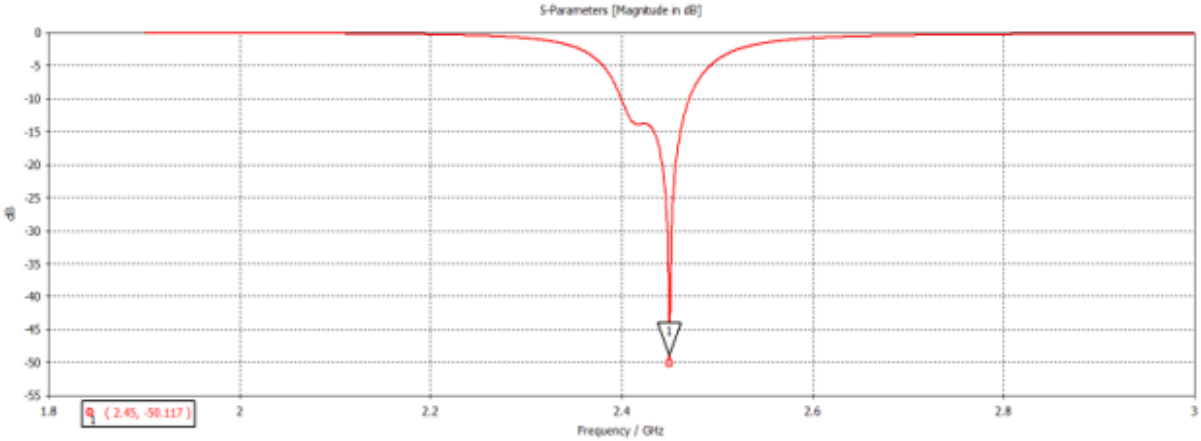


Figure 3.23: $S_{11}$ parameter of parasite patch antenna with 1 parasite element, decreased distance to the main patch.

### 3.3.2 Parasitic patches - 4 parasite

After understanding the impact that parasites will have on the antenna, the antenna shown in [50] was replicated, as can be seen in Figure 3.24. The 4 parasites have the same size and distance to the main patch being presented in Table 3.8. The original antenna in [50] was optimized to operate within the 3.2 to 5.2 GHz frequency band. Therefore, for the intended application it was then necessary to resize the antenna.

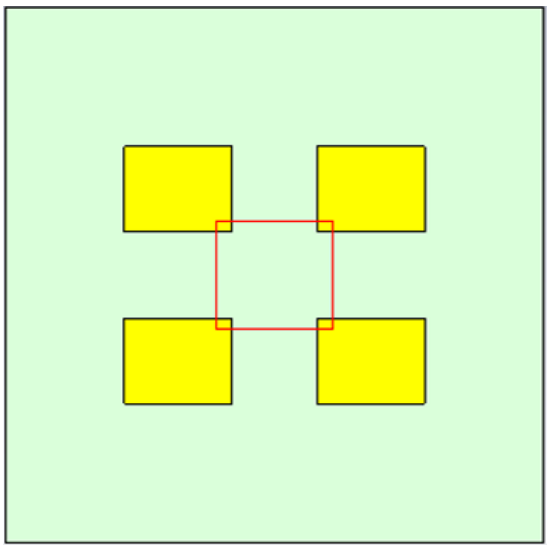

Figure 3.24: 4 parasite original antenna.

With the results obtained after the study of the impact of 1 parasite, the remaining parasites were added 1 by 1. With the increase in the number of parasites it was found that these could be grouped in diagonal pairs, as shown in Figure 3.25, thus changing the original design (4 equal parasites) to groups of 2 by 2. As can be seen in Figure 3.26 the introduction of a second parasite causes the second resonance to shift considerably, also losing much of the extra bandwidth that had been achieved.

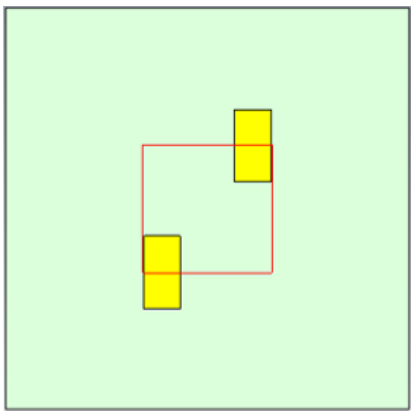

Figure 3.25: Parasite patch antenna with 2 parasite element.

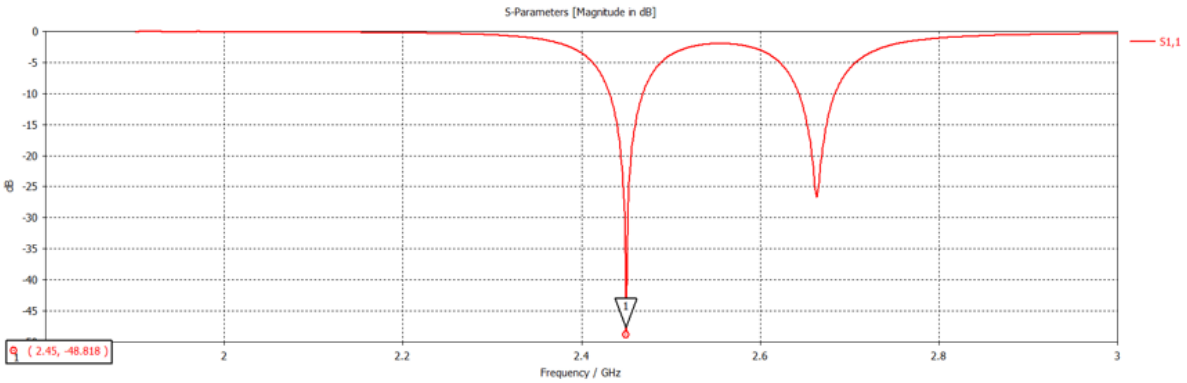


Figure 3.26: $S_{11}$ parameter of parasite patch antenna with 2 parasite element.

The second pair of parasites was then added to the antenna design, making the two pairs of parasites independent of each other. With the introduction of the second pair it was possible to move the second resonance closer to the first. It was then necessary to perform the matching of the antenna for the desired frequency band but due to the high number of variable parameters present in this antenna, its matching proved to be a challenge. In order to make it easier to match, the Optimizer tool present in the CST proved to be fundamental. After the final matching of the antenna, the antenna design is shown in Figure 3.27.

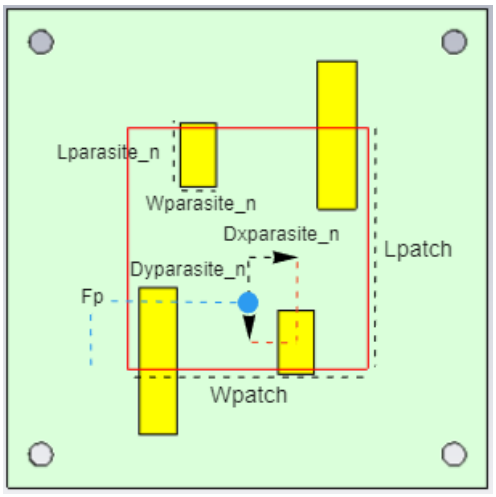


Figure 3.27: Parasite patch antenna with 4 parasite element.

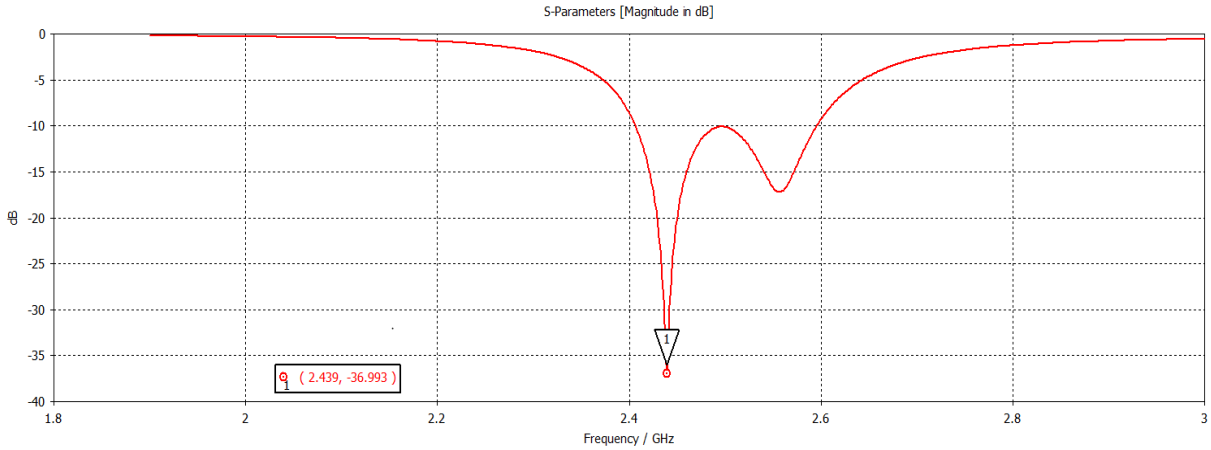


Figure 3.28: $S_{11}$ parameter of parasite patch antenna with 4 parasite element.

As can be seen in Figure 3.28 it was possible to obtain a well matched antenna for the desired frequency band. For the bandwidth, very good values were obtained, around 200 MHz, for the defined threshold of -10 dB, which was an increase of around 100 MHz when comparing to a standard microstrip patch antenna. When comparing with the results obtained in section 3.3.1.1, the addition of 3 more parasitic patches proved to be worth it since the bandwidth increased by 70 MHz. As can be seen in the Figure 3.28, between the two resonances there is a "valley" that is the closest point to the threshold value of -10 dB. For the increase of bandwidth this point is crucial because, although it is possible to increase the bandwidth, with its increase the "valley" will also rise, compromising the bandwidth. It is then necessary to establish a relationship between increasing the bandwidth and the magnitude of the "valley", this is achieved by jointly varying the width of one of the parasitic pairs and its distance on the y-axis. The combination of these two parameters makes it possible to create a relationship between increasing the bandwidth and not exceeding the set limit of -10 dB. The final antenna dimensions are presented in Table 3.10.

Table 3.10: Final dimensions parasite patch antenna.

| Parameter | Lparasite1 | Lparasite2 | Wparasite1 | Wparasite2 | $Dx_parasite1$ | $Dx_parasite2$ | $Dy_parasite1$ | $Dy_parasite2$ | Wpatch | Lpatch | Fp |
|---|---|---|---|---|---|---|---|---|---|---|---|
| Value (mm) | 8.66 | 20.05 | 4.94 | 5.16 | 8.37 | 19.11 | 16.78 | 10.64 | 32.48 | 32.42 | 7.1 |

With this design it has proven possible to increase the bandwidth of a microstrip patch antenna. Although the adaptation presented is for the antenna operating in free space, this method has the potential to meet the proposed objectives for the antenna operating in contact with the body.

### 3.3.3 Ground plane slots

After the bandwidth increase is achieved it is then necessary to ensure that the antenna is robust enough to be able to maintain the bandwidth even in contact with the body. In [59] the use of slots in the ground plane is presented as a stabilizing element for the antenna, an important factor as the human body is an unstable propagating element. In [60, 61] the authors use slots in the ground plane as a way to not only increase the stability of the antenna, causing the $S_{11}$ parameter to reduce its variation when affected by external factors, but also increase the bandwidth without compromising the size of the antenna.

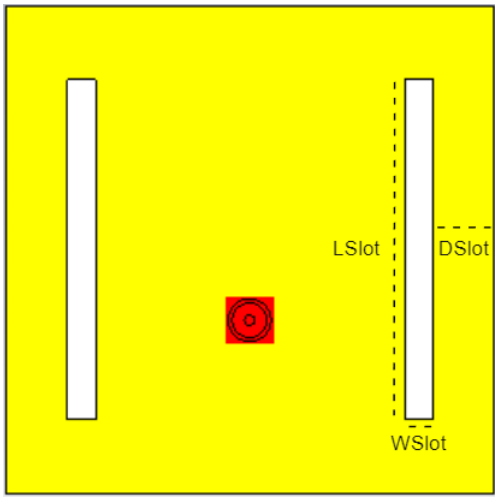


Figure 3.29: Ground plane slots.

Two equal and symmetrical slots were then introduced in the antenna ground plane presented in section 3.3.2, as shown in Figure 3.29. Their impact on the antenna was studied, as well as the variation of their parameters. As seen in Figure 3.30 the variation of the parameters of the slots influences the antenna matching. Varying the length of the slots and their distances from the edge of the substrate will vary the magnitude of the reflection coefficient and varying the width of the slots will cause the resonance frequency to shift. The addition of the slots on the ground will help in the matching of the antenna especially in contact with the human body as they make the antenna more robust to changes in the propagation medium and to body movements. In Table 3.11 are presented the parameter values of the ground plane slots.

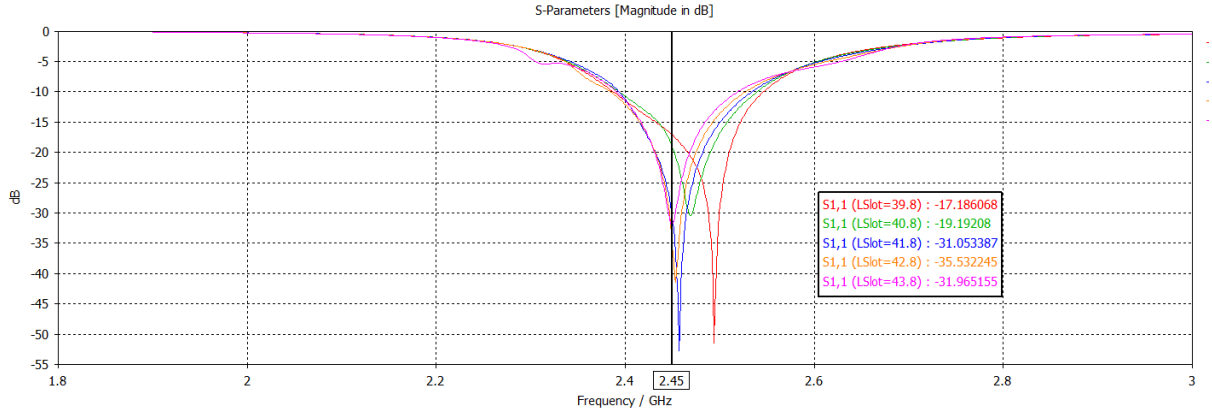


(a) Slot length variation;

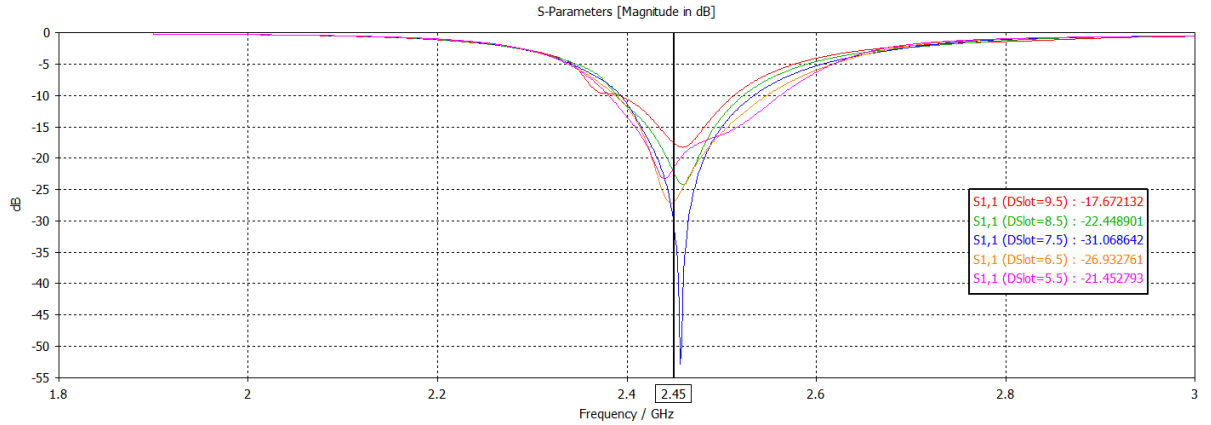


(b) Slot distance variation;

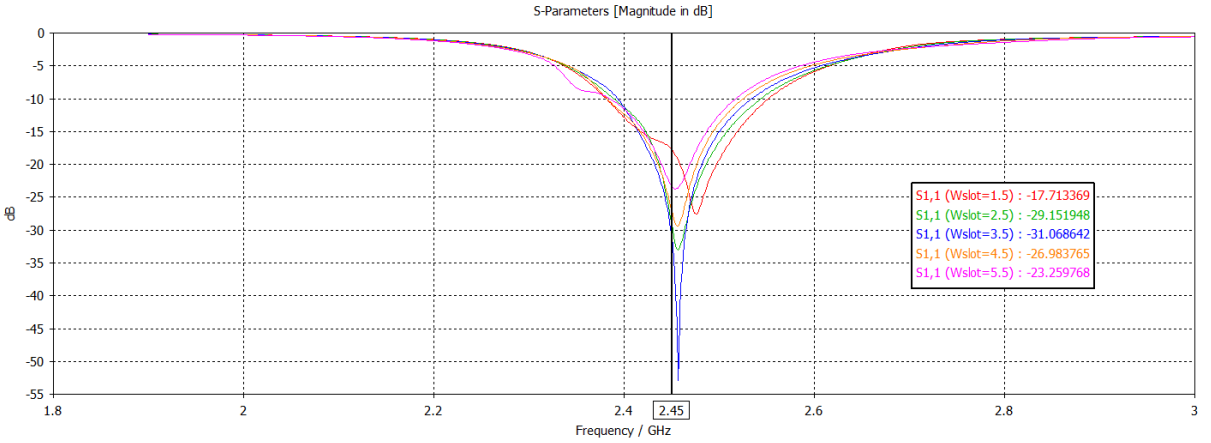


(c) Slot width variation;

Figure 3.30: Parameter variation of the parasite patch.

Table 3.11: Ground plane slots parameter values.

| Parameter | DSlot | LSlot | WSlot |
|---|---|---|---|
| Value (mm) | 19 | 41.8 | 4 |

As can be seen from Figure 3.31 the antenna is very well matched. The presence of the slots in the ground plane made the two resonances created by the main patch and the parasitic ones come together into one, thus achieving greater robustness and being able to maintain a large bandwidth of, approximately, 200 MHz.

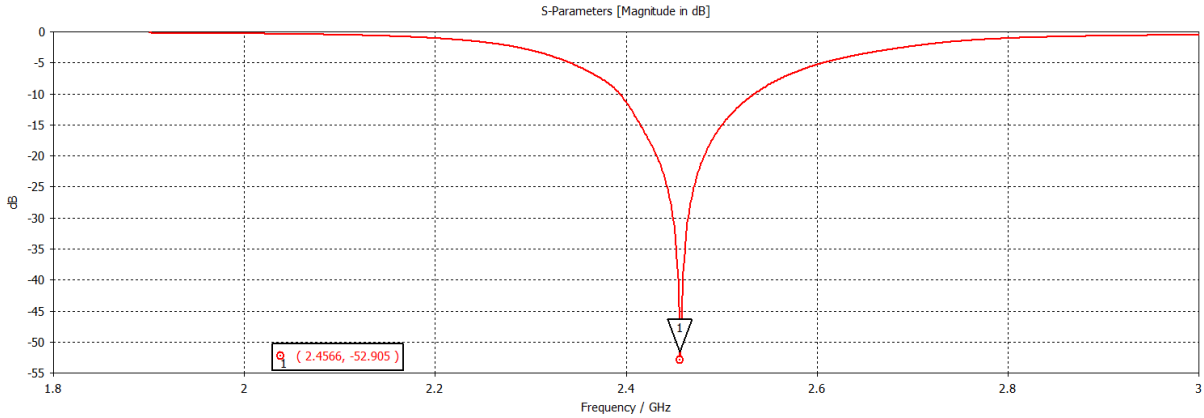


Figure 3.31: $S_{11}$ of parasitic antenna after introduction of ground plane slots.

Comparing Figure 3.31 with the values obtained without the use of slots in the ground plane (Figure 3.28), it can be concluded that the use of slots in the ground plane are an important element in antenna design. Their use will prevent the appearance of the "valley", thus preventing the antenna from mismatch.

When comparing the bandwidth values obtained with the ones presented in section 2.2.7, it is possible to conclude that the percentage values obtained by this method are very good. Although the results may be a bit misleading, since for the antennas presented in section 2.2.7, their bandwidths are considerably higher. When compared to a normal patch antenna, increases of approximately 80 % were obtained, going from 100 MHz to 180 MHz.

### 3.3.4 Cropped Patch method

With the possibility of using various methods to increase the bandwidth of a patch antenna, it is necessary to consider the target applications of these methods. After studying the presented literature, the work presented in [49] was implemented. The main objective of the proposed antenna is to reduce its size and increase its bandwidth, with its operating frequency in the 3.2 to 3.8 GHz band. The author's proposal to increase the bandwidth while maintaining a small antenna size makes this method attractive for on-body applications, since antenna size presents itself as an important

factor. By implementing this method, it is hoped to be able to increase the bandwidth of the antenna, matching it to operate in the desired frequency band.

The first implementation for this method was the author's proposed antenna replication, shown in Figure 2.11c. This antenna uses an FR4 substrate of $\epsilon_r$ = 4.4 and height ($h$) = 1.6 mm and will be fed via coaxial. To the initial patch was then cut out a triangular slot of length 'p' and width 'q'. A small triangular patch is added within the area of triangular slot which is placed 'a' and 'b' distance apart from the original triangular cut, as presented in Figure 3.32, with the parameter values shown in Table 3.12.

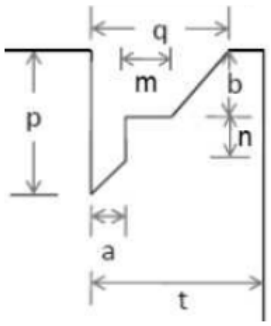


Figure 3.32: Patch Cutout [49].

Table 3.12: Parameter values of the antenna, proposed in [49].

| Parameter | $p$ | $q$ | $a$ | $b$ | $t$ | $m$ | $n$ | $W$ | $L$ |
|---|---|---|---|---|---|---|---|---|---|
| Value (mm) | 4 | 4 | 0.25 | 2.5 | 6.75 | 0.75 | 0.75 | 20 | 20 |

The antenna was then implemented in the CST, being presented in Figure 3.33. In this work stage, some changes were made regarding the substrate used: Rogers substrate was used due to its easy experimental implementation, since FR4 substrate may present volatility in the experimental process. The substrate used was then Rogers RO4360G2 with $\epsilon_r$ = 6.4 and height ($h$) = 1.524 mm. The initial parameters had to be changed since the antenna presented in [49] was designed to operate in a different frequency band from the proposed one. The antenna dimensions were then adjusted accordingly and the new parameters are presented in Table 3.13.

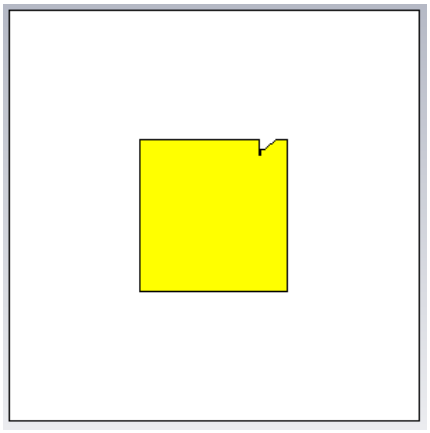

Figure 3.33: Cropped antenna version 1 - Antenna design.

Table 3.13: Cropped antenna version 1 parameters.

| Parameter | p | q | a | b | t | m | n | W | L |
|---|---|---|---|---|---|---|---|---|---|
| Values (mm) | 2.8 | 2.94 | 0.18 | 1.79 | 4.72 | 0.54 | 0.93 | 25.1 | 26 |

As can be seen in Figure 3.34, after the necessary changes the antenna is still operating for the intended frequency, the introduction of the cutout in the patch has not been shown to have increased the bandwidth of the antenna. That said, further tests were then performed in order to better understand this method for the frequency band under study.

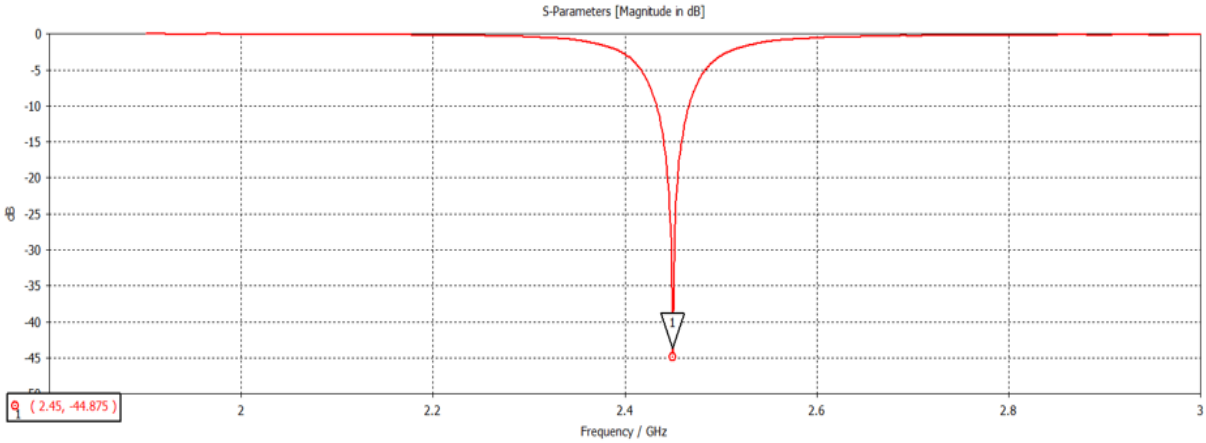


Figure 3.34: $S_{11}$ parameter of Cropped antenna version 1.

In an attempt to get a higher bandwidth more cutouts were made in the patch. An additional cut was made at the opposite end of the first cut, as shown in Figure 3.35a. With the addition of the second cut a second resonance was created as shown in Figure

3.35b, concluding that adding extra cuts will increase the bandwidth of the antenna. Using CST's Optimizer tool the antenna design was optimized in order to obtain the maximum bandwidth for the frequency band between 2.4 and 2.6 GHz. Although the bandwidth of the antenna has increased, it can be seen from Figure 3.35b, that there is a frequency band where the antenna has a matching worst than -10 dB.

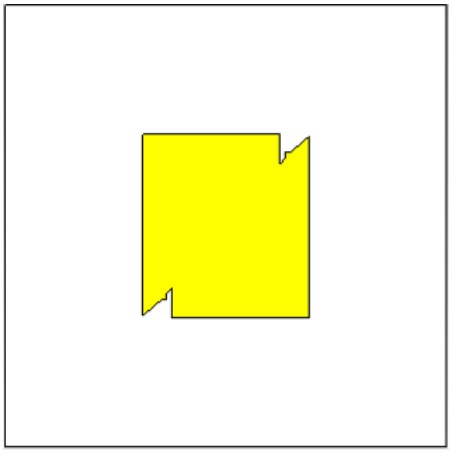

(a) Antenna design;

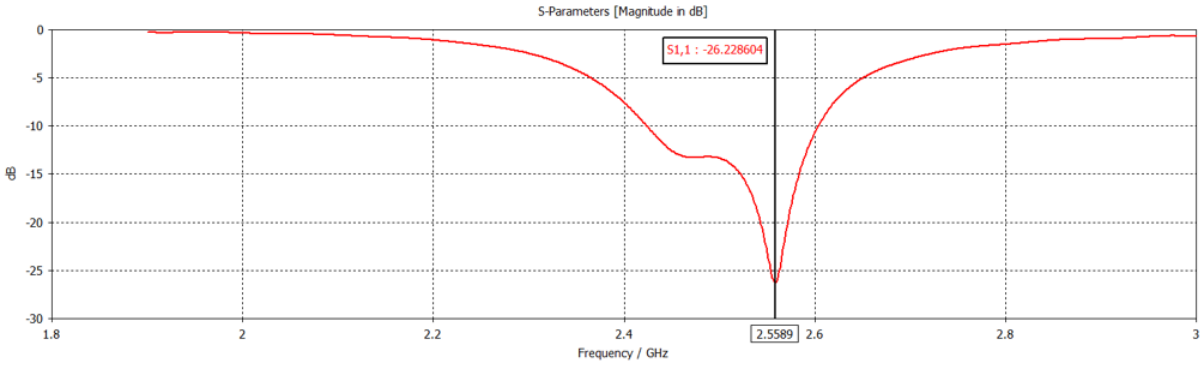


(b) $S_{11}$ parameter;

Figure 3.35: Cropped antenna version 2.

With the proof that the patch cutout causes the bandwidth to increase, 4 equal trapezoids were cut out at the corners of the patch, as presented in Figure 3.36a. The result obtained for the parameter $S_{11}$ is presented in Figure 3.36b. With the 4 cutouts it was then possible to achieve bandwidth values of approximately 180 MHz, with the antenna adapted to the desired frequency band.

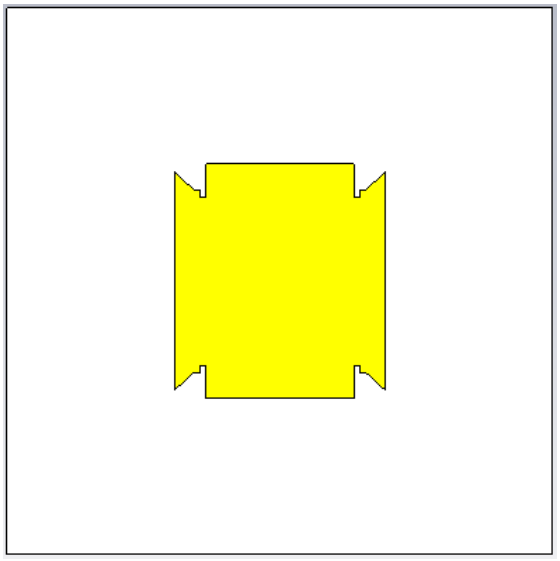

(a) Antenna design;

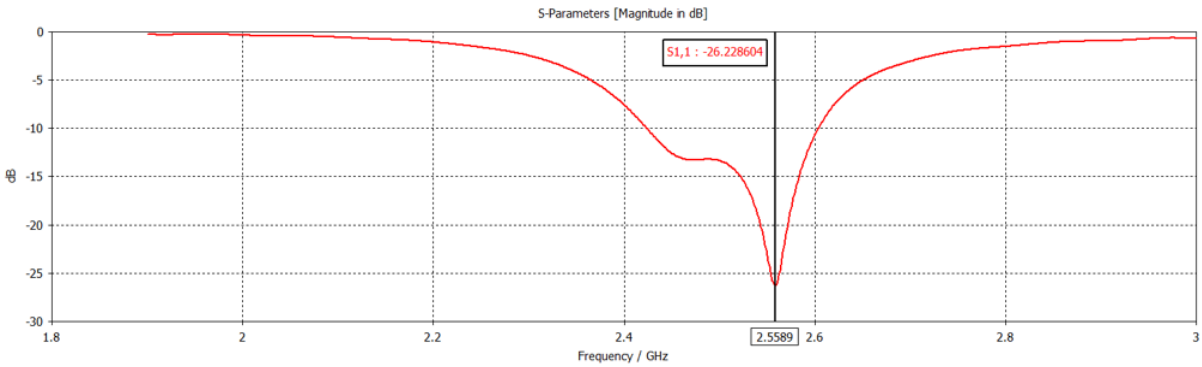


(b) $S_{11}$ parameter of Cropped antenna version 3;

Figure 3.36: Cropped antenna version 3.

In order to try to join the two resonances, as presented in the parasitic patch method, 2 symmetric slots were introduced in the ground plane, with the parameters presented in Table 3.14. The addition of the slots had the same effect as presented in section 3.3.3, the two resonances joined, obtaining bandwidth values of, approximately 130 MHz as presented in Figure 3.37.

Table 3.14: Ground plane slot parameters for Cropped antenna version 3.

| Parameter | DSlot | LSlot | WSlot |
|---|---|---|---|
| Value (mm) | 9.69 | 58.95 | 3.79 |

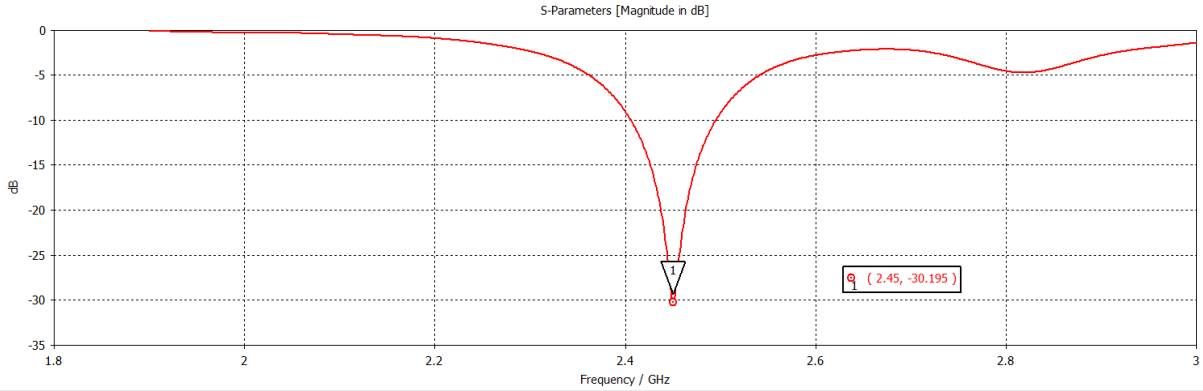


Figure 3.37: $S_{11}$ parameter of Cropped antenna version 3 with ground plane slots.

After the slots were inserted into the ground plane, the antenna was tested for operation near the human body, as shown in Figure 3.38. In order to try to ensure the adaptation of the antenna next to the body, layers of superstrate were used. The progressive method presented in section 3.2.1.3 was used in order to minimize as much as possible the influence of the body on the antenna propagation, as presented in Figure 3.39.

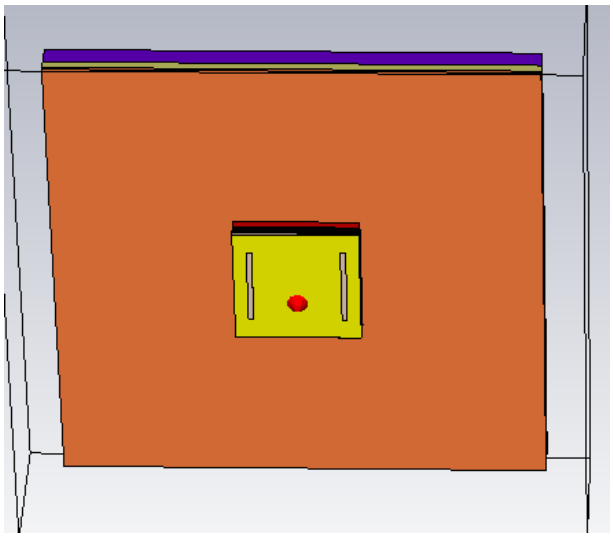

Figure 3.38: Cropped antenna version 3 in contact with the human body.

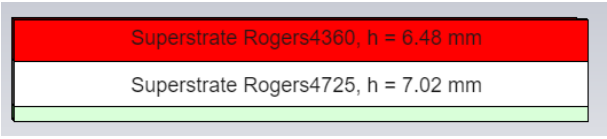


Figure 3.39: Cropped antenna version 3 - Superstrate layers.

The results obtained for the parameter $S_{11}$ are presented in Figure 3.40. Comparing with the results obtained in section 3.3.3 with those obtained with this method a large

difference is shown in terms of bandwidth, as shown in Table 3.15. Although the method of parasites presents a higher degree of complexity, this presents itself as the most appropriate option for the objectives of this project. Therefore, the study of the cropped patch method was abandoned.

Table 3.15: Bandwidth difference between the Cropped and Parasitic method.

| Method | Cropped Patch | Parasitic Patches |
|---|---|---|
| Bandwidth (MHz) | 130 | 180 |

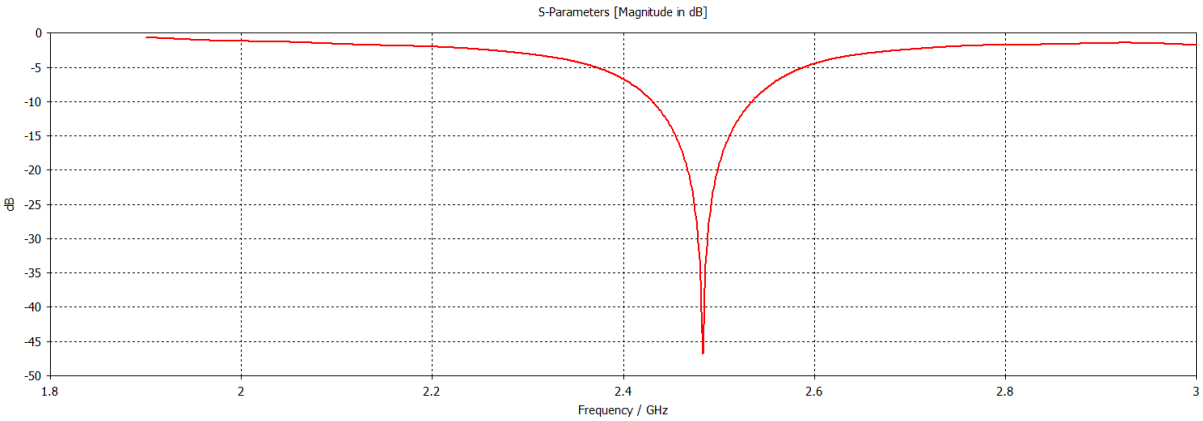


Figure 3.40: $S_{11}$ parameter of Cropped antenna version 3 with ground plane slots in contact with the human body.

## 3.4 Parasite slot antenna - Final design

With the study developed in sections 3.3.1.1 and 3.3.3 , it was possible to arrive at the final model of the antenna. This is formed by combining the use of parasitic patches together with the use of slots in the ground plane, thus obtaining a robust patch antenna of high bandwidth. With the presence of the full human chest model it was necessary to make some readjustments to the antenna, namely in the number of superstrate layers to be used and the dimensions of the antenna. With the impact of using superstrates proven in the section 3.2.1.3, a distance of 4 mm is obtained as the minimum distance for antenna adaptation. With the development of the body model and antenna it was necessary to increase the amount of superstrate layers to be used, following a progressive model. This model consist in the use of 2 different types of substrate (Rogers RO4725JXR and RO4360G2) creating a smoother transition between the antenna and the human body, as is shown in Figure 3.41. The thickness of the superstrate layers has increased considerably. Although the complexity and volume of the antenna has

increased, by increasing the superstrate layers it has been possible to ensure that the antenna can adapt to any variation that the human body may have. This topic will be addressed in section 3.4.1.

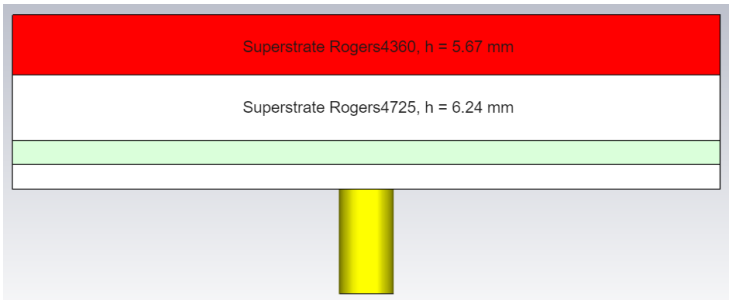


Figure 3.41: Parasite patch antenna: Final antenna design - superstrate layers.

To ensure the best possible approximation an air gap space of 0.2 mm was considered between the superstrates, as can be seen in Figure 3.42, thus simulating the roughness of the superstrates.

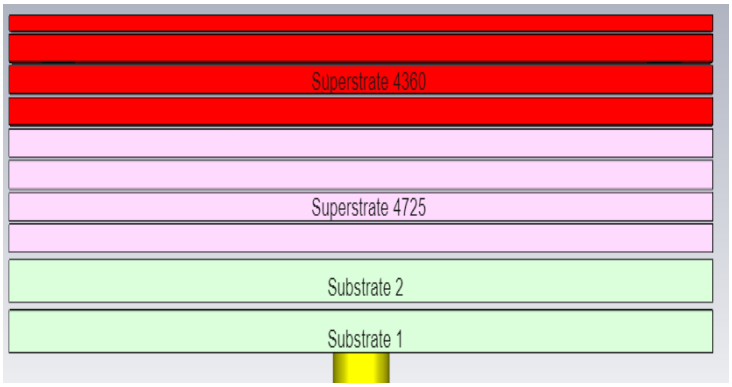


Figure 3.42: Parasite patch antenna: Final antenna design - superstrate layers with gap.

The final step in the antenna design was to create four holes where the screws needed to connect the different antenna components will be placed, as shown in Figure 3.43. The holes will be 3.2 mm in diameter with a center distance of 4.5 mm from the edges of the substrate. With the holes made it was necessary to readjust the antenna, with the values of the parameters to be presented in the Table 3.16.

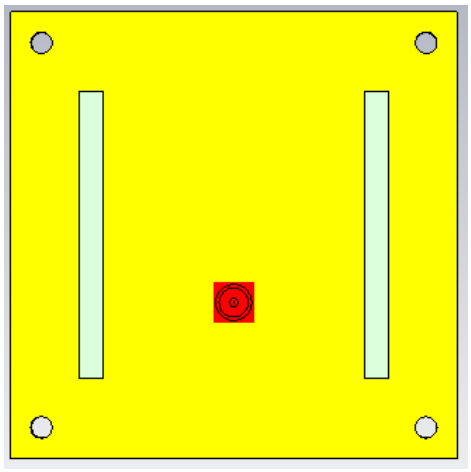

Figure 3.43: Holes created to connect all the layers of the antenna.

The final antenna design, along with the complete body model used can be seen in Figure 3.44.

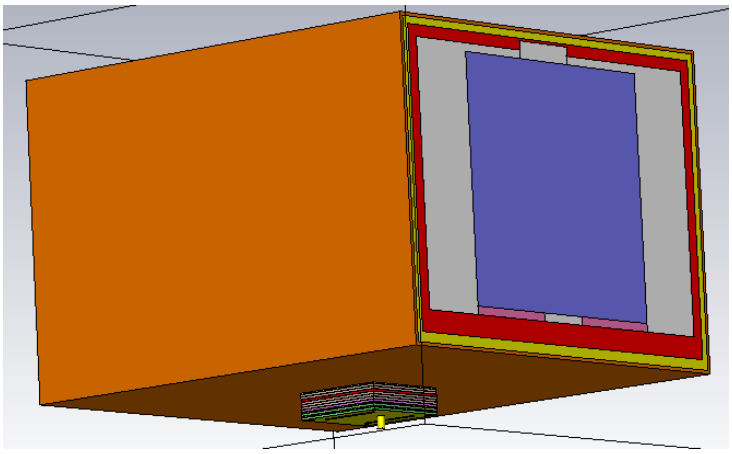

Figure 3.44: Parasite patch antenna: Final antenna design with cubic chest model.

As can be seen from the Figure 3.45 the antenna is very well adapted for the intended frequency (2.45 GHz) while maintaining the bandwidth, of about 180 MHz, for the ISM frequency band, thus being able to withstand the variations of the human body.

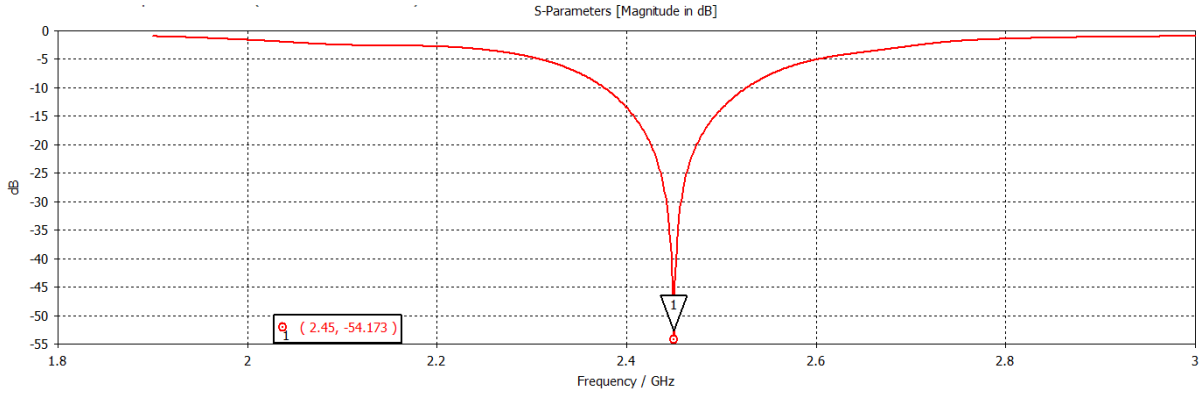


Figure 3.45: $S_{11}$ parameter for Parasite patch antenna: Final antenna design with cubic chest model.

Table 3.16: Patch slot antenna parameters after the holes for screws.

| Parameter | Wpatch | Lpatch | FP | Lparasite1 | Wparasite1 | Lparasite2 | Wparasite2 | Dxparasite1 | Dxparasite2 | Dyparasite1 | Dyparasite2 | Dslot | Lslot | Wslot |
|---|---|---|---|---|---|---|---|---|---|---|---|---|---|---|
| Value (mm) | 33 | 32.67 | 5.1 | 20.05 | 5.16 | 8.66 | 4.94 | 19.11 | 8.34 | 16.78 | 10.64 | 19 | 41.8 | 4 |

### 3.4.1 Variation of the human body layers

As discussed in the 2.2.5.1 section, the layers of the human body will vary depending on a person's age, gender, and physical constitution. In order to create a standard antenna model it is necessary that its matching is maintained whatever the subject who uses it. To do this, we varied the layers of the human body, presented in section 3.2.1.2, and checked their influence on the antenna's behavior. According to what has been discussed in the 2.2.5.1 section, the skin will have an average thickness of 3.6 mm, of the first 3 layers of the body this will have the least variation since for the study area, the human chest, the skin thickness will not have large variations. In order to cover some more unusual cases the skin thickness varied between 1.8 and 4.3 mm with the results of the parameter $S_{11}$ being presented in Figure 3.46.

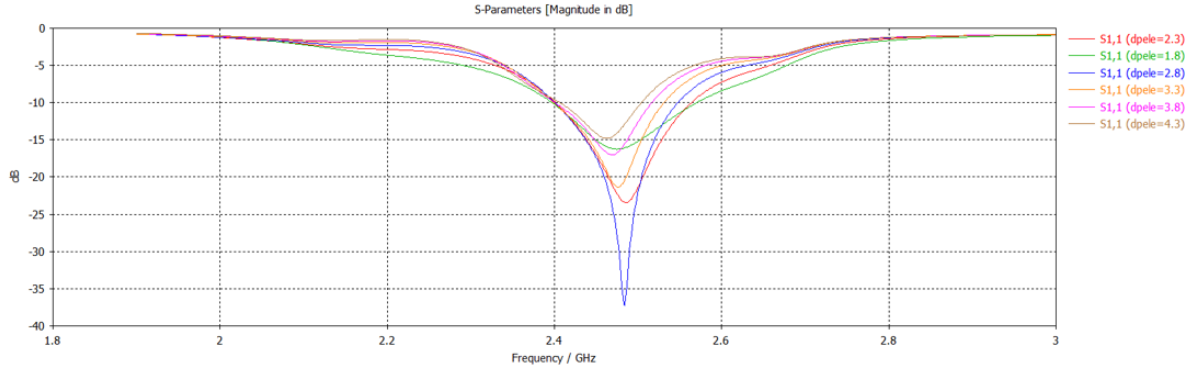


Figure 3.46: Variation of $S_{11}$ with variation of skin thickness.

As can be seen in Figure 3.46 the variation in skin thickness will cause the $S_{11}$ to vary as well as a shift in the resonant frequency of the antenna. This is the expected behavior since the skin presents a much higher $\epsilon_r$ value than the antenna components and since it is the first contact of the antenna with the human body its variation will have the greatest impact on the antenna matching. Although there are variations in the antenna's matching, it should be noted that the matching required for its proper functioning is maintained, even for the most extreme cases.

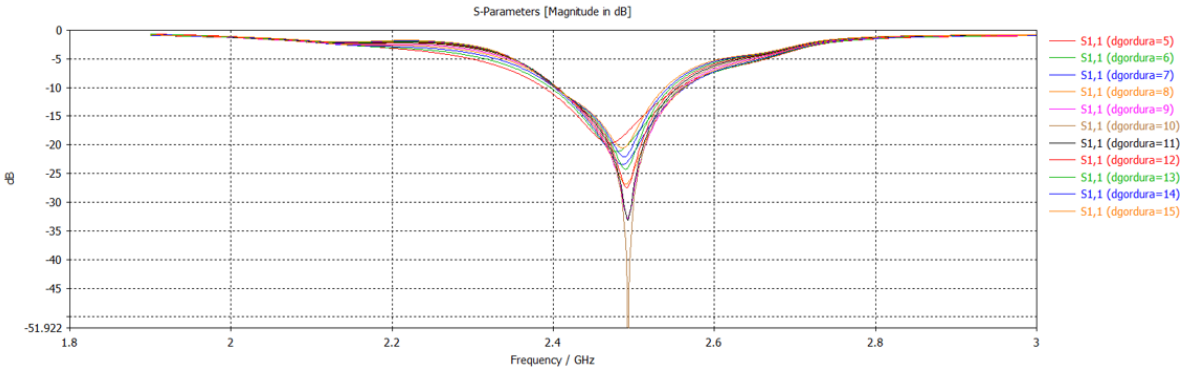


Figure 3.47: Variation of $S_{11}$ with variation of fat tissue thickness.

The second layer of the human body to be studied was the adipose layer. Of the three initial layers of the body, this is the one that presents the lowest value of $\epsilon_r$ and the one that is closest to the $\epsilon_r$ value of the antenna components. By analyzing the Figure 3.47 it is possible to conclude that, the variation of the fat layer affects the magnitude of the parameter $S_{11}$ and causes a small variation in the resonance frequency but never getting close to the mismatching, with the worst value, at 2.45 GHz, being -20 dB.

The last layer to be studied was the muscle layer. Of the three layers, this will be the one furthest from the antenna but also the one with the worst propagation conditions, due to its dielectric properties. The muscle layer was then varied with the results being shown in Figure 3.48. It can be seen that varying the thickness of the pectoral muscle will have an impact on the adaptation of the antenna, although this impact is not compromising to the operation of the antenna at 2.45 GHz.

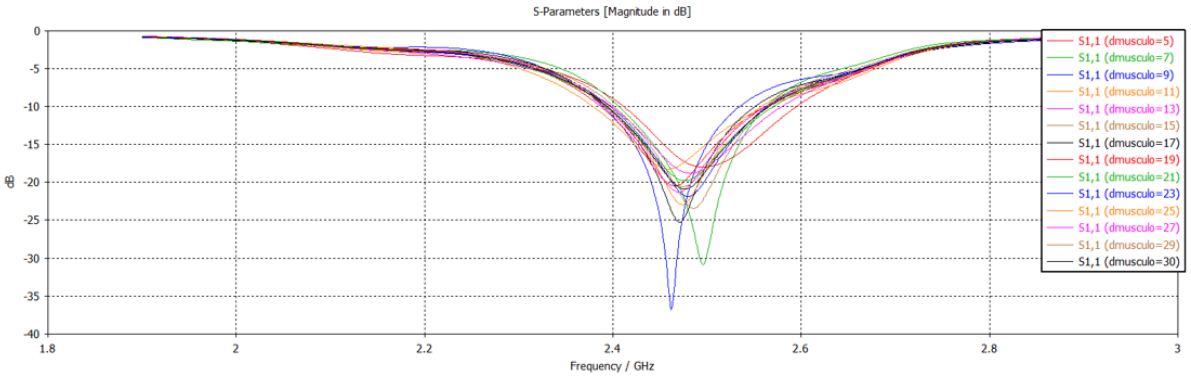


Figure 3.48: Variation of $S_{11}$ with variation of muscle thickness.

After analyzing the variation of the first 3 layers it can be concluded that they will have an impact on the antenna adaptation. In the simulation environment, the antenna always maintained the necessary adaptation to work in contact with the body, at 2.45 GHz. This behavior may not occur in real experimental environment, since there are variables that were not taken into account in these simulations as well as elements of the human body, including the presence of blood vessels. The experimental behavior of the antenna will be discussed later in this document.

### 3.4.2 Cardiac and respiratory rhythm detection

As presented in the 2.2.2 section, it is possible to detect heart and respiratory rhythm through the use of an antenna placed in contact with the body. Throughout the respiratory movement there will be a variation in the volume of air present in the lungs. This variation lead, to a change in their size. The different volumes of the lung will cause variations in their dielectric properties. The same happens for cardiac movement, the movement of the heart along the beats allows the detection of the heart rhythm. By analyzing the phase variation of the reflection coefficient ($S_{11}$) it is then possible to perform the detection of the cardiac and respiratory signals.

#### 3.4.2.1 Respiratory movement

The respiratory movement is responsible for the entry of air into our body and the consequent oxygenation of the cells as well as the elimination of the resulting carbon dioxide. This body movement will cause variations, of approximately 15 mm, throughout the entire movement, in the dimensions of the lungs [5, 62]. With the length of the lung being the parameter that vary the most. The variation in the volume of the lungs can be approximated by varying their width, length and thickness, as shown in Figure

3.49. In this section will be presented the variations of the phase of the $S_{11}$ parameter obtained, on CST, when the volume and dielectric properties of the lungs change.

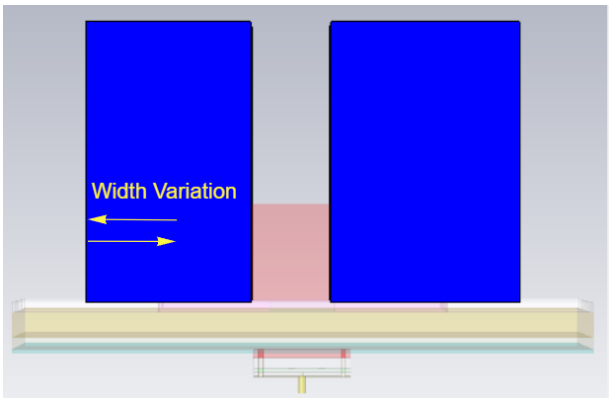


(a) Width variation;

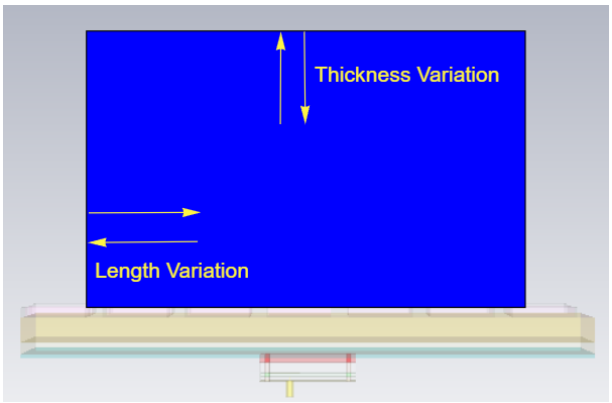


(b) Length and thickness variation;

Figure 3.49: Variation in lung dimensions.

During the study of the impact of the slots on the ground plane it was found that the variation of its width would influence the phase behavior of the reflection coefficient. Initially, and considering the values presented in the Table **??**, it was found that the resonance frequency (2.45 GHz) was in a discontinuity zone. It is then possible to conclude that the introduction of the slots into the ground plane causes the creation of discontinuity zones. A discontinuity zone is where there will be abrupt variations in the values of the phase of the $S_{11}$ parameter. That said, it is not a good decision to have the resonance frequency in this zone, since throughout the breathing motion the phase may vary in the discontinuity zone achieving incorrect results.

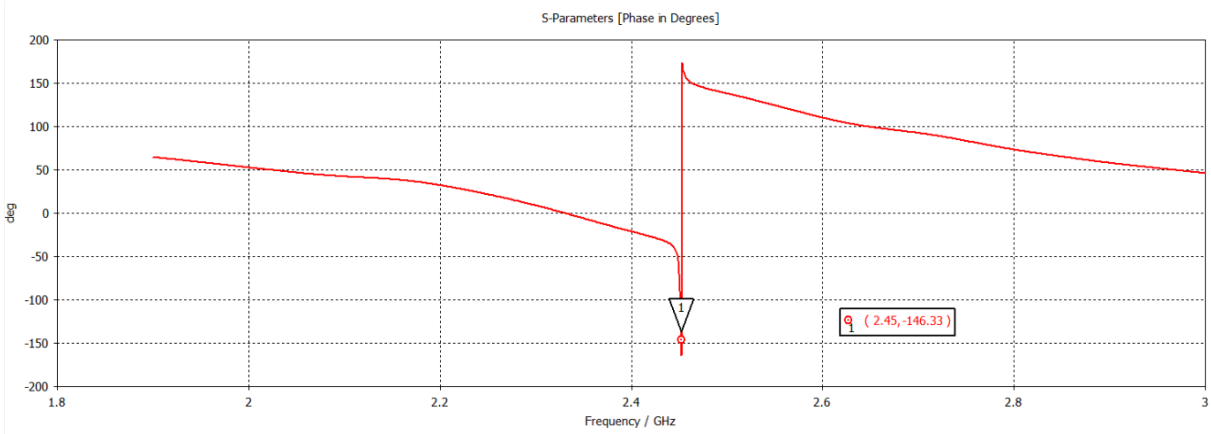


Figure 3.50: Discontinuity zone in the reflection coefficient phase.

The slots of the ground plane were then resized, along with the main patch in order to maintain the necessary matching of the antenna and avoid the existence of discontinuity zones. After resizing the antenna, the $S_{11}$ phase is shown in Figure 3.51 with the parameters changed shown in Table 3.17.

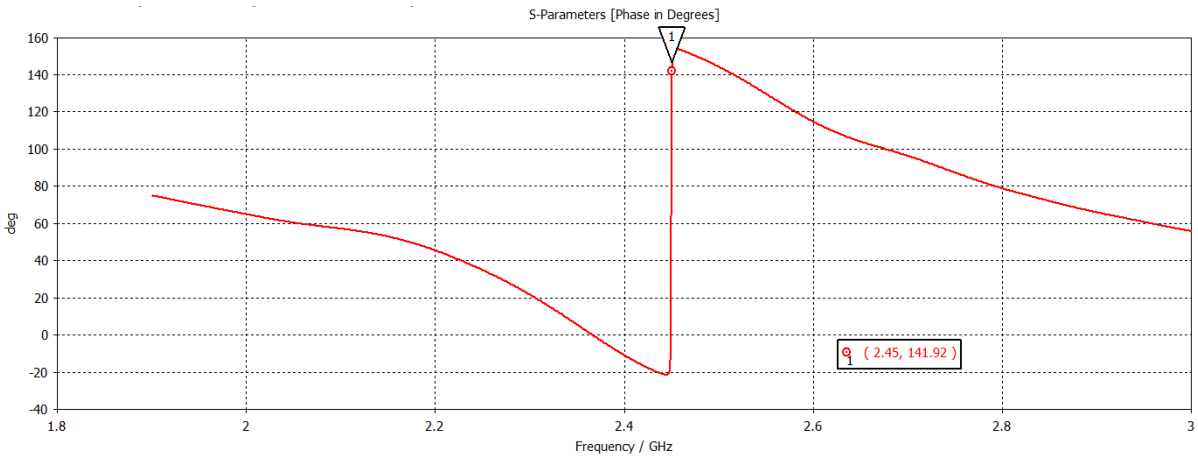


Figure 3.51: $S_{11}$ phase for the final antenna.

Table 3.17: Ground plane slots parameters after resizing.

| Parameter | Wpatch | Lpatch | Wslot |
|---|---|---|---|
| Value (mm) | 32.48 | 32.77 | 3.5 |

The first test consisted of varying the length of the lung throughout the breathing motion. For this, its length was varied by 15 mm, thus decreasing its value (since the model was built with the lungs full). In order to get as close as possible to reality, the whole model will adapt to the variations of the lungs. In order to simulate the respiratory movement, a linear regression was created where the dielectric properties of the

lungs will vary with the variation of their dimensions, following what is presented in Table 3.4. In Figure 3.52 the behavior of the phase with the variation of the lung length is presented, and its specified values are presented in Table 3.18.

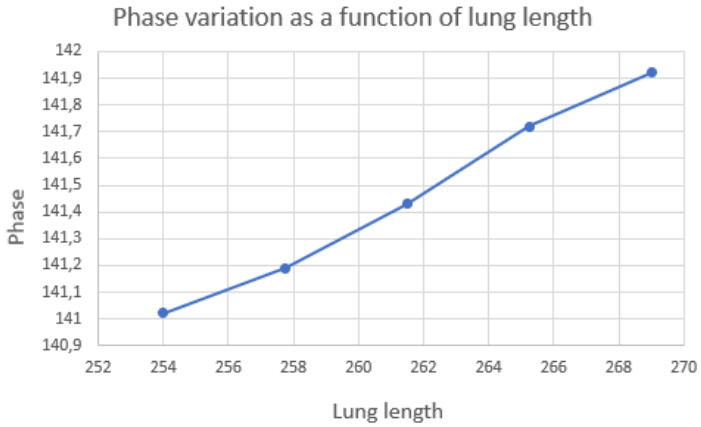


Figure 3.52: Phase variation when varying the lung length.

Table 3.18: Length variation parameters.

| Length Lung (mm) | 269 | 265.25 | 261.5 | 257.75 | 254 |
|---|---|---|---|---|---|
| Phase (°) | 141.92 | 141.72 | 141.43 | 141.19 | 141.02 |

As can be seen in Figure 3.52 the initial value of the phase (empty lung) is lower than the final value (full lung). Although the phase variation caused by the variation in lung length is small, approximately 0.9°, through this test it was possible to verify that the changes in dielectric properties together with the variation in the length of the lungs, will cause variations in the phase of the parameter $S_{11}$.

In continuation of the respiratory motion simulation, the variation of lung thickness was then simulated. As stated in [29] the lung thickness will vary 12 mm, between the empty and full position. In this case a linear regression was also created that allows the variation of the dielectric properties as a function of lung thickness. In Figure 3.53 the phase variation curve is shown, with the values shown in Table 3.19 . As it is possible to observe the thickness variation is not in the discontinuity zone, since there is a linear behavior of the phase. As in the length variation the phase variations here are small as well, approximately 0.7°. Despite these small variations it is verified that the antenna is able to detect the phase variations caused by the lung thickness variation.

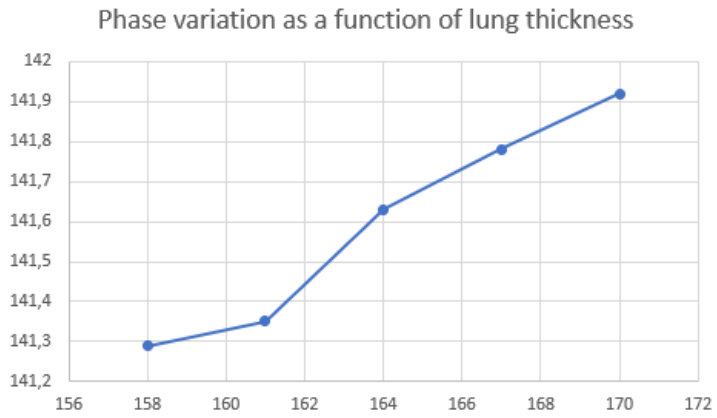


Figure 3.53: Phase variation when varying the lung thickness.

Table 3.19: Thickness variation parameters.

| Thickness Lung (mm) | 170 | 167 | 164 | 161 | 158 |
|---|---|---|---|---|---|
| Phase (°) | 141.92 | 141.78 | 141.63 | 141.35 | 141.29 |

The final dimension studied was the lung width, of the 3 this will be the one with the smallest variation [62], a variation of 3 mm is considered. In Figure 3.54 the variation of the phase as a function of the lung width is presented, it is possible to verify that the variation of the width will cause small variations in the phase of parameter $S_{11}$, approximately 0.4° as shown in Table 3.20.

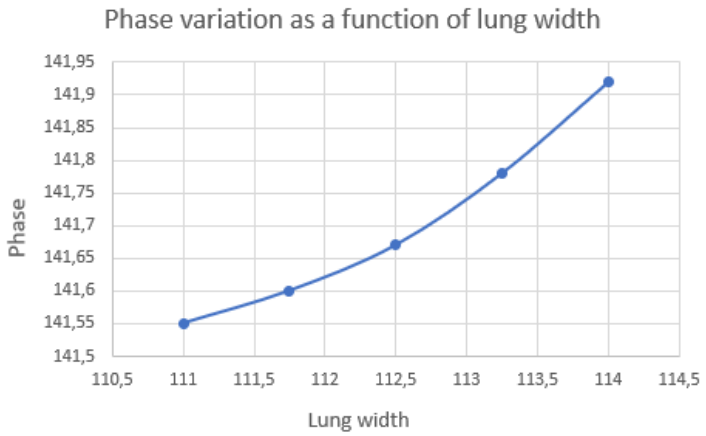


Figure 3.54: Phase variation when varying the lung width.

Table 3.20: Width variation parameters.

| Width Lung (mm) | 114 | 113.25 | 112.5 | 111.75 | 111 |
|---|---|---|---|---|---|
| Phase (°) | 141.92 | 141.78 | 141.67 | 141.6 | 141.55 |

This concludes the study of the phase variation of the reflection coefficient along the respiratory motion. Although these variations are small, with their values being presented in the Table 3.21, the designed antenna proved to be able to detect them.

Table 3.21: Total phase variation for the lungs.

| | Length | Thickness | Width |
|---|---|---|---|
| Phase variation (°) | 0.9 | 0.7 | 0.5 |

The final antenna parameters can be seen in Table 3.22.

Table 3.22: Patch slot antenna final parameters.

| Parameter | Wpatch | Lpatch | FP | Lparasite1 | Wparasite1 | Lparasite2 | Wparasite2 | Dxparasite1 | Dxparasite2 | Dyparasite1 | Dyparasite2 | Dslot | Lslot | Wslot |
|---|---|---|---|---|---|---|---|---|---|---|---|---|---|---|
| Value (mm) | 32.48 | 32.77 | 6.6 | 20.05 | 5.16 | 8.66 | 4.94 | 19.11 | 8.34 | 16.78 | 10.64 | 19 | 41.8 | 3.5 |

### 3.4.2.2 Cardiac movement

The cardiac movement is the performance of the human heart from the beginning of one heartbeat to the beginning of the next. It consists of two periods: one during which the heart muscle relaxes and refills with blood, following a period of robust contraction and pumping of blood [63]. For the cardiac motion only the variation of the heart dimension, namely the thickness, was performed, since not enough information was found on the variation of dielectric properties throughout the cardiac motion. Therefore, it is presented in Figure 3.55 the variation that will be performed to the heart.

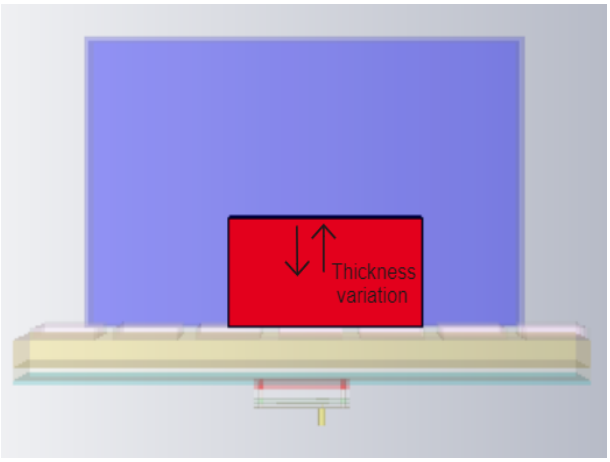


Figure 3.55: Variation of the heart dimensions.

The heart during the beat will vary about 0.5 mm [29], it was then considered heart at

its maximum size then reducing its size and verifying the phase differences obtained and presented in the Figure 3.56 and Table 3.23.

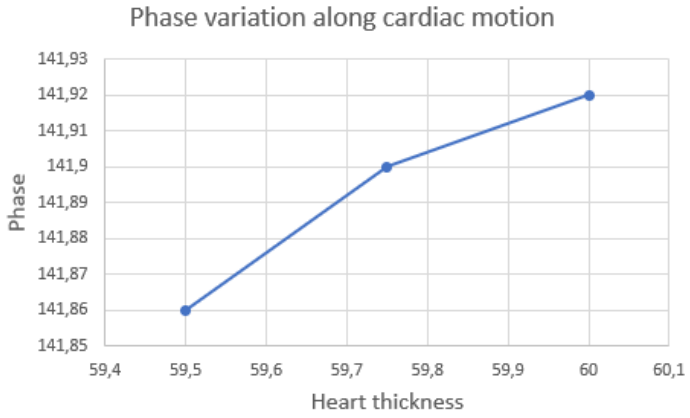


Figure 3.56: Phase variation when varying the heart thickness.

By analyzing the results obtained it is possible to verify that the phase variations caused by the movement of the heart are very low, approximately 0.06 ° .Although the phase variations are very small, it proves that the developed antenna is capable of detecting the phase variations caused by the movement of the heart.

Table 3.23: Heart thickness variation results.

| Heart thickness | 60 | 59.75 | 59.5 |
|---|---|---|---|
| Phase (°) | 141.92 | 141.9 | 141.86 |

# 4

# Experimental results

The cardiopulmonary antenna, previously developed and presented in section **??**, was built and tested at the Aveiro Telecommunications Institute. A PNA-X (Phase network Analyzer) equipment was used for the tests. During the antenna testing phase, it was possible to detect the vital signs in all the tested subjects. This chapter will explain the process of obtaining vital signs, starting with the configuration of the capture system and then presenting the results and conclusions.

## 4.1 Configuration of the measurement system

In order to analyze the variation of the antenna phase it is necessary to have a VNA (Vector Network Analyser) for that, this equipment is presented by Figure 4.1. Using a PNA-X (N5242A) from Keysight, it is then possible to analyze the phase variation of the reflection coefficient of the antenna in real time, during a given time interval and a given sampling frequency. This equipment produces a data file with the phase variation of the antenna's reflection coefficient, with the data being processed using a script developed in MATLAB.

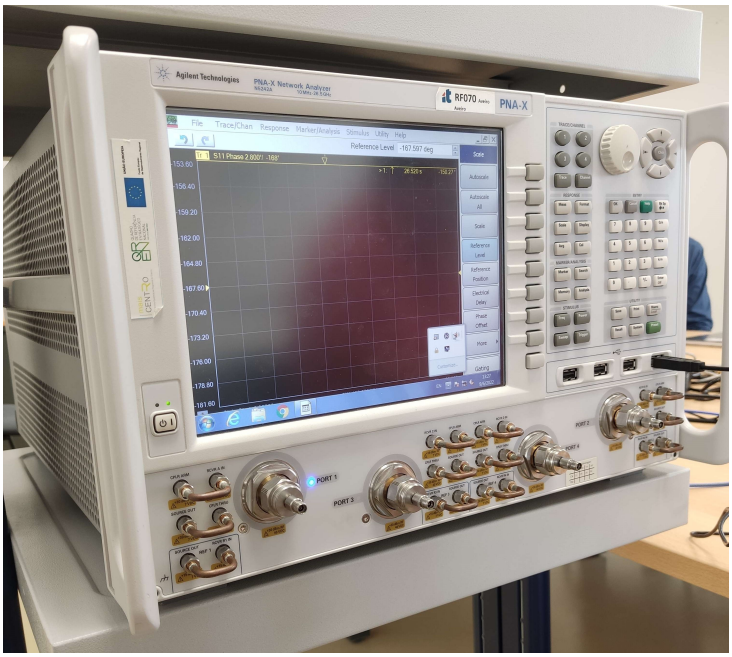


Figure 4.1: PNA (Phase Network Analyzer).

To verify and confirm the veracity of the results obtained, it is necessary to have a term of comparison. With that said, the next phase of the preparation for obtaining vital signs is to prepare the BIOPAC system, as seen in Figure 4.2. With the help of a computer, a BIOPAC system is capable of performing real-time monitoring of a person's vital signs [64]. The system used consisted of the use of a respiratory band with a transducer as can be seen in Figure 4.2b. The chest band must placed over the diaphragm and will register the variations of the perimeter of the thoracic area of the subject during the breathing movement.

(a) BIOPAC MP36;

(b) BIOPAC respiratory band;

Figure 4.2: BIOPAC system for vital signs monitoring [64].

The respiratory band will be connected to a system, as shown in Figure 4.2a, that will process the captured information and present it on the BIOPAC Student Lab 4.1 software.

The final test system will then consist of the subject where the vital signs are being measured using the developed antenna, and at the same time the subject will have the respiratory band on and his or her vital signs will also be monitored by the respiratory band. After the acquisition of signals through the two systems, the data is post-processed and evaluated in MATLAB. The final setup can be seen in Figure 4.3.

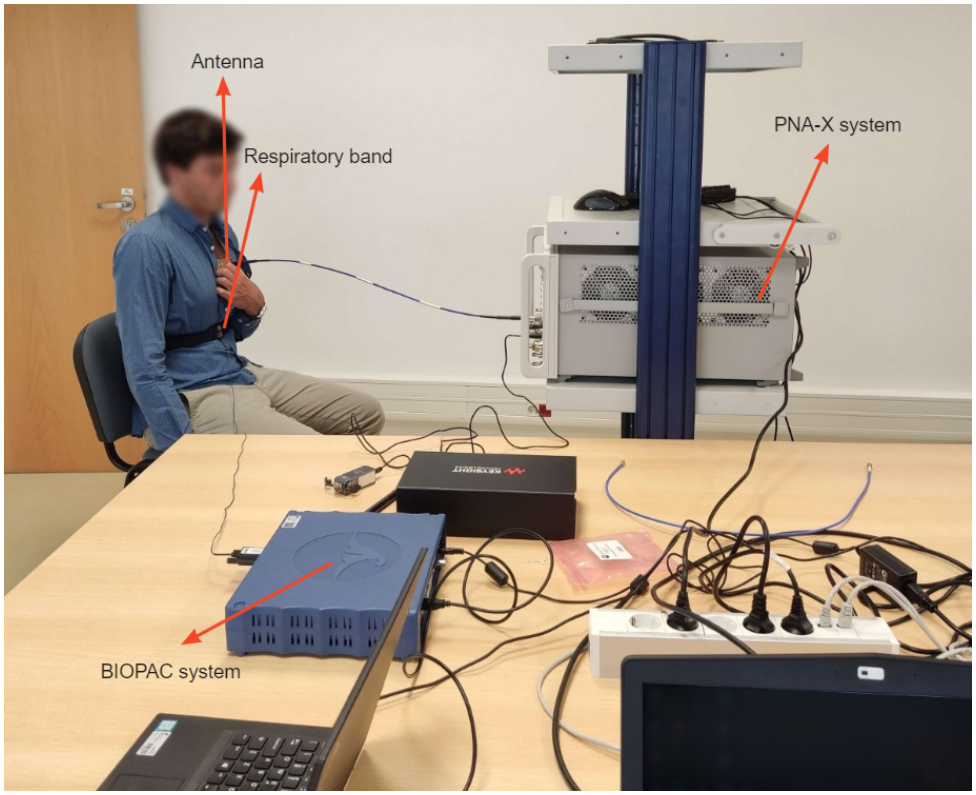


Figure 4.3: Experimental setup.

## 4.2 On-body antenna performance results

Moving from the simulation environment to the practical environment, the developed antenna was then built. As shown in Figure 4.4, the built antenna has a square dimension of 60x60x15 mm (size of the substrate plates), presenting a great robustness in terms of size due to the high number of layers that constitute it. The dimensions of the elements of the built antenna are the ones mentioned in Table 3.22.

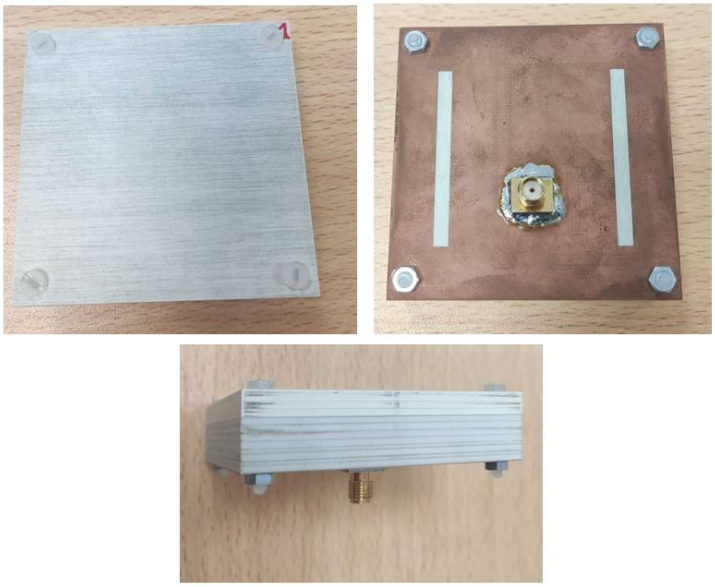

Figure 4.4: Cardiopulmonary antenna built.

To ensure that the results obtained by the PNA-X are correct, it is necessary to perform its calibration for 2.45 GHz. For this a Keysight N7555A CalKit automatic calibrator was used, like the one shown in Figure 4.5. The PNA-X was also calibrated to make measurements in the frequency range between 1.9 and 3 GHz and with a power of -10 dBm.


Figure 4.5: Electronic toolkit for VNA calibration [65].

After the PNA-X calibration process, the antenna was then connected to the equipment and measurements of its reflection coefficient ($S_{11}$) were performed, in a first phase the antenna was tested operating in free space and later in contact with the human body. As one would expect the matching levels of the antenna when operating in free space are poor, as shown in Figure 4.6 and although it is matched, the value of $S_{11}$ is around

the matching threshold (-10 dB). This is the expected behavior for this antenna since it was matched to operate in contact with the human body and not in free space.

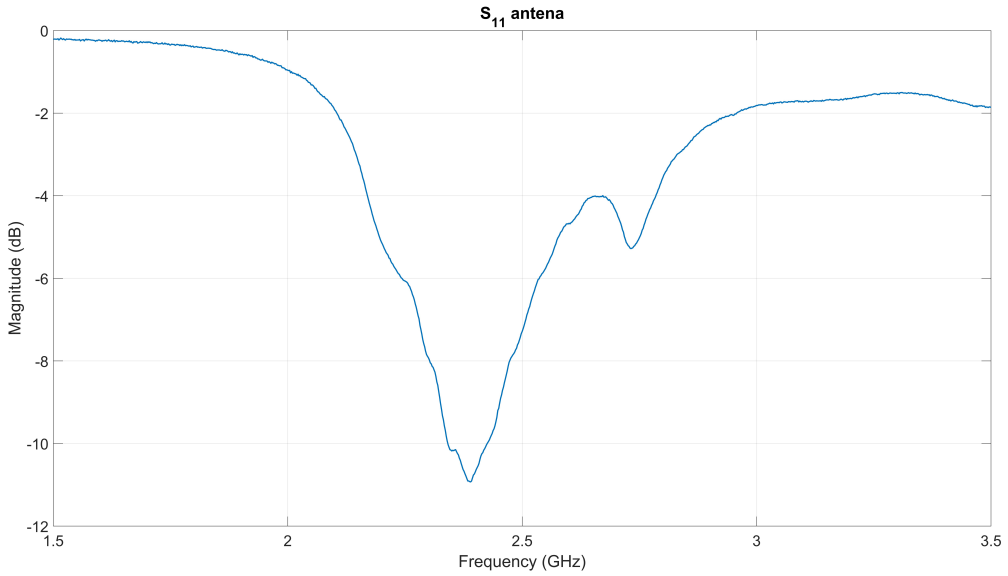


Figure 4.6: $S_{11}$ on free space.

After the first test conducted in free space, the operation of the antenna in contact with the body was tested by analyzing its reflection coefficient. For this purpose the antenna was tested on 5 different subjects, each with different body characteristics. This aspect is very important for this project since it is necessary to ensure that the antenna can, not only be matched, but also monitor vital signs in any person. For each subject the chest perimeter was measured, this measurement was performed in the armpit area since it is in that region of the chest that the antenna will be placed, the height was also measured and the test subjects were weighed, thus being able to calculate the BMI of each one, the data obtained are presented in Table 4.1. It should also be mentioned that the fact that women have a different chest physiognomy than men has been taken into account. In order to verify the functioning of the antenna subjects 3 and 4 are women.

Table 4.1: Physical characteristics of test subjects.

| | Rib cage perimeter (cm) | BMI | Gender |
|---|---|---|---|
| Subject 1 | 94 | 22.4 | M |
| Subject 2 | 95 | 23 | M |
| Subject 3 | 78 | 18.7 | F |
| Subject 4 | 89 | 22.5 | F |
| Subject 5 | 110 | 30 | M |

This was followed by the measurement of the parameter $S_{11}$, for which the antenna was positioned on the left side of the chest, above the heart. It was found that as the antenna was moved along the chest the matching of the antenna varied as well as its resonant frequency, after positional stabilization of the antenna. The first measurement of parameter $S_{11}$ was then taken and presented in Figure 4.7, it can be seen that there was a shift of the resonance frequency to approximately 2.55 GHz, this behavior is expected since the antenna was developed in a perfect environment (CST simulation environment) where it is not possible to take into account all the variations that the antenna will suffer in the real world. Despite the resonance frequency shift, the antenna is still very well suited for the ISM frequency band.

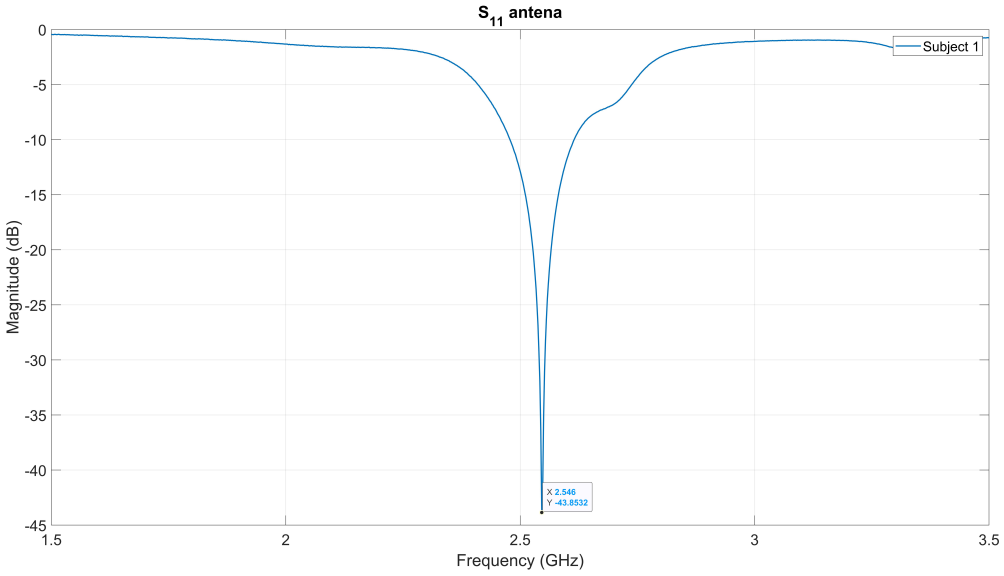


Figure 4.7: $S_{11}$ in contact with the human body - Subject 1.

The variations observed are due to the different constitutions of the various layers of the human body in each position, which may or may not be favorable for antenna

matching. It is therefore possible to conclude that the positioning of the antenna is a crucial aspect in these tests, and a frequency of 2.55 GHz was also considered for future tests, since for this frequency the antenna have a good match for all subjects. The measurement of the parameter $S_{11}$ was then performed for all 5 subjects. For each subject it was necessary to adjust the position of the antenna as well as the force with which it was placed against the body, since this aspect also has an influence on the matching of the antenna. In Figure 4.8 the parameter $S_{11}$ is presented for the 5 subjects, the results obtained were as expected, since it was expected that each subject would present different matching levels given the different physiognomies of each one of the subjects.

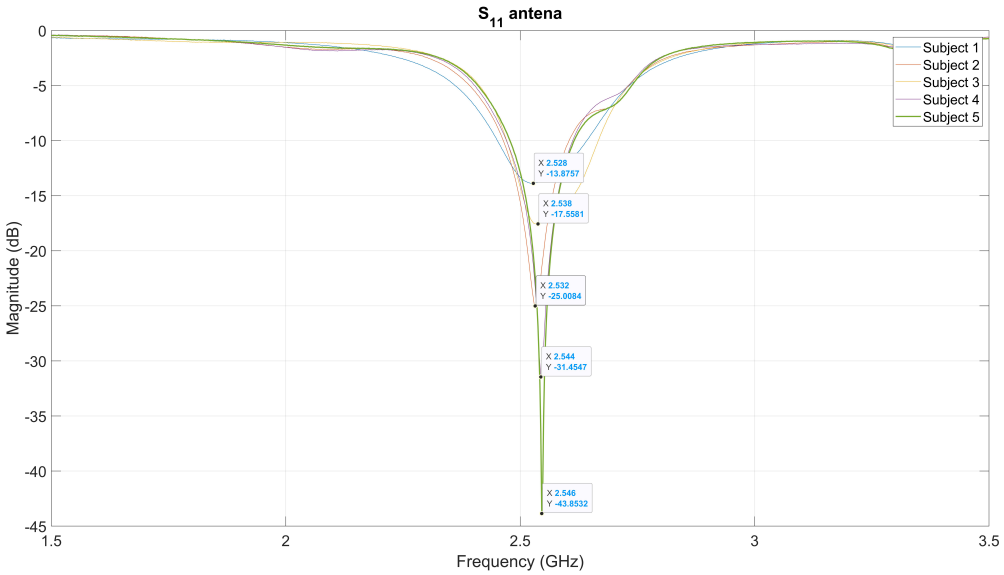


Figure 4.8: $S_{11}$ in contact with the human body - Multiple subjects.

## 4.3 Vital signs monitoring

After checking the performance of the antenna in contact with the human body, the vital signs were measured. For this test new parameters were defined in the PNA-X, namely, the sampling frequency and the test duration, as presented in Table 4.2. For the monitoring of the vital signs a temporal sweep was performed for the 2.55 GHz frequency.

Table 4.2: PNA-X parameters to vital sign detection.

| | |
|---|---|
| Sampling Frequency (Hz) | 16.67 |
| Power (dBm) | -10 |
| Sampling time (s) | 60 |

For extraction of the respiratory rhythm, the antenna was positioned at various locations on the chest in order to get the best possible signal from the PNA-X. After finding the ideal location, the subject was asked to keep the antenna in the same position and breathing calmly until the end of a sampling cycle; at the beginning of the experiment the subject took a deep breath and held his breath for 5 seconds, thus allowing a synchronization of the VNA and BIOPAC signals obtained during post-processing. The phase variation of the reflection coefficient captured by the PNA-X in subject 1 is shown in Figure 4.9. Despite the existence of some noise in the captured signal, it is possible to verify the existence of 10 peaks related to the subject's breathing, thus proving the ability of the antenna to monitor the respiratory rhythm.

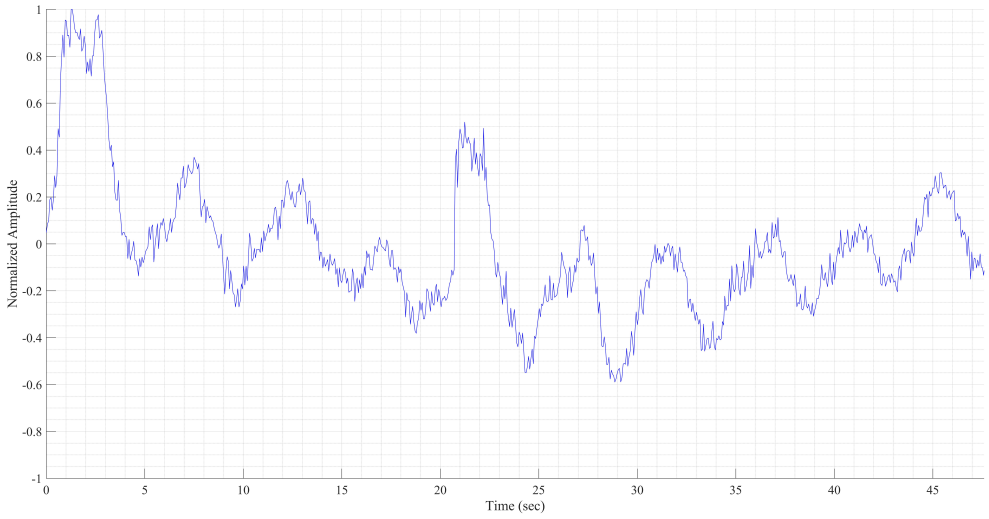


Figure 4.9: Respiration rhythm detect by the VNA - Subject 1.

Measurements were made on all subjects with the antenna and at the same time using the BIOPAC so that a comparison between the results could be made. In Figure 4.10 shows the results obtained by the antenna and the BIOPAC for subject 1. After normalization and synchronization of the signals, it can be seen that the signals are quite identical, presenting the same respiratory rhythm. The differences obtained between the two signals can be explained due to the higher quality of signal capture that

the BIOPAC has. The difficulty in ensuring that the antenna is not influenced by the surrounding environment during measurements is also a factor that influences the captured signal, another factor of influence may be the interference caused by the subject holding the antenna with his hand and lean it against the body, since the influence of the hand can be a factor of mismatching for the antenna. In an ideal case, the antenna would be placed in an immobile place and the subject would be the one approaching it.

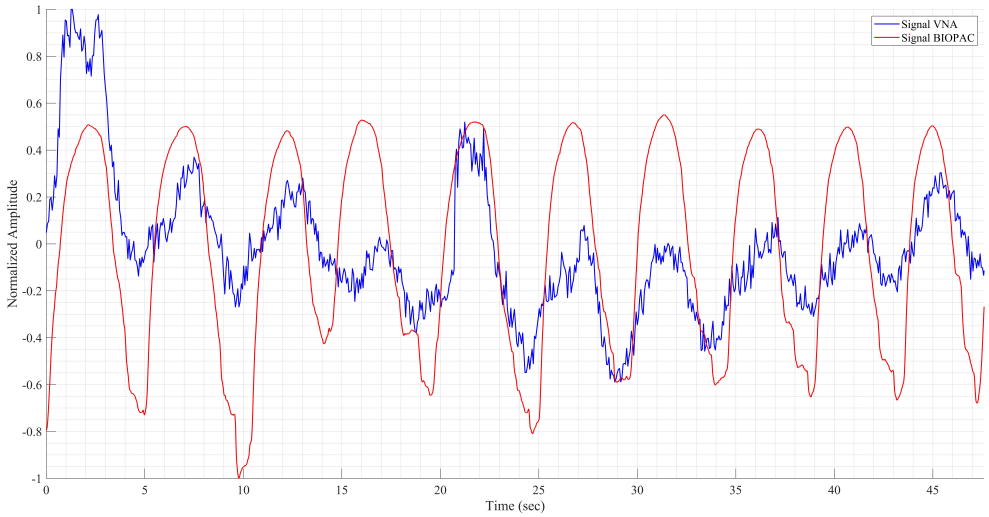


Figure 4.10: Respiration rhythm - Subject 1.

Although the antenna has been shown to be able to pick up the respiratory rate for the subject, it needs to be ensured that it can detect it for all subjects. As can be seen in Figure 4.11, the signal captured in subject 2 has high noise levels, although it is still possible to detect his breathing rhythm. The noise for this subject in particular, can be explained due to the difficulty he had in keeping the antenna fixed in the same position, having been performed several attempts, with the presented one being the one where the best results were obtained.

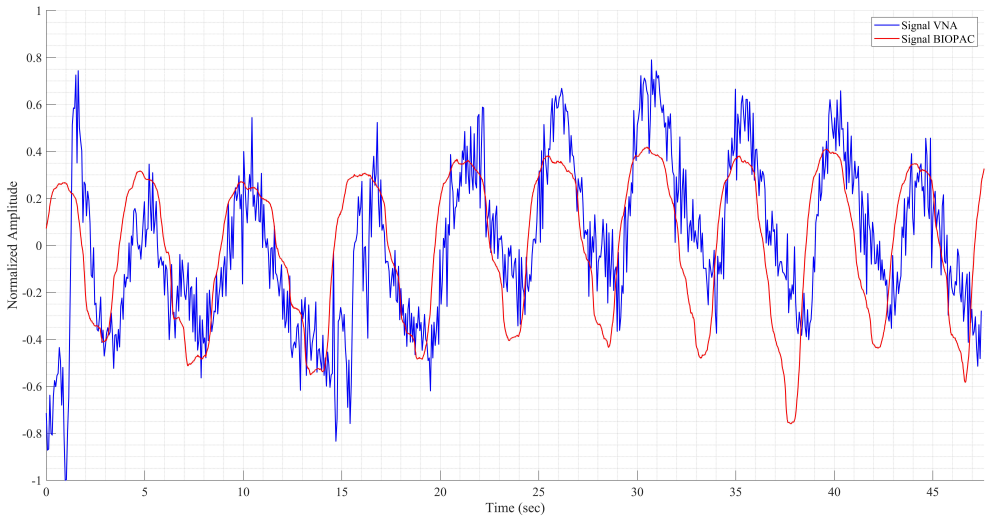


Figure 4.11: Respiration rhythm - Subject 2.

As shown in Figure 4.12 it was possible to capture the respiratory rhythm through the antenna, coinciding also with the signal captured by the BIOPAC. During the capture of the respiratory rhythm for subject 3 it was found that this was where the noise levels captured by the antenna were the lowest. This can be explained by the fact that subject 3 has the lowest BMI value and since the layers will have a smaller thickness, reducing the influence of the human body it is possible to achieve clearer signals.

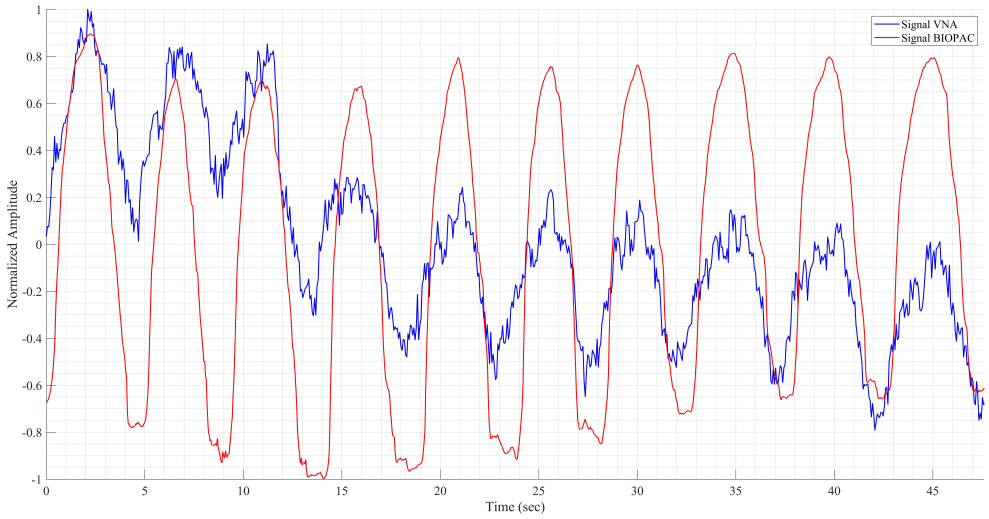


Figure 4.12: Respiration rhythm - Subject 3.

During the capture of the breathing rhythm of subject 4 it was found that this was

the subject that maintained the calmest breathing, as the number of inspirations and expirations performed was the lowest during the sampling period. The detection of the respiratory rhythm was once again proven, as shown in Figure 4.13.

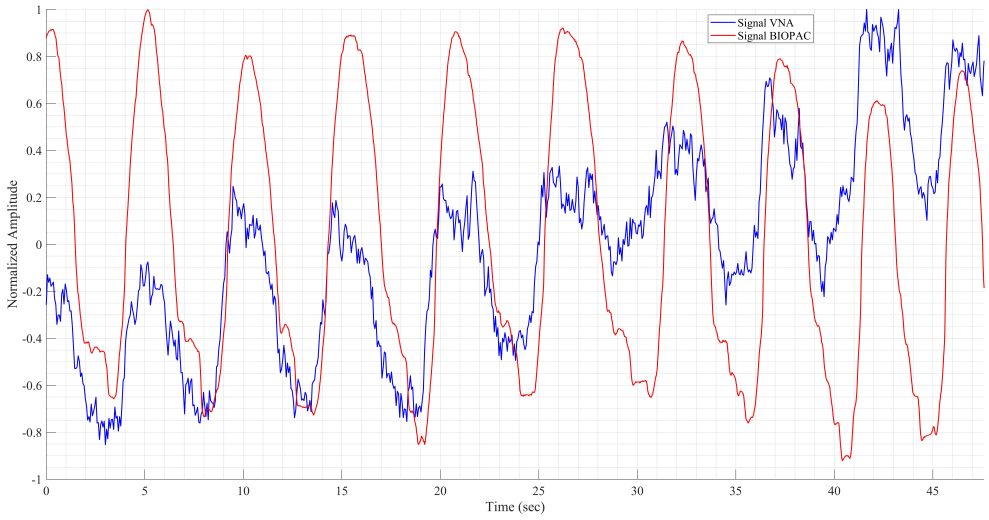


Figure 4.13: Respiration rhythm - Subject 4.

Unlike subject 4, subject 5 was the one who maintained more rapid breathing throughout the test. Although this subject had the highest chest circumference and BMI and consequently the greater amount of body mass between the antenna and the human body, this did not prove to be an obstacle for the antenna to detect the breathing rhythm, as shown in Figure 4.14.

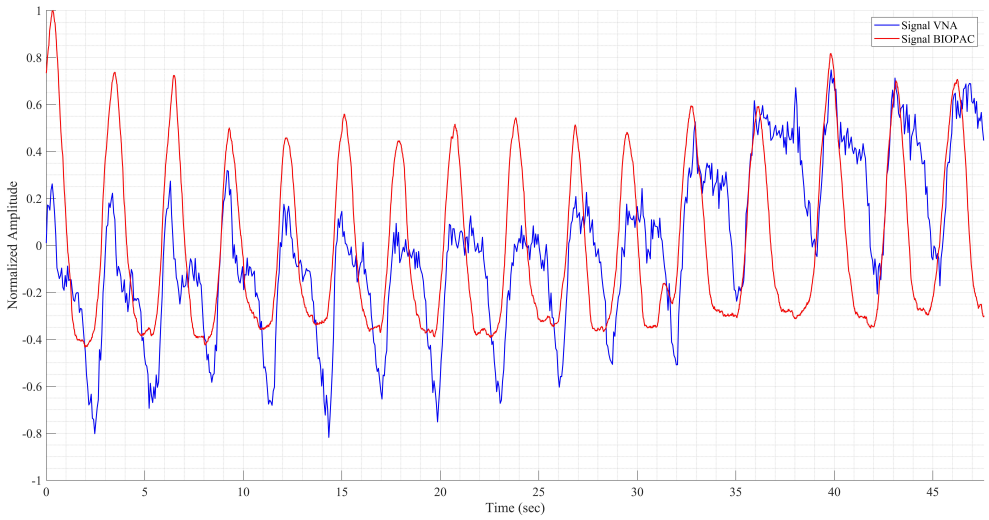


Figure 4.14: Respiration rhythm - Subject 5.

A healthy individual in normal conditions (without physical or psychological exertion) has a respiratory rate between 12 and 20 breaths per minute [66], which can reach values of 25 breaths per minute in cases of physical exertion or high levels of stress [67]. For each subject, the respiratory rate was then calculated using equations (4.1) and (4.2).

$$\Delta t = \frac{t_2 - t_1}{N_i} \tag{4.1}$$

$$F_B = \frac{1}{\Delta t} \times 60[bpm] \tag{4.2}$$

Where:

$t_1$ = Represents the peak value of the initial instant;

$t_2$ = Represents the peak value of the final instant;

$N_i$ = Number of peaks between $t_1$ and $t_2$;

The results presented in Table 4.3 consolidate the measurements performed of the respiratory rhythm, also proving the good operation of the antenna in detecting the heart rhythm, since the respiratory rhythms obtained by the antenna and by the BIOPAC are practically identical, as proved by the values of MAE (Mean Absolute Error) and RMSE (Root Mean Square Error). It is possible to verify that subjects 2 and 4 have the lowest respiratory rhythms, being a little below the average. Subject 5 has, by some margin, the fastest respiratory rate, being a little above the average.

Table 4.3: Respiratory rhythm for all subjects.

| | Respiratory rhythm PNA-X (bpm) | Respiratory rhythm BIOPAC (bpm) | Mean Absolute Error |
|---|---|---|---|
| Subject 1 | 16.34 | 16.84 | 0.166 |
| Subject 2 | 11.35 | 11.13 | |
| Subject 3 | 14.03 | 14.08 | |
| Subject 4 | 11.6 | 11.61 | |
| Subject 5 | 20.99 | 21.04 | |

The values obtained during the experimental process assimilate with those obtained through the simulations. The differences obtained can be justified by the fact that in the simulation process there are some aspects that cannot be taken into account, namely the influence of external factors, in particular the difficulty of keeping the antenna always in the same position throughout the measurements. The presence of the blood vessels may also be a reason for the noise present in the results obtained by the antenna. From the Table 4.4 it is possible to verify this. Although the phase variations observed are small, it was possible to obtain the respiratory rhythm for all subjects.

Table 4.4: Comparison between phase variations of experimental and simulated values.

| | Experimental phase variation | Simulated phase variation |
|---|---|---|
| Mean value (°) | 0.86 | 0.733 |

With these tests it was possible to conclude that the sized and built antenna fulfilled its objective of detecting the respiratory rhythm, regardless of the person who used it.

# 5

# Conclusions and Future work

## 5.1 Conclusion

The main objective of this dissertation was to develop a robust cardiopulmonary antenna, on the ISM band of 2.45GHz, that would allow the detection of vital signs in any subject, regardless of their physical constitution. Thus, we tried to fill a gap in the bibliography regarding the use of on-body antennas for vital signs monitoring. The developed antennas were simulated using the CST Studio Suite 2019 software.

Firstly, the study of traditional methods for vital signs monitoring was performed, verifying that, although these are reliable methods and used worldwide, for certain types of patients they may not be the most adequate, being necessary the development of alternative methods where the antenna developed is included.

Next, a review of the literature on the use of On-Body antennas to vital signs monitoring as well as the influence of the human body on this antennas was performed. This study was fundamental in the choice of the type of antenna to be used. The authors reported important characteristics that an antenna should have in order to work in contact with the human body, namely a ground plane that covers the entire antenna with the microstrip patch antenna being presented as the best option. The human body will be the biggest obstacle to the antenna matching. The different dielectric properties of each layer, as well as different thicknesses for each person, make creating a standard antenna type a challenge.

To ensure that the antenna could be matched to the body, it was necessary to make changes to the design of a conventional patch antenna. The contact of the radiating element with the body was shown to cause the antenna to completely mismatch. The use of superstrates is critical in this type of applications, as it allows for a smooth transition between propagation medium, considerably decreasing the mismatch caused by the human body.

During the literature review it was found that for certain physiognomies, the antenna operation could be compromised. In order to solve this problem the bandwidth of the antenna was increased. Patch antennas are typically antennas with a small bandwidth with several ways to increase the bandwidth for these antennas being discussed in the literature. Two methods were implemented. The use of a cropped patch was one of them. The cuts made on the patch allowed for a second resonance to be created, thus increasing the bandwidth. Several tests were made, starting with 1 crop and finishing with 4. The best result, regarding the bandwidth, was obtained with 4 crops, achieving values of, approximately, 130 MHz when operating in contact with the human body.

The second method implemented was the use of parasitic patches. An initial study was done using 1 parasitic patch placed on a substrate plate which was placed above the main patch. In further studies the number of parasites was increased up to 4. The use of parasites proved to be similar to the cropped patch, its use creates a new resonance frequency increasing the bandwidth of the antenna to values close to 180 MHz when operating in contact with the human body.

The final step to both methods was the introduction of 2 symmetrical ground plane slots. Its addition allow for the two resonances to come together, increasing the bandwidth and allowing the antenna to keep a better matching. With the studies to both methods completed, it was observed that the parasitic method presented the better results. The bandwidth obtained for the cropped method was considerably lower than the obtained in the parasitic method, 130 and 180 MHz respectively, with the values obtained with the parasitic method being an increase of, approximately 70 % when comparing to a normal microstrip patch antenna. Because of that the cropped method was abandoned.

The capability to detect variation in the phase of the reflection coefficient was then tested. This variations will allow the antenna to monitor the vital signs. Using the CST software a human body model for the human chest was created. This model was created to be as realistic as possible to the actual human chest, with all its layers and components included. Varying the dimensions and dielectric properties of the lungs and heart was possible to detect variations in the phase of the $S_{11}$ parameter. Although

the variations detected were small, 0.9 ° for the lungs and 0.06 ° for the heart, it was possible to verify that the antenna was capable to detect the vital signs.

With the antenna capability of detect the vital signs on a simulation environment confirmed, the antenna was then built and tested. A PNA-X was used and the antenna was tested in 5 different subjects, all of them with different body types, with the antenna keeping its matching to all of the subjects. The subjects used a BIOPAC system that allowed also to monitor the vital signs. Both of the signs obtained were post-processed and compared.

Comparing the results obtained by the antenna with the ones obtained by the BIOPAC, the ability of the antenna to monitor the respiratory rhythm was proved. Using the MATLAB software the respiratory rhythm of all the subjects was calculated. When comparing the respiratory rhythms obtained by the antenna, it is possible to concluded that they are very similar to the ones obtained by the BIOPAC since the MAE value is very small.

Despite the different physiognomies of the test subjects, the antenna not only always maintained its adaptation but was able to monitor the respiratory rhythm of all subjects, facing the obstacles created by the human body and overcoming them.

## 5.2 Future Work

In this dissertation the use of an on-body antenna as a method of monitoring vital signs was studied. The antenna obtained presents a high degree of complexity, given its number of layers of different components. Due to the time limitation of the dissertation it was not possible to verify if there would be a more optimized method for obtaining a high bandwidth patch antenna, and this may be a topic for future development. The reduction of the number of layers of the antenna and consequent optimization of the obtained design can also be a point of improvement in future works, thus reducing the complexity and size of the antenna. To ensure that the antenna works, increasing the number of test subjects will be an option for future tests. With the increase in test subjects it will also be necessary to diversify the age range, also trying to cover as many physiognomies as possible. The incorporation of the antenna in immobile objects, for example a hospital gurney, may result in better results, since the subject or another person will not have to hold the antenna and place it in contact with the body, thus avoiding a point of possible interference in the results obtained.

# References


[1] World Health Organization, *Cardiovascular diseases*, Accessed: 2021-11-25. [Online]. Available: http://www.who.int/cardiovascular_diseases/en/.

[2] Darcy Marciniuk, Tom Ferkol, Arth Nana, Maria Montes de Oca, Klaus Rabe, Nils Billo, and Heather Zar, "Respiratory diseases in the world. realities of today–opportunities for tomorrow", *African Journal of Respiratory Medicine Vol*, vol. 9, no. 1, 2014.

[3] *Electrocardiogram (ecg or ekg): Procedure and results*, https://www.verywellhealth.com/the-electrocardiogram-ecg-1745304, Accessed: 2021-11-25.

[4] Jennifer A. Alison and Frits M.E. Franssen, "Optimizing health in chronic lung diseases: What did we learn from the experts in pulmonary rehabilitation?", *Respirology*, vol. 24, pages 916–917, 9 2019.

[5] Abubakar Tariq, "Vital signs monitoring using doppler radar and on-body antennas", 2013, PhD thesis, University Of Birmingham.

[6] Ehsaneh Shahhaidar, Olga Boric-Lubecke, Reza Ghorbani, and Michael Wolfe, "Electromagnetic generator: As respiratory effort energy harvester", in *2011 IEEE Power and Energy Conference at Illinois*, 2011, pages 1–4. DOI: 10.1109/PECI.2011.5740494.

[7] Andrea A. Serra, Paolo Nepa, Giuliano Manara, Giovanni Corsini, and John L. Volakis, "A single on-body antenna as a sensor for cardiopulmonary monitoring", *IEEE Antennas and Wireless Propagation Letters*, vol. 9, pages 930–933, 2010.

[8] *Multi-functional health patch from imec*, https://www.electronicsweekly.com/news/business/489127-2016-11/, Accessed: 2021-11-30.

[9] *The earliest medical device innovators*, Accessed: 2022-05-05. [Online]. Available: https://www.mddionline.com/rd/earliest-medical-device-innovators.

[10] Yahya and Lingnan Rahmat-Samii Song, "Advances in communication and biomedical antenna developments at the ucla antenna lab: Handheld, wearable, ingestible, and implantable [bioelectromagnetics]", *IEEE Antennas and Propagation Magazine*, pages 102–115, 2021.

[11] Andrea A. Serra, Paolo Nepa, Giuliano Manara, Giovanni Corsini, and John L. Volakis, "A single on-body antenna as a sensor for cardiopulmonary monitoring", *IEEE Antennas and Wireless Propagation Letters*, vol. 9, pages 930–933, 2010.

[12] DL Gorgas and J McGrath, "Vital signs and patient monitoring techniques", *Clinical Procedures in Emergency Medicine: 4th ed.,(JR Roberts and JR Hedges, Eds.), Philadelphia,: Saunders*, pages 3–28, 2004.

[13] David G Wilson, Peter L Cronbach, D Panfilo, Saul E Greenhut, Berthold P Stegemann, and John M Morgan, "Reconstruction of an 8-lead surface ecg from two subcutaneous icd vectors", *International Journal of Cardiology*, vol. 236, pages 194–197, 2017.

[14] Michael V Scanlon, "Acoustic monitoring of first responder's physiology for health and performance surveillance", in *Sensors, and Command, Control, Communications, and Intelligence (C3I) Technologies for Homeland Defense and Law Enforcement*, SPIE, vol. 4708, 2002, pages 342–353.

[15] Eric Derom, Chris Van Weel, Giuseppe Liistro, Johan Buffels, Tjard Schermer, Ernst Lammers, Emiel Wouters, and Marc Decramer, "Primary care spirometry", *European Respiratory Journal*, vol. 31, no. 1, pages 197–203, 2008.

[16] G Ramachandran and M Singh, "Three-dimensional reconstruction of cardiac displacement patterns on the chest wall during the p, qrs and t-segments of the ecg by laser speckle inteferometry", *Medical and Biological Engineering and Computing*, vol. 27, no. 5, pages 525–530, 1989.

[17] Barbara A Phillips, Michael I Anstead, and Daniel J Gottlieb, "Monitoring sleep and breathing: Methodology: Part i: Monitoring breathing", *Clinics in chest medicine*, vol. 19, no. 1, pages 203–212, 1998.

[18] Carolina Teixeira de Sousa Gouveia, "Bio-radar", 2017, Master Thesis, Universidade de Aveiro.

[19] Richard Ribón Fletcher and Sarang Kulkarni, "Wearable doppler radar with integrated antenna for patient vital sign monitoring", *2010 IEEE Radio and Wireless Symposium, RWW 2010 - Paper Digest*, pages 276–279, 2010.

[20] Changzhi Li and Jenshan Lin, "Recent advances in doppler radar sensors for pervasive healthcare monitoring", *2010 Asia-Pacific Microwave Conference*, pages 283–290, 2010.

[21] Akshith Ullal, Bo Yu Su, Moein Enayati, Marjorie Skubic, Laurel Despins, Mihail Popescu, and James Keller, "Non-invasive monitoring of vital signs for older adults using recliner chairs", *Health and Technology*, vol. 11, pages 169–184, 1 Jan. 2021.

[22] Diogo Malafaya, Sara Domingues, and Helder P. Oliveira, "Domain adaptation for heart rate extraction in the neonatal intensive care unit", *Proceedings - 2020 IEEE International Conference on Bioinformatics and Biomedicine, BIBM 2020*, pages 1082–1086, Dec. 2020.

[23] B. Gupta, S. Sankaralingam, and S. Dhar, "Development of wearable and implantable antennas in the last decade: A review", *2010 10th Mediterranean Microwave Symposium, MMS 2010*, pages 251–267, 2010.

[24] Andreas Christ, Anja Klingenböck, Theodoros Samaras, Cristian Goiceanu, and Niels Kuster, "The dependence of electromagnetic far-field absorption on body tissue composition in the frequency range from 300 mhz to 6 ghz", *IEEE Transactions on Microwave Theory and Techniques*, vol. 54, pages 2188–2194, 5 May 2006.

[25] Constantine A Balanis, *Modern antenna handbook*. John Wiley & Sons, 2011.

[26] I. B. Shirokov, I. V. Serdyuk, and R. F. Dubrovka, "Investigation of the dielectric cover influence on the microstrip antenna's characteristics", *2008 4th International Conference on Ultrawideband and Ultrashot Impulse Signals, UWBUSIS 2008*, pages 130–132, 2008.

[27] Manickam Karthigai Pandian and Thangam Chinnadurai, "Design and optimization of rectangular patch antenna based on fr4, teflon and ceramic substrates", *Recent Advances in Electrical & Electronic Engineering (Formerly Recent Patents on Electrical & Electronic Engineering)*, vol. 12, pages 368–373, 4 Jul. 2018.

[28] Anacom, "Icp-anacom autoridade nacional de comunicações qnaf 2008 anexo 1 tabela de atribuição de frequências",

[29] A. Tariq and H. Ghafouri-Shiraz, "On-body antenna for vital signs and heart rate variability monitoring", *LAPC 2011 - 2011 Loughborough Antennas and Propagation Conference*, 2011.

[30] Kang Hee Sim, Moon Sook Hwang, Sun Young Kim, Hye Mi Lee, Ji Yeun Chang, and Moon Kyu Lee, "The appropriateness of the length of insulin needles based on determination of skin and subcutaneous fat thickness in the abdomen and upper arm in patients with type 2 diabetes", *Diabetes and Metabolism Journal*, vol. 38, pages 120–133, 2 2014.

[31] Adel Y. I. Ashyap, Samsul Haimi Bin Dahlan, Zuhairiah Zainal Abidin, Muhammad Inam Abbasi, Muhammad Ramlee Kamarudin, Huda A. Majid, Muhammad Hashim Dahri, Mohd Haizal Jamaluddin, and Akram Alomainy, "An overview of electromagnetic band-gap integrated wearable antennas", *IEEE Access*, vol. 8, pages 7641–7658, 2020.

[32] Y. Q. Tan, S. Ahdi Rezaeieh, A. Abbosh, and S. Mustafa, "Defining optimum frequency range for heart failure detection system considering thickness variations in human body tissues", *Proceedings of the 2013 International Conference on Electromagnetics in Advanced Applications, ICEAA 2013*, pages 1280–1282, 2013.

[33] Pamela Di Donato, Dominique Penninck, Marco Pietra, Mario Cipone, and Alessia Diana, "Ultrasonographic measurement of the relative thickness of intestinal wall layers in clinically healthy cats", *Journal of feline medicine and surgery*, vol. 16, pages 333–339, 4 2014.

[34] Nahid Rahmani, Mohammad Ali Mohseni-Bandpei, Mahyar Salavati, Roshanak Vameghi, and Iraj Abdollahi, "Normal values of abdominal muscles thickness in healthy children using ultrasonography", *Musculoskeletal science practice*, vol. 34, pages 54–58, Apr. 2018.

[35] Tetsuro Hida, Kei Ando, Kazuyoshi Kobayashi, Kenyu Ito, Mikito Tsushima, Tomonori Kobayakawa, Masayoshi Morozumi, Satoshi Tanaka, Masaaki Machino, Kyotaro Ota, Shunsuke Kanbara, Sadayuki Ito, Naoki Ishiguro, Yukiharu Hasegawa, and Shiro Imagama, "Ultrasound measurement of thigh muscle thickness for assessment of sarcopenia", *Nagoya Journal of Medical Science*, vol. 80, page 519, 4 Nov. 2018.

[36] AbdElrahman Mohamed and Mohammad Sharawi, "Ltcc based patch antenna for biomedical applications at ism band", in *2016 IEEE 5th Asia-Pacific Conference on Antennas and Propagation (APCAP)*, 2016, pages 409–410.

[37] N. Alexopoulos and D. Jackson, "Fundamental superstrate (cover) effects on printed circuit antennas", *IEEE Transactions on Antennas and Propagation*, vol. 32, no. 8, pages 807–816, 1984.

[38] L. Ferreira and P. Pinho, "Antena para transferência de potência sem fios para alimentação de dispositivos biomédicos", 2021, Master Thesis, Instituto Politécnico de Lisboa.

[39] Ubaid Ullah, Mohd Fadzil Ain, Nor Muzlifah Mahyuddin, Mohamadariff Othman, Zainal Arifin Ahmad, Mohd Zaid Abdullah, and Arjuna Marzuki, "Antenna in ltcc technologies: A review and the current state of the art", *IEEE Antennas and Propagation Magazine*, vol. 57, pages 241–260, 2 Apr. 2015.

[40] Jia Zhu, Senhao Zhang, Ning Yi, Chaoyun Song, Donghai Qiu, Zhihui Hu, Bowen Li, Chenghao Xing, Hongbo Yang, Qing Wang, and Huanyu Cheng, "Strain-insensitive hierarchically structured stretchable microstrip antennas for robust wireless communication", *Nano-Micro Letters*, vol. 13, 1 Dec. 2021.

[41] Daniel H Schaubert, David M Pozar, and Andrew Adrian, "Effect of microstrip antenna substrate thickness and permittivity: Comparison of theories with experiment", *IEEE Transactions on Antennas and Propagation*, vol. 37, no. 6, pages 677–682, 1989.

[42] Hugo F Pues and Antoine R Van De Capelle, "An impedance-matching technique for increasing the bandwidth of microstrip antennas", *IEEE transactions on antennas and propagation*, vol. 37, no. 11, pages 1345–1354, 1989.

[43] Sang-Hyuk Wi, Yong-Bin Sun, In-Sang Song, Sung-Hoon Choa, I-S Koh, Yong-Shik Lee, and Jong-Gwan Yook, "Package-level integrated antennas based on ltcc technology", *IEEE Transactions on Antennas and Propagation*, vol. 54, no. 8, pages 2190–2197, 2006.

[44] Sang-Hyuk Wi, Jung-Min Kim, Tae-Hoon Yoo, Hyun-Jin Lee, Jae-Yeong Park, Jong-Gwan Yook, and Han-Kyu Park, "Bow-tie-shaped meander slot antenna for 5 ghz application", in *IEEE Antennas and Propagation Society International Symposium (IEEE Cat. No. 02CH37313)*, IEEE, vol. 2, 2002, pages 456–459.

[45] Pekka Ikonen and Sergei Tretyakov, "On the advantages of magnetic materials in microstrip antenna miniaturization", *Microwave and Optical Technology Letters*, vol. 50, no. 12, pages 3131–3134, 2008.

[46] RC Hansen and Mary Burke, "Antennas with magneto-dielectrics", *Microwave and optical technology letters*, vol. 26, no. 2, pages 75–78, 2000.

[47] Sang-Hyuk Wi, Yong-Shik Lee, and Jong-Gwan Yook, "Wideband microstrip patch antenna with u-shaped parasitic elements", *IEEE Transactions on Antennas and Propagation*, vol. 55, no. 4, pages 1196–1199, 2007. DOI: 10.1109/TAP.2007.893427.

[48] A.K. Shackelford, Kai-Fong Lee, and K.M. Luk, "Design of small-size wide-bandwidth microstrip-patch antennas", *IEEE Antennas and Propagation Magazine*, vol. 45, no. 1, pages 75–83, 2003. DOI: 10.1109/MAP.2003.1189652.

[49] Ujjal Chakraborty, Samiran Chatterjee, Santosh Kumar Chowdhury, and Partha Pratim Sarkar, "A comact microstrip patch antenna for wireless communication", *Progress In Electromagnetics Research C*, vol. 18, pages 211–220, 2011.

[50] Herve Legay and L Shafai, "New stacked microstrip antenna with large bandwidth and high gain", *IEE Proceedings-Microwaves, Antennas and Propagation*, vol. 141, no. 3, pages 199–204, 1994.

[51] Constantine A Balanis, *Antenna Theory: Analysis and Design*. John Wiley & Sons, 2015.

[52] Udit Raithatha and S Sreenath Kashyap, "Microstrip patch antenna parameters, feeding techniques & shapes of the patch–a survey", *International Journal of Scientific & Engineering Research*, vol. 6, no. 4, pages 981–984, 2015.

[53] *Coaxial-fed rectangular patch antenna – ansys optics*, Accessed: 2022-01-05. [Online]. Available: https://optics.ansys.com/hc/en-us/articles/360042538213-Coaxial-fed-rectangular-patch-antenna.

[54] *Dielectric properties » it'is foundation*, Accessed: 2022-02-05. [Online]. Available: https://itis.swiss/virtual-population/tissue-properties/database/dielectric-properties/.

[55] IMG Pedersen, JJ Hermans, and JFM Molenbroek, "Measurements of the sternum for better cardiopulmonary resuscitation", in *39th Annual Conference of the Nordic Ergonomics Society, Lysekil, Sweden*, Nordic Ergonomic Society, 2007, pages 1–8.

[56] Daniela D'Alessio, Claudia Giliberti, Marcello Benassi, and Lidia Strigari, "Potential third-party radiation exposure from patients undergoing therapy with 131i for thyroid cancer or metastases", *Health physics*, vol. 108, no. 3, pages 319–325, 2015.

[57] Sarah Kathryn Lynch, "Characterization of rib cortical bone thickness changes with age and sex", Ph.D. dissertation, Wake Forest University, 2015.

[58] *False ribs hi-res stock photography and images - alamy*, Accessed: 2022-03-05. [Online]. Available: https://www.alamy.com/stock-photo/false-ribs.html.

[59] Raj Kumar, JP Shinde, and MD Uplane, "Effect of slots in ground plane and patch on microstrip antenna performance", *International journal of recent trends in engineering*, vol. 2, no. 6, page 34, 2009.

[60] Jieh-Sen Kuo and Kin-Lu Wong, "A compact microstrip antenna with meandering slots in the ground plane", *Microwave and optical technology letters*, vol. 29, no. 2, pages 95–97, 2001.

[61] Xue-Xia Yang, Bing-Cheng Shao, Fan Yang, Atef Z Elsherbeni, and Bo Gong, "A polarization reconfigurable patch antenna with loop slots on the ground plane", *IEEE Antennas and Wireless Propagation Letters*, vol. 11, pages 69–72, 2012.

[62] Gary H Kramer, Kevin Capello, Brock Bearrs, Aimée Lauzon, and Lysanne Normandeau, "Linear dimensions and volumes of human lungs obtained from ct images", *Health physics*, vol. 102, no. 4, pages 378–383, 2012.

[63] R. Boutchko, "Emission tomography motion compensation", *Comprehensive Biomedical Physics*, pages 213–227, 2014. DOI: 10.1016/B978-0-444-53632-7.00105-2.

[64] *Body strap for rsp transducers | rxstrap-rsp | consumable, education, research | biopac*, Accessed: 2022-09-10. [Online]. Available: https://www.biopac.com/product/rsp-strap/.

[65] *N7555a electronic calibration module (ecal), dc-26.5 ghz, 2-port | keysight*, Accessed: 2022-09-10. [Online]. Available: https://www.keysight.com/br/pt/product/N7555A/electronic-calibration-module-ecal-dc-26-5-ghz-2-port.html.

[66] *Vital signs*, Accessed 2022-09-10. [Online]. Available: https://my.clevelandclinic.org/health/articles/10881-vital-signs.

[67] Michelle A Cretikos and Rinaldo Bellomo, "Respiratory rate: The neglected vital sign", vol. 188, 2 2008. [Online]. Available: http://www.ncepod.org.uk/2005.htm.